

Dissertation

submitted to the
Combined Faculties for the Natural Sciences and for Mathematics
of the Ruperto-Carola University of Heidelberg, Germany

for the degree of
Doctor of Natural Sciences

presented by
M.Sc. (Hons) Muhammad Sayyar Khan
born in Mardan, NWFP, Pakistan
Oral-examination: November 21st, 2008

**The role of sulfite reductase in assimilatory
sulfate reduction in *Arabidopsis thaliana***

Referees: Prof. Dr. Rüdiger Hell

Prof. Dr. Thomas Rausch

Table of Contents

Summary	1
Zusammenfassung	2
1 Introduction	3
1.1 Importance of sulfur for the plants and agriculture.....	3
1.2 An overview of uptake and assimilation of sulfur in higher plants.....	4
1.3 Role of ATP sulfurylase in sulfate reduction.....	7
1.4 Role of APS reductase in sulfate reduction.....	8
1.5 Role of sulfite reductase in sulfate reduction.....	9
1.6 Comparison of Arabidopsis sulfite reductase with sulfite reductases from other organisms	10
1.7 Sulfur and selenium: uneven twins in plant and human nutrition.....	10
1.8 Relevance of selenium metabolism in plants.....	11
1.9 Goals in Se-metabolism.....	13
1.10 Aims of the project.....	14
2 Materials and methods	15
2.1 Chemicals and Consumables.....	15
2.2 Enzymes.....	17
2.3 Technical Equipment.....	18
2.4 Biological Material.....	20
2.4.1 Bacterial Stains.....	20
2.4.2 Plant Material.....	20
2.5 Growth Conditions.....	20
2.5.1 Growth of Bacteria.....	20
2.5.1.1 Preparation of competent cells.....	21
2.5.1.1 Transformation of bacteria with DNA.....	21
2.5.2 Growth of Plants.....	22
2.5.2.1 Growth on soil.....	22
2.5.2.2 Sterilization of seeds.....	22
2.5.2.3 Hydroponical cultures.....	22
2.5.2.4 Germination on agar-dishes.....	23
2.5.2.5 Chemical complementation of <i>sir1-1</i> mutants.....	23
2.5.2.6 Stable transformation and screening of Arabidopsis.....	23
2.6 Molecular Biological Methods.....	24
2.6.1 Isolation of genomic DNA from plants.....	24
2.6.2 Isolation of total mRNA	24
2.6.3 Genotyping and molecular characterization of T-DNA insertions.....	24
2.6.4 cDNA synthesis and semi-quantitative RT-PCR analysis.....	25
2.6.5 Determination of the transcript levels by using custom made microarray.....	25
2.6.6 Separation of nucleic acids by agarose gel electrophoresis.....	26
2.6.7 DNA sequencing.....	26
2.7 Biochemical Methods.....	26
2.7.1 Recombinant expression and purification of AtSiR under native conditions.....	26
2.7.2 Recombinant expression and purification of AtSiR under denatured conditions.....	27
2.7.3 Antibody production.....	28

2.7.4	Antibody testing for SiR Protein.....	28
2.7.5	Isolation of soluble proteins from plants.....	28
2.7.6	Determination of the protein concentration.....	29
2.7.7	Determination of enzymatic activities	29
2.7.7.1	Determination of SiR activity.....	29
2.7.7.3	Determination of SAT activity.....	30
2.7.7.4	Determination of sulfite oxidase activity.....	30
2.7.8	Separation of proteins by SDS-polyacrylamide gel electrophoresis.....	30
2.7.9	Immunological detection of SiR protein.....	31
2.7.10	Immunological detection of SAT and OAS-TL proteins.....	32
2.7.11	Determination of metabolites and element contents.....	32
2.7.11.1	Quantification of the anions sulfate, phosphate, and nitrate.....	33
2.7.11.2	Determination of OAS after derivatization with AccQ-Tag.....	33
2.7.11.3	Determination of thiol metabolites after derivatization with monobromobimane.....	33
2.7.11.4	Determination of leaf chlorophyll contents.....	34
2.7.11.5	Determination of glucosinolates	34
2.7.12.6	Determination of total CNS contents.....	34
2.7.12.7	Determination of sulfolipids.....	35
2.7.12.8	Determination of total sulfur and selenium through Inductively Coupled Plasma Emission Spectroscopy.....	35
2.8	Physiological methods.....	36
2.8.1	Analysis of metabolic fluxes.....	36
2.8.1.1	Incorporation of ^{35}S into thiols and protein from $^{35}\text{SO}_4^{2-}$	36
2.8.1.2	Incorporation of ^3H into OAS, thiols and protein from ^3H -serine.....	36
2.8.1.3	Isolation of radiolabeled metabolites	37
2.8.1.3.1	Isolation of OAS and thiol metabolites.....	37
2.8.1.3.2	Isolation of the protein fraction after radiolabel feeding experiments..	38
2.8.1.4	Determination of incorporated radioactivity by liquid scintillation counting	38
2.9	Cloning.....	38
2.9.1	Vectors.....	38
2.9.2	PCR for cloning.....	39
2.9.3	DNA digestion with restriction enzymes.....	39
2.9.4	Constructs.....	39
2.9.4.1	Construct for genetic complementation and overexpression of <i>SiR</i>	39
2.9.4.2	Construct for the overexpression of recombinant AtSiR in <i>E. coli</i>	40
2.9.5	Primers and oligonucleotides	40
2.9.5.1	Primers used for sequencing.....	40
2.9.5.2	Primers used for genotyping and characterization of the T-DNA borders....	41
2.9.5.3	Primers used for RT-PCR analysis.....	41
2.9.5.4	Primers used for cloning	41
2.10	Statistical analyses.....	41
3.	Results	42
3.1.	Isolation and characterization of the T-DNA insertion line <i>sir1-1</i>	42
3.1.1	Characterization of T-DNA insertion site in <i>sir1-1</i>	42
3.1.2	<i>sir1-1</i> contains a single insertion.....	43
3.1.3.	Growth phenotype and total biomass of homozygous <i>sir1-1</i> plants.....	44
3.1.4.	Transcription analysis.....	45

3.1.5. Enzymatic activity of SiR in <i>sir1-1</i> and Col-0 plants.....	46
3.2 Analysis of sulfur-containing metabolites and related compounds.....	47
3.2.1 Analysis of thiol contents.....	47
3.2.2 Analysis of O-acetylserine (OAS) and sulfite contents	48
3.2.3 Analysis of sulfite contents.....	49
3.2.4 Analysis of inorganic anions.....	50
3.2.5 Analysis of total carbon, nitrogen and sulfur ratio	51
3.2.6 Analysis of glucosinolate contents.....	51
3.2.7 Analysis of sulfolipids contents	52
3.2.8 Analysis of chlorophyll contents.....	53
3.3 Enzymatic assays and protein analysis.....	54
3.3.1 Overexpression and purification of AtSiR protein	54
3.3.2 Antibody testing.....	55
3.3.3 Immunological detection of SiR Protein.....	56
3.3.4 Enzymatic activity and immunological detection of SAT and OAS-TL.....	57
3.3.5 Enzymatic activity of sulfite oxidase.....	58
3.4 impacts of chemical and genetic complementations on <i>sir1-1</i>	59
3.4.1 <i>sir1-1</i> can be partially complemented by GSH or sulfide.....	59
3.4.2 Genetic complementation of homozygous <i>sir1-1</i>	60
3.4.3 SiR activity in genetically complemented <i>sir1-1</i> and <i>SiR</i> overexpressor lines ...	62
3.4.4 Metabolite contents in genetically complemented <i>sir1-1</i> and <i>SiR</i> overexpressor lines	63
3.4.5 Response of <i>sir1-1</i> , Col-0, genetically complemented and <i>SiR</i> overexpressor lines towards cadmium exposure.....	64
3.5 In vivo experiments for determination of incorporation rates.....	66
3.5.1 Incorporation of the radioactively labeled sulfate into thiols.....	66
3.5.2 Incorporation of the radioactively labeled sulfate into protein.....	68
3.5.3 Incorporation of the ³ H serine into OAS and thiols.....	68
3.6 Sulfur metabolism in seeds.....	70
3.6.1 Determination of total carbon, nitrogen, sulfur and inorganic anions in the seeds	70
3.6.2 Glucosinolate, thiols and OAS contents in the seeds	71
3.7 Transcriptional analysis of sulfur metabolism related genes in <i>sir1-1</i> and Col-0.....	72
3.7.1 Impact of reduced sulfide synthesis on the expression of sulfur metabolism related genes in the leaves of <i>sir1-1</i>	72
3.7.2 Impact of reduced sulfide synthesis on the expression of sulfur metabolism related genes in the roots of <i>sir1-1</i>	74
3.8 Sulfur and selenium (Se) uneven twins in plant metabolism.....	76
3.8.1 Selenite and selenate treatment increase total sulfur contents in Arabidopsis.....	76
3.8.2 Selenite and selenate treatment increase total selenium contents in Arabidopsis.	77
3.9 Isolation and characterization of a 2nd T-DNA insertion line for <i>SiR</i>	78
3.9.1 Characterization of T-DNA insertion in <i>sir1-2</i>	78
3.9.2 <i>sir1-2</i> contains a single insertion.....	79
3.9.3 Phenotype of homozygous <i>sir1-2</i> seedlings.....	80
3.9.4 Transcription analysis.....	80
3.9.5 <i>sir1-2</i> can be partially complemented by GSH or sulfide.....	81
4 Discussion.....	83
4.1 Arabidopsis <i>sir1-1</i> is severely affected in growth.....	83
4.2 Consequences of the T-DNA insertion for the plant's metabolism.....	84

4.3 SiR activity creates a bottleneck in sulfate reduction	87
4.4 The activity of SiR is crucial in the response of plants towards cadmium exposure....	88
4.5 The impact of reduced sulfide synthesis on the expression of sulfur metabolism-related genes.....	90
4.6 Response of Arabidopsis lines towards selenium fertilization.....	93
References.....	96
Supplementary data.....	106
List of abbreviations.....	111
Acknowledgments	112

Summary

Reductive assimilation of inorganic sulfate to sulfide is an essential metabolic process in higher plants for the synthesis of cysteine and all downstream compounds containing reduced sulfur in the cell. Sulfite reductase (SiR) plays a central role in the assimilatory sulfate reduction pathway by catalyzing the reduction of sulfite to sulfide. An Arabidopsis T-DNA insertion line (*sir1-1*) with an insertion in the promoter region of *SiR* was isolated in order to address the exact role of SiR *in vivo*. Homozygous *sir1-1* plants are viable, but severely affected in growth. They flower and set viable seeds, albeit later than wild-type plants grown under the same conditions. Evaluation of *SiR* transcript levels in the leaves of *sir1-1* plants revealed that the mRNA was down-regulated to about 50% of wild-type level. Consequently, the amount of SiR protein and the activity of SiR was reduced in the same manner. The significant differences between the leaves of *sir1-1* compared to wild-type plants for most of the sulfur-containing and other related compounds suggests strong perturbations in the entire metabolism of *sir1-1* plants. A reduction of 25.6-fold and 32.7-fold in the incorporation of ³⁵S label into cysteine and GSH fractions, respectively, of *sir1-1* leaves compared to wild-type plants was observed, suggesting that the activity of SiR generates a severe bottleneck in the assimilatory sulfate reduction pathway. Investigations of the transcript levels through microarray analysis revealed that the expression of many genes related to sulfur metabolism was altered in response to reduced sulfide synthesis. Out of 920 selected genes related to sulfur metabolism, the expression of 67 genes in the leaves and 180 genes in the roots of *sir1-1*, were significantly up- or down-regulated compared to wild-type. The high affinity sulfate transporters, *SULTR 1;1* and *SULTR 1;2* showed a significant up-regulation in the roots of *sir1-1* compared to Col-0. The up-regulation of the high affinity sulfate transporters in the roots of *sir1-1* suggest that instead of steady-state sulfate levels, the amount of reduced sulfur present in the cell, likely forms the signal for their induction. The preliminary results for a second T-DNA insertion line (*sir1-2*) strongly indicate that an insertion more closer to the gene, in the promoter region of *SiR* causes early seedling lethality. All results point towards the exclusiveness of SiR for sulfite reduction and that its optimal activity is essential for the normal growth of Arabidopsis plants. Treatment of different Arabidopsis lines with selenate, which is chemically similar to sulfate, caused an increase in the total sulfur and selenium contents of the plants, possibly due to the up-regulation of sulfate transporters.

Zusammenfassung

Reduktive Assimilation von anorganischem Sulfat zu Sulfid ist in höheren Pflanzen ein essentieller metabolischer Prozess für die Synthese von Cystein und allen daraus resultierenden Verbindungen mit reduziertem Schwefel in der Zelle. Sulfid Reduktase (SiR) spielt eine zentrale Rolle in der assimilatorischen Sulfatreduktion, indem es die Reduktion von Sulfid zu Sulfid katalysiert. Eine Arabidopsis T-DNA Insertionslinie (*sir1-1*) mit einer Insertion in der Promotor-Region von *SiR* wurde isoliert, um die genaue Rolle von SiR *in vivo* zu untersuchen. Die homozygote *sir1-1* Pflanzen waren zwar lebensfähig, aber stark im Wachstum beeinträchtigt. Homozygote *sir1-1* Pflanzen blühen und produzieren lebensfähige Samen, wenn auch später als Wildtyp-Pflanzen. Die Ermittlung von *SiR* Transkriptmengen in Blättern der *sir1-1* Pflanzen zeigte, dass die mRNA zu 50 % der Wildtyp-Level herunterreguliert war. Die Menge an SiR Protein sowie die SiR-Aktivität waren entsprechend reduziert. Die signifikanten Unterschiede zwischen Blättern von *sir1-1* und Col-0 Pflanzen der meisten schwefelhaltigen und anderen in Beziehung stehenden Verbindungen deuten auf eine starke Störung im gesamten Stoffwechsel von *sir1-1* Pflanzen hin. Es wurde eine Reduzierung der Inkorporation von ³⁵S-Markierung von 25,6-fach in Cystein- und 32,7-fach in GSH-Fractionen in *sir1-1* Blättern im Vergleich zum Wildtypen beobachtet. Dies deutet darauf hin, dass SiR-Aktivität einen schwerwiegenden Engpass im Schwefel-Stoffwechsel darstellt. Microarray-Analysen zeigten, dass die Expression vieler Schwefelstoffwechsel-assoziiierter Gene als Antwort auf die reduzierte Sulfid-Synthese geändert war. Von 920 selektierten Schwefelstoffwechsel-assoziierten Genen war die Expression von 67 Genen in Blättern und 180 Genen in Wurzeln von *sir1-1* signifikant hoch- oder herunterreguliert im Vergleich zum Wildtypen. Die hochaffinen Sulfattransporter, *SULTR 1;1* und *SULTR 1;2*, zeigten eine signifikante Hochregulierung in den Wurzeln von *sir1-1* Pflanzen. Daher stellen wahrscheinlich nicht die steady-state Sulfatgehalte, sondern die Menge von reduziertem Schwefel in der Zelle das Signal für die Induktion der hochaffinen Sulfat-Transporter dar. Die vorläufigen Ergebnisse mit einer zweiten T-DNA Insertionslinie (*sir1-2*) legen nahe, dass eine Insertion, die in der Promotorregion näher am Gen von *SiR* liegt, frühe Keimlingslethaliät hervorruft. Alle Ergebnisse deuten darauf hin, dass SiR das exklusive Enzym für Sulfid-Reduktion ist und dass seine optimale Aktivität für normales Wachstum von Arabidopsis-Pflanzen essentiell ist. Behandlung von verschiedenen Arabidopsis-Linien mit Selenat, das chemisch dem Sulfat sehr ähnlich ist, verursachte einen Anstieg in den Gesamtgehalten von Schwefel und Selen, was eine Folge der Aktivierung der Sulfat-Transporter sein könnte.

1 Introduction

1.1 Importance of sulfur for the plants and agriculture

Sulfur is one of the least abundant essential macronutrient in plants. Plants take up sulfur from the soil mainly in the form of sulfate via roots. However, the abundance of sulfate in the pedosphere varies widely. In general the major portion of sulfate taken up by the plants is reduced and metabolized into organic compounds essential for structural growth, whereas the rest of sulfate in plant tissue is stored in the vacuoles. Plant species vary greatly in their sulfur requirements and an adequate and balanced S nutrition play a crucial role in the production, quality and health of the plants. The reactivity of sulfur in different oxidation and reduction states makes it one of the most versatile element in biology. It not only serves as a structural component but also has essential functions in cells (Saito, 2004). It is present in amino acids (cysteine and methionine), vitamins and cofactors (biotin and thiamine, CoA, and S-adenosyl methionine), oligopeptides (glutathione and phytochelatins), and a variety of other secondary products (glucosinolates, e.t.c.) (Saito, 2004). The sulfur containing amino acids play a key role in the structure, conformation, and function of proteins and enzymes. The thiol groups (sulfhydryl) of cysteine residues play a significant role in various functional reactions. In proteins the thiol groups of cysteine maintain protein structure by forming disulfide bonds between two cysteine residues via oxidation. In glutathione and cysteine the thiol groups are often involved in the redox cycle by two thiol \leftrightarrow disulfide conversion, which is a very versatile interchange for redox control and allow plants to mitigate against oxidative stress (Leustek and Saito 1999). The nucleophilic nature of the thiol group, specially that of glutathione, play a role in detoxification of xenobiotics by direct conjugation with thiol group mediated by glutathione *S*-transferase. Glutathione is also important in detoxification of heavy metals through phytochelatins, that are synthesized from glutathione. Sulfur-containing secondary compounds present in some species play an important role in the defense of plants against herbivores and pathogens. For example glucosinolates which are stored in specialized cells of certain plant species are enzymatically degraded by myrosinases and yield a variety of biologically active compounds such as thiocyanates, isothiocyanates, and nitriles (Graser et al., 2001; Reichelt et al., 2002; Wittstock and Halkier, 2002). The glucosinolate-myrosinase system, often termed as 'mustard oil bomb', is assumed to be an important mechanism in plant-herbivore and plant-pathogen interactions (Mikkelsen et al., 2002).

The supply of sulfur in agro-ecosystems is not always optimal for plant growth and quality. Sulfur deficiency in agricultural crops or grassland have been reported in different regions of the world (Dobermann et al., 1998; Zhao et al., 2002; Malhi et al., 2005). Sulfur deficiency in western Europe has become common due to a dramatic reduction in the sulfur inputs from the atmosphere (McGrath et al., 2002). For example the deposition of atmospheric sulfur in many areas of the United Kingdom has decreased from 70 kg ha⁻¹ year⁻¹ in the 1970's to less than 10 kg ha⁻¹ year⁻¹ in the early 2000s (Zhao et al., 2008). Fertilization of sulfur is required in such areas to avoid low crop quality and yield. Due to higher requirements of sulfur, *Brassica* crops and multiple-cut grasses are more prone to sulfur deficiency than other crops (Zhao et al., 2008). In seed proteins of several crops, the levels of the sulfur-containing amino acids, cysteine and methionine are low from nutritional point of view for animals. Enhancing methionine levels via genetic engineering is one of the target traits in biotechnology. As sulfur assimilation is strongly linked to nitrogen assimilation the deficiency of sulfur not only affects a wide range of important biological functions in the plants that are directly linked to sulfur, but also leads to the inefficient use of nitrogen. The inefficiency of the sulfur deficient crop, therefore, leads to increased nitrogen losses to the environment. Brown et al. (2000) showed that the application of sulfur at a sulfur-deficient grassland site reduced nitrate leaching to drainage water by 5-72%. Therefore, correcting sulfur deficiency on one hand has positive effect on yield and on the other hand benefits the environment. Interest in the nutra- and pharmaceuticals value of sulfur-containing plant products has recently increased. Several complementary pieces of evidence suggest that sulfur-containing phytochemicals such as isothiocyanates derived from methylsulphinylalkyl glucosinolates may be important in reducing the risk of cancer (Talalay and Fahey, 2001). For example sulforaphane, a hydrolysis product of 4-methylsulfinylbutyl glucosinolate has been shown to induce cell cycle arrest and apoptosis in HT29 human colon cancer cells *in vitro* (Gamet-Payrastre et al., 2000).

1.2 An overview of uptake and assimilation of sulfur in higher plants

The uptake and reduction of sulfate in higher plants and its subsequent assimilation into organic sulfur compounds proceeds through a highly coordinated mechanism via the assimilatory sulfate reduction pathway (Hawkesford and De Kok, 2006) (Fig. 1). Uptake of

sulfur as sulfate into the roots from soil is almost exclusively catalyzed by sulfate transporters. After the uptake of sulfate into the roots from the soil, it is then distributed throughout the plants. A number of genes involved in the uptake and distribution of sulfate have been reported including 14 genes in *Arabidopsis* (Hawkesford, 2003; Yoshimoto et al., 2003). These are classified into five different subfamilies, named Sultr1 to 5, according to their cellular and subcellular expression and possible functioning (Hawkesford and Wray, 2000; Hawkesford and De Kok, 2006). The high-affinity sulfate transporter proteins, Sultr1;1 and Sultr1;2, are localized to root epidermal cells and are responsible for the initial uptake of sulfur from the rhizosphere (Takahashi et al., 2000; Yoshimoto et al., 2002). Low affinity transporters belonging to Sultr2 and Sultr3 subfamilies are localized to vascular tissues and thought to be involved in the uptake of sulfate from plant apoplasts into vascular cells. The transporters of Sultr4 subfamily are thought to be responsible for the efflux of sulfate from the vacuole to the cytoplasm (Kataoka et al., 2004). The functions of Sultr5 subfamily transporters are less well characterized (Hawkesford and De Kok, 2006). There are no reports available indicating sulfate transport activity for Sultr5 subfamily, either *in planta* or in expression systems such as yeast. The possibility remains that these transporters have a substrate other than sulfate (Hawkesford, 2008). In fact, it has been recently shown that Sultr5;2 is required for the efficient uptake and translation of molybdate in *Arabidopsis thaliana* and is therefore termed as molybdate transporter (MTO1) (Tomatsu et al., 2007)

For assimilation, sulfate needs to be activated to adenosine 5'-phosphosulfate (APS), in which sulfate is linked by an anhydride bond to a phosphate residue by consumption of ATP and concomitant release of pyrophosphate. This activation is the sole entry step for the metabolism of sulfate and is catalyzed by ATP sulfurylase (ATPS; EC 2.7.7.4). However, APS can also be phosphorylated by APS kinase to 3'-phosphoadenosyl 5'-phosphosulfate (PAPS). PAPS serves as source of activated sulfate for sulfotransferases (SOT) that catalyzes sulfation of a variety of compounds such as glucosinolates, flavonoids, and jasmonates. Multiple isoforms of SOT exist in higher eukaryotes due to the structural diversity of the biological acceptors sulfate groups (Klein and Papenbrock, 2004). The product of the ATP sulfurylase, i.e. APS and pyrophosphate must be further metabolized immediately by the enzymes APS reductase, APS kinase, and pyrophosphatase due to the reaction equilibrium of ATP sulfurylase, which favors the reverse direction (Saito, 2004). The activity of ATP

sulfurylase is found in chloroplast and cytosol. However, all four isoforms of ATP sulfurylase in *Arabidopsis* likely encode plastidic forms and the cytosolic isoform is speculated to be produced from one of these four genes by using a different translational start codon (Hatzfeld et al., 2000). Since the next step, i.e. the reduction of sulfite to sulfide takes place exclusively in the plastids, the actual role of cytosolic ATP sulfurylase is not clear. It is hypothesized that the APS formed in the cytosol may not be directly involved in assimilation but may rather participate in sulfation through PAPS formation (Rotte and Leustek, 2000). Subsequently, APS is further reduced by APS reductase (APR; EC 1.8.4.9) or phosphorylated by APS kinase to PAPS. APR is exclusively localized to the plastids and *in vivo* it exists as a homodimer most probably linked by a disulfide bond of the conserved cysteine residue (Kopriva and Koprivova, 2004). The reduction of APS to sulfite by APR requires two electrons that are derived from glutathione. Sulfite is further reduced to sulfide by sulfite reductase (SiR; EC 1.8.7.1). The reaction catalyzed by SiR requires the transfer of six electrons provided by NADPH in chemotrophic organisms and ferredoxins in higher plants. As the electrons are supplied to ferredoxins from PSI in photosynthetic cells, in this respect sulfate assimilation is therefore linked to photosynthesis.

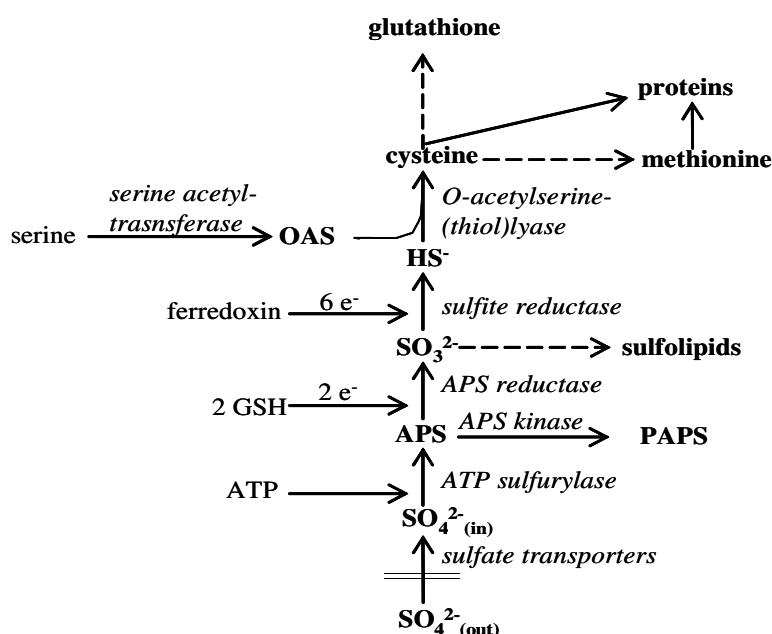


Fig. 1 Assimilatory sulfate reduction pathway in higher plants.

Enzymes along with their products and substrates are shown. APS, adenosine 5'-phosphosulfate; PAPS, 3'-phosphoadenosyl 5'-phosphosulfate; OAS, *O*-acetylserine. Dashed lines represent multiple reaction steps

The proper combination of different isoforms of ferredoxin, ferredoxin-NADPH⁺ reductase, and sulfite reductase play an critical role in efficient reduction of sulfite (Yonekura-Sakakibara et al., 2000). The sulfite reductase found in the plant cells is exclusively localized in plastids of photosynthetic and nonphotosynthetic tissues and exists as a homodimer containing a siroheme and an iron-sulfur cluster per subunit (Saito, 2004). A molybdenum enzyme, sulfite oxidase, that catalyzes the oxidation of sulfite to sulfate, has also been detected in plants (Eilers et al., 2001). However, this enzyme is localized in peroxisomes and is likely responsible for detoxification of sulfite rather for chloroplast-based assimilation. Sulfite can also be withdrawn from the primary assimilatory sulfate reduction pathway for the biosynthesis of sulfolipids in a two step reaction process. Sulfide produced by SiR is finally incorporated into the carbon and nitrogen containing skeleton of *O*-acetylserine (OAS) to form cysteine. Two enzymes, serine acetyltransferase (SAT; EC 2.3.1.30) and *O*-acetylserine (thiol)lyase (OAS-TL; EC 2.5.1.47), are responsible for this step. In contrast to the plastidic localization of the enzymes of sulfate reduction, SAT and OAS-TL are found in three major compartments of plant cells (Saito, 2000), i.e. the cytosol, mitochondrion and chloroplast. SAT catalyzes the formation of OAS by acetylation of serine under consumption of acetyl-coenzyme A, whereas OAS-TL incorporates sulfide into OAS to form cysteine. SAT and OAS-TL form a multi-enzyme complex called cysteine synthase complex (Hell et al., 2002). The synthesis of cysteine, which is regarded as the starting point for the production of methionine, GSH, and a variety of compounds containing reduced sulfur, marks the terminal step of sulfur assimilation.

1.3 Role of ATP sulfurylase in sulfate reduction

The mechanism responsible for the uptake, reduction of sulfate and its subsequent assimilation into organic sulfur compounds is tightly regulated (Hawkesford and De Kok, 2006). The assimilatory reduction of sulfate to sulfide is an essential requirement for the production of organic compounds containing reduced sulfur. Because of the strategic position of ATP sulfurylase at the entry point, its regulatory role in sulfate assimilation has been investigated (Logan et al., 1996; Lappartient et al., 1999). In general, the activity and steady-state mRNA level of ATP sulfurylase were increased upon sulfur starvation and decreased when reduced form of sulfur such as cysteine or glutathione was fed to the plants. However, the changes in the activity and mRNA level, which are limited to roots, are relatively small,

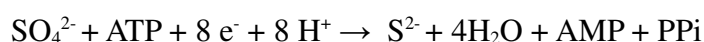
i.e. approximately 2-fold or even less. The regulatory role of ATP sulfurylase in sulfate assimilation was also demonstrated in transgenic Indian Mustard lines that overexpress ATP sulfurylase from *Arabidopsis* in the leaves. These lines not only accumulated glutathione but also showed increased resistance to SeO_4^{2-} , a toxic analog of SO_4^{2-} (Pilon-Smits et al., 1999). However, overexpression of ATP sulfurylase in Bright Yellow 2 tobacco cells (Hatzfeld et al., 1998) showed that the abundance of ATP sulfurylase was not limiting for cell metabolism in these cells.

1.4 Role of APS reductase in sulfate reduction

The regulatory role of APR in assimilatory sulfate reduction has also been investigated by many researchers and several complementary pieces of evidence suggest that APR play a critical role in the regulation of sulfate assimilation. Its activity changes rapidly in a variety of plant species after sulfur starvation, exposure to reduced sulfur compounds, and heavy-metal stress (Leustek and Saito, 1999). As sulfate assimilation is also strongly connected to nitrogen assimilation (Brunold and Suter, 1984), the role of APR with respect to nitrogen metabolism has also been investigated. In *Arabidopsis*, withdrawal of nitrogen from the growth media for 3 days led to a decrease of APR activity, whereas no significant change in the OAS-TL and thiol content was observed (Koprivova et al., 2000). The changes in APR activity in all these experiments were corresponding to the changes in its mRNA, suggesting the fact that APR is primarily regulated at the transcription level. However, in addition to that a further post-translational level of APR by redox process has also been suggested (Bick et al., 2001). The role of APR in the control of flux of the pathway has also been demonstrated in $^{35}\text{SO}_4^{2-}$ feeding experiments (Vauclare et al., 2002). These tracer experiments with $^{35}\text{SO}_4^{2-}$, performed in the presence of 0.5 mM L-cysteine or glutathione revealed that APR plays a critical role in the control of flux of the pathway. As the uptake of sulfate in these experiments was even more inhibited by glutathione than APS reduction, it is therefore, not entirely clear how the exact contribution of these individual steps in the control of flux of the pathway were organized. These experiments, however, clearly suggest that APR share the control of flux with sulfate uptake system. It is important to note that like ATP sulfurylase, the induction of APR by sulfur starvation (Gutierrez-Marcos et al., 1996; Takahashi et al., 1997) and heavy-metal stress (Heiss et al., 1999; Lee and Thomas Leustek, 1999) was limited to roots.

1.5 Role of sulfite reductase in sulfate reduction

Sulfite reductase completes the reduction process of sulfate with electron from reduced ferredoxin. In contrast to other enzymes of the assimilatory sulfate reduction pathway, SiR is encoded by a single copy gene in Arabidopsis (Bork et al., 1998). Plant SiR is a soluble protein of 65 KDa and contain a single siroheme and (4Fe-4S) cluster as prosthetic groups (Nakayama et al., 2000). Plant-type ferredoxin (Fd) is a small (11 Kda), one electron carrier protein with a single (2Fe-2S) cluster and acts as the physiological electron donor for SiR (Yonekura-Sakakibara et al., 2000). The efficient intermolecular electron transfer is facilitated by the formation of a transient electron transfer complex between Fd and SiR with 1:1 stoichiometry (Akashi et al., 1999). The molecular interaction between Fd and SiR from maize leaves revealed that two interaction sites of Fd: region 1 including Glu-29, Glu-30, Asp-34 and region 2 including Glu-92, Glu-93, Glu-94 are critical for interaction with SiR (Saitoh et al., 2006). The high affinity of SiR ($K_m =$ approximately $10 \mu\text{M}$) for SO_3^{2-} ensures the efficient metabolism of sulfite (Leustek and Saito, 1999). SiR does not appear to be appreciably regulated at the transcript level (Bork et al., 1998). However, Feeding of OAS to nitrogen deficient Arabidopsis led to an increase in mRNA levels of *SiR* (Koprivova et al., 2000). Similarly application of methyl jasmonate has also resulted in increased mRNA levels of *SiR* (Jost et al., 2005). Interestingly, in pea and maize, SiR has also been found to play a role in compacting nucleoids in the plastids (Sekine et al., 2007). The functional form of chloroplast DNA exist in a DNA-protein complex form called nucleoid (Kuroiwa, 1991). SiR was suggested to repress DNA synthesis (Cannon et al., 1999) and transcription (Sekine et al., 2002) within nucleoids. The release of SiR from the plastid nucleoids activated transcription activity due to relaxation in the DNA compaction, whereas, the addition of exogenous SiR increased DNA compaction, which then led to the repression of the transcription. On the basis of these observation it was proposed that in the plastid nucleoids transcription is regulated through DNA compaction by SiR (Sekine et al., 2002). The reduction of SO_4^{2-} to S^{2-} consumes 732 kJ mol^{-1} and requires 8 electrons, out of which six electrons are contributed by SiR (Leustek and Saito, 1999).



However, inspite of its large contribution in terms of electrons in the overall reduction of sulfate and the essential requirement of sulfide for incorporation into organic matter, very

little attention has been given to this enzyme. The exact role of SiR in terms of regulation of sulfate assimilation or control of flux of the pathway needs to be thoroughly investigated.

1.6 Comparison of Arabidopsis sulfite reductase with sulfite reductases from other organisms

The amino acid sequence deduced from pea *SiR* (*PsSiR*) was found to exhibit significant homology with *SiR* from various other organisms (Sekine et al., 2007). The similarity of the putative mature *PsSiR* was found to be 85% with *Arabidopsis thaliana* *SiR* (*AtSiR*), 91% with *Nicotiana tabaccum* *SiR* (*NtSiR*), 79% to *Zea mays* *SiR* (*ZmSiR*), and 79% with *Oryza sativa* *SiR* (*OsSiR*) in these analyses. Moreover, the hemoprotein subunit (CysI) of *E. coli* (*EcCys*), *Cyanidioschyzon merolae* *SiR* A (*CmSiRA*) and *SiR* B (*CmSiR B*) showed 48%, 59% and 57% similarity, respectively, to *PsSiR*. The three dimensional structure of *E. coli* CysI determined with the help of X-ray crystallography indicated that the siroheme and 4Fe-4S cluster are retained within the active site of the enzyme through four cysteine ligands i.e. Cys434, Cys440, Cys479, and Cys483 (Crane et al., 1995). Moreover, four basic amino acid residues i.e. Arg83, Arg153, Lys215, and Lys217, were found to be involved in the coordination of the substrate to the siroheme. These residues were found to be completely conserved in all *SiRs*. Phylogenetic analysis of *SiRs* showed that all *SiRs* of flowering plants were monophyletic in their origin (Sekine et al., 2007), and originated from cyanobacterial *SiR* (Kopriva et al., 2008).

The structure and sequence of *SiR* is quite similar to nitrite reductase (*NiR*), which catalyzes an equivalent reduction step in nitrate assimilation, i.e. a six electron reduction of nitrite to ammonia, using ferredoxin as an electron donor. In *Arabidopsis*, *SiR* shows 19% identity with nitrite reductase at amino acid level which indicate that these genes may have the same evolutionary origin (Kopriva et al., 2008). Phylogenetic analysis showed that both *SiR* and *NiR* arose from an ancient gene-duplication in Eubacteria, before the primary endosymbiosis that give rise to plastids (Kopriva et al., 2008).

1.7 Sulfur and selenium: uneven twins in plant and human nutrition

Selenium (Se) is an essential element for animals including humans (Dhillon and Dhillon, 2003; Rayman, 2000; Rayman, 2002). Being a group VIA element of the periodic table, its properties are quite similar to sulfur (Broadley et al., 2006; White et al., 2007). Like sulfur, it

also exists in several oxidation states as selenide (Se^{2-}), elemental selenium (Se^0), selenite (Se^{4+}) and selenate (Se^{6+}) (White et al., 2004). The role of selenium in higher plants has not yet been found, although some resistant plants growing on seleniferous soils, including some species of *Astragalus* and *Stanleya*, are able to accumulate selenium to very high concentrations (Feist and Parker, 2001; Pickering et al., 2003). On the basis of their abilities to accumulate Se, plants species have been divided into three groups: 'non-accumulator', 'Se-indicator', and 'Se-accumulator' (Ihnat, 1989; Wu, 1998; Dhillon and Dhillon, 2003; Ellis and Salt, 2003). Due to its many similar chemical properties S and Se are thought to share the initial route for the uptake and assimilation. Plants acquire Se primarily as selenate (SeO_4^{2-}), which enters root cells through high affinity sulfate transporters (Terry et al., 2000; White et al., 2004; White et al., 2007), but selenite and organic selenium compounds are also taken up readily (Asher et al., 1977; White et al., 2004). The sulfate transporters differ in their selectivity between sulfate and selenate and several of them are believed to contribute to selenate uptake and accumulation (White et al., 2007). Upon uptake, the reduction of selenate to selenide follow the same route as specified for the reduction of sulfate to sulfide (Fig. 2). Upon reduction to selenide, the last step of assimilation of selenide to form selenocysteine proceeds in a similar way as specified for the sulfide assimilation to form cysteine (Sors et al., 2005a).

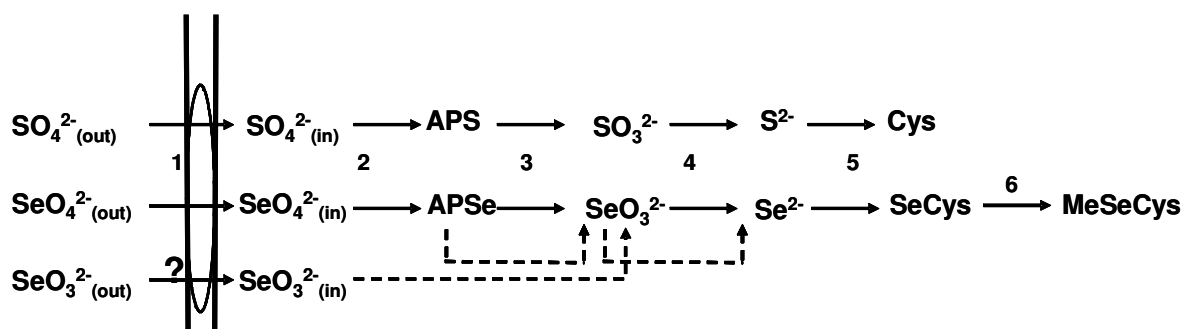


Fig. 2 Comparison of assimilatory sulfate/selenate reduction pathway in higher plants.

The dotted lines indicate the possible non-enzymatic steps. 1, sulfate transporters; 2, ATP sulfurylase; 3, APS reductase; 4, sulfite reductase; 5, *O*-acetylserine (thiol) lyase; 6, selenocysteine methyltransferase

1.8 Relevance of selenium metabolism in plants

Interest in selenium metabolism is derived from two primary areas, human nutrition and environmental remediation (Sors et al., 2005b). Although Se is an essential micronutrient for

humans and animals at very low doses but toxic at high dosage (Vinceti et al., 2001). The latter fact has sparked further interest in the phytoremediation of selenium (Berken et al., 2002; Wu, 2004). Being a worldwide problem, there is a demand for the cleanup of selenium-contaminated soils through different strategies. For instance phytoremediation that makes use of suitable plants to stabilize, remove, or detoxify pollutants could be a potentially promising technology in this respect. Overexpression of the gene encoding selenocysteine methyltransferase (SMT) from selenium hyperaccumulator *Astragalus bisulcatus* in *Arabidopsis* and Indian mustard (*Brassica juncea*) has been reported to result in increased selenium tolerance, accumulation and volatilization (LeDuc et al., 2004). An even more substantial accumulation of selenium in Indian mustard was achieved in the double transgenic lines overexpressing both, ATP sulfurylase and SMT (LeDuc et al., 2006). Another important reason responsible for the interest in Se metabolism is related to human nutrition. Various organic forms of Se and their anticarcinogenic properties against certain types of cancer have been comprehensively documented (Combs and Gray, 1998; Ip, 1998; Reid et al., 2002; Whanger, 2002; Whanger, 2004) and promoted research interest in the development of anticarcinogenic selenium-enriched nutritional supplements (Orser et al., 1999). A wide array of products are formed during the course of metabolism of selenium (Ganther and Lawrence, 1997). The amount and the chemical form of selenium that are produced during the course of metabolism are the determinants of its biological activity as an essential nutrient, cancer preventive agent or toxicant (Ganther, 1999). Methylation is a major pathway for selenium metabolism in microbes, plants and animals, that can produce less toxic forms (Ganther, 1999). The role of a number of methylated forms of selenium tested for cancer prevention (Ip and Ganther, 1991; Ip et al., 1991) revealed that the monomethylated forms of Se have strong effects on carcinogenesis compared to other forms. These metabolites were lacking some of the toxic effects that are associated with other forms such as selenite (Ganther and Lawrence, 1997; Ip, 1998). Among different monomethylated forms of selenium, methylselenocysteine serves as a reservoir (Ganther, 1999). Many of the biological actions ascribed to Se are in most cases thought to be mediated through the action of different selenoproteins. The selenoproteins incorporate Se cotranslationally as a selenocysteine residue that is fully ionized at physiological pH and acts as a very efficient redox catalyst (Beckett and Arthur, 2005). Among the 30 selenoproteins that have been

identified so far bioinformationally, six are glutathione peroxidase, three are iodothyronine deiodinases, and three are thioredoxin reductases (Kryukov et al., 2003).

1.9 Goals in Se-metabolism

There is considerable interest in the development of crops with enhanced desirable Se contents, primarily due to the pivotal role of several Se-containing compounds in human health. Given the fact that sulfur and Se share the initial route for the uptake and assimilation due to their similar chemical properties, simultaneous increase of both S and Se-containing compound appears to be a major challenge for plant scientists. Unintended interactions are most likely to happen. While pursuing any strategies for developing Se-enriched crops, the unintended interaction of Se with other compounds has to be taken into consideration. For instance, the use of a commercially available broccoli variety enriched in Se through Se fertilization in animal cancer trials (Finley et al., 2000; Finley, 2003) revealed that, as a result of selenium fertilization the production of sulforaphane, a cancer preventive sulfur-containing compounds, was inhibited by about 75% compared with uninitialized controls (Charron et al., 2001). In view of these considerations the production of the so-called selenium-enriched functional foods without significantly compromising plant health and other equally important bioactive compounds is a major challenge. To overcome such challenges a comprehensive knowledge of the genes affecting sulfur and selenium uptake, assimilation and metabolism coming from model organisms is indispensable.

1.10 Aims of the project

It is quite surprising that in spite of catalyzing one of the most energy consuming and critical step in the assimilatory sulfate reduction, very little attention has been given to characterize the exact role of SiR in the assimilatory sulfate reduction pathway. There are several open questions regarding the exact role of SiR in the assimilatory sulfate reduction pathway. Sulfide, being a prerequisite for the synthesis of cysteine, its production through the six electron transfer reduction of sulfite by SiR, is therefore a necessary step for the production of organic compounds containing reduced sulfur. To date it is not entirely clear whether sulfite reductase is the exclusive enzyme for sulfite reduction in higher plants. The exclusiveness of SiR for sulfite reduction is further challenged by the existence of NiR in plants, which catalyzes an equivalent reduction step in nitrogen assimilation and share 19% identity at amino acids level with SiR. Moreover, both of these enzymes catalyze six electron reduction steps using Fd as an electron donor. All these observations led to speculations that in plants NiR might be able to carry out sulfite reduction as well up to some extent. Moreover, the possibility of other unknown enzymes carrying out sulfite reduction in the pathway could also not be entirely excluded. Besides addressing the question regarding the exclusiveness of SiR, the impact of no or reduced sulfide synthesis through SiR knockout/down on the primary sulfur metabolism was also a major aim of this particular project. The impact of reduced SiR activity on the primary and secondary sulfur-containing metabolites was expected to provide useful informations to address the question whether sulfite reduction really creates a bottleneck in sulfate assimilation. The response of sulfur-metabolism related genes towards reduced sulfide synthesis in the leaves and roots of *Arabidopsis* will be documented to characterize the *in vivo* role of SiR in the regulation of the entire pathway.

Recently, there is considerable interest in selenium metabolism due health promoting properties of several selenium compounds. However, being members of the same group (group VIA) of the periodic table, sulfur and selenium share many similar chemical properties. The impact of selenium fertilization on sulfur metabolism for the long term production of the so-called “Se-enriched food” will be studied to find a suitable strategy to enhance selenium contents in the plants without significantly affecting plant health and other critical sulfur containing compounds.

2 Materials and methods

2.1 Chemicals and Consumables

Chemicals:

AccQ-Tag TM	Waters, Milford (USA)
Acetic acid Netherlands)	JT Baker, Deventer, (The
Agar (Germany)	Sigma-Aldrich, Steinheim
Agarose	Serva, Heidelberg (Germany)
Albumin fraction V (BSA)	Roth, Karlsruhe (Germany)
Ammoniumsulfate	Acros Organics, Geel (Belgium)
Ampicillin (sodium-salt)	Roth, Karlsruhe (Germany)
Bacto trypton (Germany)	BD Biosciences, Heidelberg
Bacto yeast extract (Germany)	BD Biosciences, Heidelberg
Cadmiumchloride (UK)	Fisher Scientific, Loughborough
Coomassie brilliant blue G250	Merck, Darmstadt (Germany)
L-Cysteine Netherlands)	Duchefa, Haarlem (The
Dithiotreitol (Germany)	Sigma-Aldrich, Steinheim
DNA loading buffer	Peqlab, Erlangen (Germany)
DNA ladder 2-Log (Germany)	New England Biolabs, Frankfurt

2 Materials and methods

Ethidiumbromide (Germany)	Sigma-Aldrich, Steinheim
Ethylendiamintetraacetate (Germany)	Sigma-Aldrich, Steinheim
Ethylenglycoltetraacetate	Serva, Heidelberg (Germany)
Fe-EDTA	Merck, Darmstadt (Germany)
Imidazole (Germany)	Sigma-Aldrich, Steinheim
Isopropyl- β -D-thiogalactopyranoside Netherlands)	Duchefa, Haarlem (The
Kanamycin Netherlands)	Duchefa, Haarlem (The
β -Mercaptoethanol	Merck, Darmstadt (Germany)
Micro agar Netherlands)	Duchefa, Haarlem (The
Monobromobimane	Synchem, Kassel (Germany)
Nickelchloride (Germany)	Sigma-Aldrich, Steinheim
<i>O</i> -acetylserine-HCl	Bachem, Bubendorf (Switzerland)
Protein Standard Mark12 TM	Invitrogen, Karlsruhe (Germany)
Phenylmethylsulfonylfluoride (Germany)	Sigma-Aldrich, Taufkirchen
Rotiphorese [®] Gel 30	Roth, Karlsruhe (Germany)
Roti [®] -Quant Bradford reagent	Roth, Karlsruhe (Germany)
Sodiumazide (Germany)	AppliChem, Darmstadt

Sodiumsulfide	Sigma-Aldrich, Steinheim
Sodiumthiosulfate	Sigma-Aldrich Buchs, Buchs (Switzerland)
Tetramethylethyldiamine	Roth, Karlsruhe (Germany)

All not listed chemicals were obtained in analysis grade from the above mentioned companies or from Biomol, Boehringer or Riedel-de-Häen.

Consumables:

CentriconConcentrators	Amicon, Beverly, MA (USA)
Dialysis tube Visking	Roth, Karlsruhe (Germany)
2D-Quant-Kit	Amersham, San Francisco, CA, (USA)
NAP5 TM -columns	Amersham, Braunschweig (Germany)
Nitrocellulose transfer membrane Protran	Schleicher & Schuell, Dassel (Germany)
Protean IEF system electrode wigs	Bio-Rad, Munich (Germany)
QIAprep Spin Miniprep Kit	Qiagen, Hilden (Germany)
ReadyStrip TM IPG strips	Bio-Rad, Munich (Germany)
Rotilabo syringe filters (0.45 µM)	Roth, Karlsruhe (Germany)

Further consumables corresponded to the usual laboratory equipment.

2.2 Enzymes

<i>Taq</i> -DNA-Polymerase (5 U/µl)	New England Biolabs, Beverly (USA)
Platenium <i>taq</i> -DNA polymerase	Invitrogen, Karlsruhe (Germany)
Phusion <i>taq</i> -DNA polymerase (Germany)	New England Biolabs, Frankfurt

3.3 Technical Equipment

Autoclave Sanoklav (Germany)	Sanoklav, Bad Überkingen-Hausen
Conditioning cabinet Percival Intellus (Germany)	CLF Laborgeräte GmbH, Emersacker
Cooling block Thermostat KBT-2 133	HLC, Bovenden (Germany)
Electroporator EasyJect Optima	EquiBio, Ashford (UK)
Fast Prep System Bio101 Thermosavant	Qbiogene, Carlsbad, CA (USA)
Fraction collector LKB FRAC-100	Pharmacia, Freiburg (Germany)
Gel-Dokumentation Gel Jet Imager 2000	Intas, Göttingen (Germany)
Growth chambers	Waiss, Gießen (Germany)
Heating block Thermostat HBT-2 132	HLC, Bovenden (Germany)
Horizontal shaker The Belly Dancer	Stovall, Greensboro, NC (USA)
HPLC-Systems:	
1. Column Nova-Pak [®] C18 3,9x150mm	Waters, Milford (USA)
Column Nova-Pak [™] C18 4,6x250mm	Waters, Milford (USA)
W600 controlle	Waters, Milford (USA)
W600E pump	Waters, Milford (USA)
W717plus autosampler	Waters, Milford (USA)
FP-920 fluorescence detector	Jasco, Groß-Umstadt
2. ICS 1000	Dionex, Idstein (Germany)
Column Ion Pak [®] AS9-HC 2x250mm	Dionex, Idstein (Germany)
AS 50 autosampler	Dionex, Idstein (Germany)
Hose pump PA-SF	IKA Labortechnik, Staufen (Germany)
Incubation shaker Innova 4300	New Brunswick Scientific, Nürtingen

(Germany)

Incubation shaker Multitron	Infors, Bottmingen (Germany)
Mini-Protean 3 elektrophoresis and blot system	Bio-Rad, Munich (Germany)
Nanodrop Spectrophotometer ND-1000	NanoDrop Technologies, Wilmington, DE (USA)
PerfectBlue doublegel system Twin ExW S	Peqlab, Erlangen (Germany)
Photometer Uvikon _{XL}	Secoman, Kandsberg (Germany)
PlateReader Fluostar Optima (Germany)	BMG Labtechnologies, Offenburg
Protean IEF Cell	Bio-Rad, Munich (Germany)
Protean II xi Cell	Bio-Rad, Munich (Germany)
Sterile bench Lamin Air 2448 and HB 2472 (Germany)	Heraeus Instruments, Osterode
Spectral photometer LKB Ultraspec III	Pharmacia, Freiburg (Germany)
Ultrasonicator Sonoplus GM 70 with tip UW 70	Bandelin Electronic, Berlin (Germany)
Ultrasound waterbath Transsonic 460	Elma, Singen (Germany)
Centrifuges:	
Beckman J2-21 with JA-20 rotor	Beckman, Munich (Germany)
or with SS-34 rotor	DuPont, Bad Homburg (Germany)
Megafuge 1.0 R with BS 4402/A Rotor (Germany)	Heraeus Instruments, Osterode
Microcentrifuge 5415C and 5417R	Eppendorf, Hamburg (Germany)
Sorvall RC5C with GSA Rotor	DuPont, Bad Homburg (Germany)

Further devices corresponded to the usual laboratory equipment.

Softwares:

Chromleon 7.1	Dionex, Idstein (Germany)
Intas GDS Application 1.51	Intas, Göttingen (Germany)
Fluostar Optima 1.30 (Germany)	BMG Labtechnologies, Offenburg

Millenium32	Waters, Milford, MA (USA)
Sigma Plot 8.0SP	SS Inc., Munich
Sigma Stat 3.0	SPSS Inc., Munich
Unicorn 4.12	Amersham, Braunschweig
Vector NTI 9.0.0	Invitrogen, Karlsruhe

2.4 Biological Material

2.4.1 Bacterial Stains

For cloning *Escherichia coli* strain XL1-B was used (*endA1 gyrA96 hsdR17 lac recA1 relA1 supE44 thi-1 [F'proAB lacI^q ZΔM15 Tn10(Tetr)]*). For overexpression of recombinant AtSiR protein HMS 174 (*(F' recA hsdR(r_{k12}-m_{k12}⁺) rifr (DE3))*) strain was used. Transformation of *Arabidopsis* plants with AtSiR was carried out with strain AGL1 (C58, RecA) with pTiBo542DT-DNA T_i plasmid.

2.4.2 Plant Material

Arabidopsis thaliana ecotype Columbia-0 (Col-0) was used as wild-type control in all experiments described in the results except Se fertilization experiments in which the SAT and SMT overexpressor lines were compared with their respective empty vector control line in the same background. Two T-DNA insertion lines for AtSiR; further annotated as *sir1-1* and *sir1-2* in the Col-0 background were obtained from GABI KAT collection center. *sir1-1* and *sir1-2* are described in the results. *Arabidopsis thaliana* belongs to family *Brassicaceae* and order Capparales. The experiments were performed either on soil-grown or on hydroponically-grown plants.

2.5 Growth Conditions

2.5.1 Growth of Bacteria

Bacteria were routinely grown in LB-medium (1% tryptone, 1% NaCl, 0.5% Yeast extract, pH 7 with NaOH). The LB-media for plates was solidified by adding 1% agar. The media

was cooled down to approximately 60°C after autoclaving, followed by the addition of selectable antibiotics under sterile conditions. Overexpression of recombinant proteins in bacteria by using the pET system (Novagen, 1999) was carried out by inoculating 1000 ml LB-medium with 1/25 volume of the respective overnight culture. The culture was grown under selective pressure at 37°C on a horizontal shaker with 220 rpm. At an OD_{600nm} of 0.8, the expression of the recombinant protein was induced with 100 µg/µl IPTG. Expression was allowed for 4h at 37°C and 220 rpm, before the cells were harvested by centrifugation for 10 min with 6,000 x g at 4°C. The bacterial sediment was frozen with liquid nitrogen and stored at -80°C.

2.5.1.1 Preparation of competent cells

Approximately 250 ml of LB-medium (section 2.5.1) without antibiotics was inoculated with 10 ml of overnight culture and grown until an OD₆₀₀ of 0.5-0.8 was reached. The culture was then cooled on ice and centrifuged at 1500 x g for 15 min at 4°C. Electrocompetent bacteria were prepared on ice by several resuspension steps followed by centrifugation at 1500 x g for 15 min at 4°C as follow. First the pellet was washed with sterile ice-cold water two times (250 and 125 ml, respectively). Afterwards, bacteria were successively resuspended in 125 and 50 ml of 10% cold glycerol. Finally, the pellet was resuspended in 2 ml of 10% glycerol, and distributed in aliquots of 40 µl. These aliquots were immediately shock-frozen in liquid nitrogen and stored in a -80°C freezer until usage.

2.5.1.1 Transformation of bacteria with DNA

Electroporation for the transformation of electrocompetent bacteria was carried out through EasyJect Optima electroporator (Equibio) set according to the built-in protocol. For plasmid transformation 1 µl (approx. 20 ng) of DNA was used. Shortly before transformation the competent cells were thawed on ice for approximately 5 min followed by the addition and incubation of DNA for 10 min. Immediately after the electric impulse, bacteria were suspended in 1 ml LB-medium (section 2.5.1) without antibiotics and grown for 1 h at 37°C (*E. coli*) or 3-5 h at 28°C (*Agrobacterium*). Appropriate amount of the bacterial culture was then plated on the solid LB agar plates (section 2.5.1) containing selective marker.

2.5.2 Growth of Plants

2.5.2.1 Growth on soil

The seeds were sowed on humid soil (Tonsubstrat from Ökohum, Herbertingen substituted with 20% (v/v) vermiculit and 2% (v/v) quartz sand) and stratified for three days at 4°C. Plants were kept in the climate chamber under short day conditions (8.5 h light). The light intensity in the growth chamber was set to 100 $\mu\text{mol photons m}^{-2} \text{s}^{-1}$, whereas, the relative humidity (RH) was kept at 50%. The temperature during the day and night were set at 22°C and 18°C, respectively. Seeds were directly germinated on soil, and 2 weeks-old seedlings were transferred to individual pots for further growth. Plants were transferred to long day conditions (16 hours light at 22°C and 8 h dark at 19°C, light intensity 160 $\mu\text{mol photons m}^{-2} \text{s}^{-1}$) after seven weeks of growth.

2.5.2.2 Sterilization of seeds

Adequate amount of seeds (50-100 mg) were soaked for 10 minutes in 1 ml of sterile water containing 0.1 % (v/v) Tween-20. They were then surface sterilized with 1 ml 70% EtOH for 1 min, followed by incubation in 6% Na-hypochloride for 5 min. Finally, the seeds were washed four times with sterile water and dried on sterile filter paper. Seeds were plated on solid media for germination (section 2.5.2.3 and 2.5.2.4). Afterwards, plates were wrapped with paraffin film and placed vertically in a growth incubator after 48 hours of stratification at 4°C.

2.5.2.3 Hydroponical cultures

Hydroponical cultures of *Arabidopsis thaliana* were used for the exposure of plants to cadmium. Surface-sterilized seeds (section 2.5.2.2) were germinated on agar in microcentrifuge tubes as described by Tocquin et al. (2003). The microcentrifuge tubes were placed into sterilized pipettip-boxes filled with modified ½ Hoagland medium (see below). Individual seedlings were transferred after 16 days to large pots containing 5 l of the same medium. Hydroponically grown plants were kept under short day conditions (section 2.5.2.1).

Modified ½ Hoagland medium:

Macroelements:

Microelements:

2.5 mM $\text{Ca}(\text{NO}_3)_2 \times 4\text{H}_2\text{O}$	40 μM Fe-EDTA
2.5 mM KNO_3	25 μM H_3BO_3
0.5 mM $\text{MgSO}_4 \times 6\text{H}_2\text{O}$	2.25 μM $\text{MnCl}_2 \times 4\text{H}_2\text{O}$
0.5 mM KH_2PO_4	1.9 μM $\text{ZnSO}_4 \times 7\text{H}_2\text{O}$
	0.15 μM $\text{CuSO}_4 \times 5\text{H}_2\text{O}$
	0.05 μM $(\text{NH}_4)_6\text{Mo}_7\text{O}_{24} \times 4\text{H}_2\text{O}$

ad pH 5.8 to 6.0 with 5 N KOH

2.5.2.4 Germination on agar-dishes

For germination experiments under exposure to cadmium, surface-sterilized seeds (section 2.5.2.2) were placed onto solid Arabidopsis medium (Haughn and Somerville, 1986) but with Fe-HBED instead of Fe-EDTA and 0.8% micro-agar. The sterile-filtered Fe-HBED was added to the medium after autoclaving. After three days of stratification at 4°C in the dark, the petri-dishes were placed upright into a conditioning cabinet with 8.5h of 83 $\mu\text{E m}^{-2}\text{s}^{-1}$ light per day and a temperature of 22°C during the light and 18°C in the dark. Seeds were either germinated on cadmium-free medium for five days and then seedlings were transferred to dishes containing 0 μM , 25 μM , 50 μM or 100 μM cadmium, or the seeds were germinated on cadmium-containing medium from the very beginning.

2.5.2.5 Chemical complementation of *sir1-1* mutants

For phenotypic complementation of homozygous *sir1-1* plants, surface sterilized seeds (section 2.5.2.2) of homozygous *sir1-1* and Col-0 plants were germinated hydroponically in eppendorf tubes placed in small boxes containing ½ Hoagland medium (section 2.5.2.3). The ½ Hoagland medium in the small boxes (0.5 L) was exogenously supplied either with a final concentration of 1 mM GSH or 0.1 mM Na_2S . The media was exchanged every two days.

2.5.2.6 Stable transformation and screening of Arabidopsis

Transformation of homozygous *sir1-1* and Col-0 plants were carried out by floral dip according to the protocol by (Clough and Bent, 1998). A single colony of Agrobacterium bearing the respective binary vector was inoculated in a 4 ml of LB-medium (section 2.5.1) overnight starting culture containing appropriate selectable markers at 28°C. After 20 h the 4

ml overnight culture was inoculated in 300 ml LB selection medium and grown for 35-40 h at 28°C. Bacteria were centrifuged at 6,000 x g for 15 min at 4°C and resuspended in a solution containing 50 g/l sucrose and 300 µl/l Silwet 77 (Lehle seeds, Round Rock, TX, USA) at OD₆₀₀=0.8-1. Arabidopsis flowering stalks were dipped in a bacterial solution for 15 seconds and left in humid, low light conditions for 24 h.

The transformants were grown directly on soil and were sprayed with commercial BASTA herbicide (Bayer Crop Science) when plants were 2-3 weeks old. Seedlings were sprayed with a final concentration of 200 mg/l glufosinate ammonium (BASTA). BASTA spray was carried out two times in a 4-day interval. Resistant seedlings were transferred to individual soil pots and grown under standard conditions (section 2.5.2.1).

2.6 Molecular Biological Methods

2.6.1 Isolation of genomic DNA from plants

DNA was isolated from a single rosette leaf for genotypic determination of Arabidopsis plants according to Edwards et al.(1991). However, for molecular characterization of T-DNA borders, DNA was isolated with Amersham Nucleon Phyto Pure Plant DNA Extraction Kit (Amersham, GE Healthcare, Munich, Germany) according to manufacturer's protocol.

2.6.2 Isolation of total mRNA

For semi-quantitative reverse transcription PCR (RT-PCR) analysis of *sir1-1* and Col-0, RNA was isolated from the leaves of 7 weeks old soil grown plants using RNeasy Plant Mini Kit (QIAGEN, Hilden, Germany) according to the manufacturer's protocol.

2.6.3 Genotyping and molecular characterization of T-DNA insertions

Genotyping was performed by PCR. The *sir1-1* line was screened with genomic primers 605 and 606 together with left T-DNA specific border primer 432, whereas, the *sir1-2* line was screened with genomic primers 605, 606, 1038 and T-DNA specific left border primer 1037 (section 2.9.5.2). Genetically complemented lines were screened with primers 605 and 606

for the wild-type allele and 606 and 432 for the T-DNA insertion.

To figure out the exact location T-DNA insertion site in the *sir1-1* and *sir1-2* line, T-DNA flanking sequences were amplified using a primer binding inside the respective T-DNA border and a primer binding to the genomic DNA outside of the insertion. For the amplification of the left border of *sir1-1* and *sir1-2*, primers 606 and 432, and 1037 and 1038, respectively were used. The PCR products were purified from agarose gels after separation by agarose gel electrophoresis and sequenced (Seqlab, Göttingen, Germany) from both sides using the same primers combination.

A standard 25 µl PCR reaction consisted of 2.5 µl of 10x taq buffer, 0.5 µl of 10 mM dNTPs, 20 pmol of each primer, 1 µl of the template DNA and 0.2 µl of the Taq polymerase from (New England Biolabs, Frankfurt am Main, Germany).

2.6.4 cDNA synthesis and semi-quantitative RT-PCR analysis

Total RNA (1 µg) (section 2.6.2) was used for the synthesis of the first strand cDNA, using M-MLV Reverse Transcriptase (Promega) according to the manufacturer's protocol. For analysis of homozygous *sir1-1* plants, the wild-type *SiR* allele of the seven weeks old soil grown plants was amplified using primer 569 and 570. Constitutively expressed actin 7 (*AtACT7*) was used as a control with primers 364 and 365 (section 2.9.5.3). The PCR was carried out using platinum taq polymerase (New England Biolabs, Frankfurt) with the following conditions: initial denaturation 5 min at 95°C was followed by 55 second denaturation step at 94°C, 30 sec annealing step at temperature characteristic for each primer pair and 45 sec extension step at 72°C. Sample sets were taken out after 31, 32 and 34 cycles. Quantification of the transcript level was done using a quantification software (gel-pro^(R) Express, Media Cybernetics, Inc, Silver Spring, USA). The expression of wild-type *SiR* allele in Col-0 and *sir1-1* was normalized according to the expression of their respective actin 7 allele.

2.6.5 Determination of the transcript levels by using custom made microarray

Design and production of the microarray: 50mer oligonucleotides of 912 selected genes were

synthesized by Ocimum Biosolutions, Inc. (Frankfurt, Germany) with an N-terminal aminolinker and checked for cross hybridization with the Smith-Waterman alignment. The microarray contains all the probes in four randomized replicates to avoid positional effects. Sample preparation, hybridization, and evaluation were performed according to Haas et al. (2008).

2.6.6 Separation of nucleic acids by agarose gel electrophoresis

Fragment of DNA were separated from agarose gels of varying concentrations (0.8% to 2%) depending on the size of the DNA fragments. Agarose was dissolved in 1x TBE buffer (90 mM Tris, 90 mM boric acid, 0.5 mM EDTA) through heating. After cooling down the gel to ~50°C, ethidium bromide was added to a final concentration of 0.7 µg/ml. After mixing the samples with a corresponding volume of loading buffer consisting of 0.25 % bromophenol blue, 0.25% xylene cyanole and 40% glycerol, appropriate volumes of the samples were loaded on the gel. Electrophoresis gels were run at 100-130 V in 1x TBE buffer and documented using INTAS GDS system (Intas, Göttingen, Germany).

2.6.7 DNA sequencing

All sequencing was carried by SeqLab ; All samples for sequencing were prepared according to the company i.e SeqLab (Göttingen, Germany) instructions. Contigs were assembled from the sequenced data and analyzed in Vector NTI9 Suite (Invitrogen, Karlsruhe, Germany).

2.7 Biochemical Methods

2.7.1 Recombinant expression and purification of AtSiR under native conditions

Overexpression of recombinant AtSiR protein from Arabidopsis in *E. coli* (strain HMS 174, section 2.4.1) using the pET system was carried out as described in section 2.5.1. After centrifugation the bacterial pellets were resuspended in 5 ml of binding buffer (50 mM Tris pH 8, 250 mM NaCl, and 10 mM imidazole), and sonicated for 5 minutes at 40% cycle using Baudelin Sonoplus GM70 sonicator. Cell debris were removed by centrifugation at 47,000 x

g for 10 min at 4°C and filtration of the supernatant through a filter with 0.45 µm pores. Immobilized metal affinity chromatography (IMAC) was used to purify the SiR fusion protein from the bacterial extract by the metal-chelating properties of the His-tag. A HiTrap™ column was loaded with nickel-ions and equilibrated with 5 ml of binding buffer. For binding of the recombinant SiR, the cells-free bacterial extract in the binding buffer containing 0.5 mM PMSF was circulated over the column for 1 h. The flow rate during the purification was adjusted to 1 ml/min. Unspecifically bound bacterial proteins were washed from the column with 10 ml of the wash buffer (50 mM Tris pH 8, 250 mM NaCl, and 100 mM imidazole). The recombinant SiR was eluted from the column by elution buffer (50 mM Tris pH 8, 250 mM NaCl, and 250 mM imidazole) and individual fractions of 1 ml were collected. Protein amounts and purities were verified by Bradford measurements (section 2.7.6) and SDS gel electrophoresis ((section 2.7.8). The column was stored in 0.02% NaN₃ at 40C, after elution of Ni-ions with 10 ml of 10 mM EDTA..

2.7.2 Recombinant expression and purification of AtSiR under denatured conditions

As the concentration of purified recombinant *AtSiR*, due to solubility reasons, was much less than the desired concentration needed for the production of the antibody. A method for purification under denaturing conditions was used according to the QIAGEN manual with a few modifications (QIA Expressionist). The bacterial pellet (section 2.5.1) was resuspended in binding buffer (50 mM Tris pH 8, 250 mM NaCl,), and sonicated for 5 minutes at 40% cycle using Baudelin Sonoplus GM70 sonicator. Afterwards, PMSF was added to final concentration of 1 mM. The suspension was centrifuged at 47,000 x g 10 min at 4°C. The supernatant was discarded and the pellet was resuspended in buffer B (100 mM NaH₂PO₄, 10 mM Tris, 8 M urea, 10 mM imidazole, pH 8). After centrifugation at 47,000 x g 10 min at 4°C, the supernatant was supplemented with 50 µl of 200 mM PMSF and filtered through a 0.45 µm filter attached to a syringe. The extract was then subjected to Ni²⁺ affinity chromatography using a HiTrap™ Chelating HP Column with a flow rate of 1 ml/min. The column was prepared in exactly the same manner as described for the purification of the *AtSiR* under native condition in section 2.7.1. *AtSiR* was bound to the column by continuous flow in a closed circuit for 1 h, then washed with 10 ml of buffer C (100 mM NaH₂PO₄, 10

mM Tris, 8 M urea, 10 mM imidazole, pH 6.10). Fractions were eluted with 8 ml of buffer D (100 mM NaH₂PO₄, 10 mM Tris, 8 M urea, 15 mM imidazole, pH 5.5) and 6 ml of buffer E (100 mM NaH₂PO₄, 10 mM Tris, 8 M urea, 30 mM imidazole, pH 4.3). The 2nd and 3rd fractions (1 ml) eluted with buffer E were highly pure.

2.7.3 Antibody production

Due to lower concentration of the recombinant *AtSiR* protein under native conditions, recombinant SiR proteins were purified under denaturing conditions and sent to Pineda (Pineda Antibody Service, Berlin, Germany) for the production of antibodies in the rabbit against *A. thaliana* SiR protein.

2.7.4 Antibody testing for SiR Protein

The antiserum for *AtSiR* was tested against different concentrations of the purified recombinant *AtSiR* along with the preimmune serum to check the specificity and sensitivity of the antiserum. After transfer on the nitrocellulose, the membrane was cut in stripes and incubated with different concentrations of preimmune serum and antiserum. Stripes were blocked with 5% BSA in TBS for 2 h, and washed twice with TBS. Afterwards, different dilutions of the antiserum and different concentrations of the recombinant *AtSiR* protein and crude plant extracts were tested along with preimmune serum as a control side by side to check the specificity and sensitivity of the antibody.

2.7.5 Isolation of soluble proteins from plants

Total protein were isolated from the leaves of seven weeks old soil-grown plants. Approximately 150-200 mg FW leaf material from each individual plant was ground in liquid nitrogen and extracted in 500 µl of extraction buffer (50 mM HEPES/KOH pH 7.4, 10 mM KCl, 1 mM EDTA, 1 mM EGTA, 10% glycerol) supplemented with 0.5 mM PMSF and 30 mM DTT. The extraction was achieved by vortexing of the samples for 15 min on ice. Cell debris were removed by two steps of centrifugation at 25,000 x g for 10 min at 4°C. The supernatant was desalted by size-exclusion chromatography using a NAP-5 column (Amersham, Braunschweig, Germany) and thereby transferred to resuspension buffer (50

mM HEPES-KOH pH 7.5, 1 mM EDTA, 2 mM DTT and 0.5 mM PMSF) according to manufacturer's protocol.

2.7.6 Determination of the protein concentration

Determination of a protein concentration was performed according to Bradford (1976) with bovine serum albumine (BSA) as a standard. 10 µl of appropriately diluted sample or standard was mixed with 250 µl of Roti[®]-Quant Bradford reagent in a well of a 96-well-plate. After incubation at room temperature for 5 min, the absorbance at 595 nm was measured in the Fluostar Optima plate reader and the concentration of the samples was determined on the basis of a standard calibration curve.

2.7.7 Determination of enzymatic activities

2.7.7.1 Determination of SiR activity

The activity of SiR was determined by coupling sulfide, the product of SiR, to excess of OAS-TL in the presence of OAS. The assay was performed at 25⁰C for 1 h in a total volume of 0.1 ml, containing 49 µl of the plant crude extract (section 2.7.5) into a mixture of 25 mM HEPES; pH 7.8, 1 mM Na₂SO₃, 5 mM OAS, 1 µg of recombinant OAS-TLC from *A. thaliana*, 10 mM DTT, 30 mM, NaHCO₃, 15 mM Na₂S₂O₄, and 5 mM methyl viologen. The reaction was stopped by precipitation of the proteins upon addition of 50 µl 20% TCA. The samples were centrifuged at 25,000 x g for 10 min at 4°C. The supernatant was transferred quantitatively to new safe lock eppendorf tube, followed by the addition of 200 µl ninhydrin solution and 100 µl of 100% acetic acid. Afterwards, the samples were incubated in a water bath for 10 min at 99°C. The ninhydrin solution contains 250 mg ninhydrin dissolved in a mixture of 6 ml of 100 % acetic acid and 4 ml of concentrated HCl. The samples were cooled down at room temperature, followed by the addition of 550 µl of 100% ethanol to each sample. The amount of cysteine was determined photometrically according to Gaitonde (1967) to with a cysteine standard calibration curve.

2.7.7.2 Determination of OAS-TL activity

Determination of enzymatic OAS-TL activity was achieved by quantification of the reaction product cysteine. The reaction was carried out in an assay of 0.1 ml volume, containing 1-2 µg of leaf protein (section 2.7.5) diluted in 65 µl of water, 50 mM HEPES; pH 7.5, 5 mM Na₂S, 5 mM DTT, 10 mM OAS. The reaction was started by the addition of master mix to the crude extract and incubation at 25°C for 5 minutes. The reaction was stopped by precipitation of the proteins with 50 µl 20% TCA. The produced cysteine was determined according to Gaitonde (1967).

2.7.7.3 Determination of SAT activity

SAT activity was assayed by coupling to the OAS-TL reaction (Nakamura et al., 1987). The entire OAS that was generated by SAT was converted to cysteine by excess of OAS-TL activity. Subsequently, the cysteine obtained was determined after Gaitonde, (1967). To ensure a high excess of OAS-TL activity during coupling of both reactions, all SAT activity determinations were supplemented with 2 units of purified recombinant OAS-TL. In a reaction volume of 100 µl, 58 µl of the crude protein extracts from leaves (section 2.7.5) were assayed to obtain a measurable signal.

The master mix consisted of 50 mM HEPES; pH 7.5, 10 mM Na₂S, 5 mM DTT, 10 mM serine, 1 mM Ac-CoA, and 2 U of recombinant OAS-TL A from *A. thaliana*. The reaction was allowed to proceed for 30 min at 25°C and was stopped by precipitation of the proteins with 50 µl 20% of TCA.

2.7.7.4 Determination of sulfite oxidase activity

The activity of sulfite oxidase extracted from leaves of hydroponically-grown *sir1-1* and Col-0 plants was assayed in cooperation with R. Hänsch and R.R. Mendel, Univ. Braunschweig. The specific activity of sulfite oxidase was determined as described in (Eilers et al., 2001).

2.7.8 Separation of proteins by SDS-polyacrylamide gel electrophoresis

Proteins were separated on discontinuous polyacrylamide gels consisting of separating (lower) gel and stacking (upper) gel according to Laemmli, (1970). BioRad MiniProtean II

gel system (BioRad, München, Germany) was used to pour and run the gels. 10% separating gels consisted of 3.3 ml of acrylamide/bis reagent Rotigel 30 (Carl Roth), 2.5 ml buffer (1.5 M Tris HCL pH 8.8), 100 µl 10% SDS and 4 ml water. Gels were polymerized by adding 100 µl of 10% ammonium persulfate (APS) and 4 µl of TEMED (Carl Roth). 5% stacking gels were prepared by mixing 2.7 ml water, 0.5 ml buffer (1 M Tris HCL pH 6.8), 0.67 ml Rotigel 30 and 40 µl 10% SDS, polymerized by adding 40 µl of 10% APS and 4 µl TEMED. Samples for the gel electrophoresis were prepared by mixing appropriate amount of protein with 5x Laemmli buffer, consisting of 10% SDS, 20% glycerol, 25% β-Mercaptoethanol and 0.1% bromophenol blue in 100 mM Tris-HCl pH 7. Samples were cooked at 95°C for 5 min and loaded on the gel. The running buffer used for gel electrophoresis consisted of 25 mM Tris-HCl pH 8.3, 0.192 M glycine and 0.1 % SDS. The gel was initially run at 70-80 V for the stacking gel and then at 120-150 V for the separating gel. Proteins were stained with Coomassie solution (50% methanol, 1% acetic acid and 0.1% Coomassie Brilliant Blue G-250 or R-250) for 30 minutes and destained with a destaining solution consisted of 20% ethanol and 10% acetic acid.

2.7.9 Immunological detection of SiR protein

Western blot protocol for SiR was optimized by testing different buffer systems (TBS and PBS), different blocking solutions (5% BSA or 5% skimmed milk), and by adding 0.1% Tween to primary and secondary antibody solution. The protocol presented below describes the best obtained results using the anti-*AtSIR* antibody. For immunodetection, proteins separated by SDS-PAGE (section 2.7.8) were transferred to a nitrocellulose membrane according to Towbin et al. (1979). Mini-Protean III chambers (BioRad) were used for the transfer in blotting buffer (0.02 M Tris-HCl pH 8.0, 0.15 M glycine, 0.04% SDS, 20% methanol). Transfer of proteins was allowed for 16h at 4°C with a constant current of 45 mA. After the transfer the nitrocellulose membrane was stained with Ponceau (0.1% Ponceau S (w/v) in 5% acetic acid) for 15-20 minutes to visualize the marker bands and check the quality of transfer. The dye was then briefly washed out with water, staining was documented by photographing and the membrane was incubated in blocking solution (5% milk in 1x PBS) overnight on the shaker at 4°C. The blocking solution was washed two times for 10 min with PBS (0.08 M Na₂HPO₄, 0.02 M NaH₂PO₄ and 0.1 M NaCl). The membrane was then

incubated with the primary antibody (1:2000 dilution) for 4 hours at room temperature. For this purpose the solution used for the dilution of the primary antibody contained 0.5% milk, 1x PBS, and 0.1% Tween). The membrane was washed 3 times for 5 minutes with 1x PBS and then incubated with 1:5000 dilution of the secondary antibody (AntiRabbit IgG Alkaline Phosphatase Conjugate, Sigma) for 2 hours. After washing of the membrane with PBS buffer and equilibration in AP-buffer (100 mM Tris pH 9.5, 100 mM NaCl, 5 mM MgCl₂), the secondary antibody was detected with NBT and BCIP as described in Sambrook et al. (1989).

2.7.10 Immunological detection of SAT and OAS-TL proteins

For the immunological detection of SAT and OAS-TL, non-stained resolved protein gels were transferred onto the nitrocellulose membrane using the Mini Trans-Blot system (BioRad). The transfer and ponceau (0.1% Ponceau S (w/v) in 5% acetic acid) staining was done in exactly the same way as described for SiR western blot analysis in section 2.7.9. The membrane was destained with TBS buffer (20 mM Tris, 137 mM NaCl, pH 7.6) and the marker was properly marked. The membrane was washed and blocked with 5% BSA (BSA in 1x TBS) for 2 hours. The membrane was then incubated with the primary antibody of OAS-TL (1:1000) and SAT (1:7500) in 0.5% BSA for 2 hours at room temperature. The membranes were washed twice with 1x TBS for 10 min, followed by incubation with 1:5000 diluted secondary antibody (AntiRabbit IgG Alkaline Phosphatase Conjugate, Sigma) for 1.5 h. Detection of the secondary antibody was carried out with NBT and BCIP as described in Sambrook et al. (1989).

2.7.11 Determination of metabolites and element contents

Metabolites (except for sulfolipids and glucosinolates) were extracted from 50-100 mg of fresh weight powdered leaf material from seven weeks old soil-grown plants and from their mature seeds in 1 ml 0.1 M HCl for 15 min by shaking on ice. Cell debris were collected by two centrifugation steps with 20,000 x g at 4°C and the supernatant extract was transferred to a clean microrcentrifuge tube.

2.7.11.1 Quantification of the anions sulfate, phosphate, and nitrate

The metabolite extract (section 2.7.11) was diluted 10-fold prior to application of the sample (25 μ l). The sample was separated by anion exchange chromatography using an IonPac AS9-HC 2 x 250 mm column (Dionex) that was connected to an ICS 1000 (Dionex). A carbonate buffer (8 mM NaCO₃, 1 mM NaHCO₃) served as mobile phase with a flow rate of 0.3 ml/min. Separated ions were detected with a conductivity detector (Dionex) and quantified on the basis of standard calibration curves for each ion by using the Chromeleon 7.1 software provided by the manufacturer.

2.7.11.2 Determination of OAS after derivatization with AccQ-Tag

OAS was quantified after derivatization with AccQ-TagTM (Waters). Derivatization was performed according to the manufacturer's specifications in a volume of 50 μ l containing 35 μ l 0.2 M borate buffer; pH 8.8 and 10 μ l 3 mg/ml AccQ-Tag in acetonitrile. 5 μ l of the metabolite extract (section 2.7.11) were used for the derivatization. The derivatized amino acids were separated by reverse phase liquid chromatography (LC) using a Nova-PakTM C18, 3.9 x 150 mm column (Waters) as described in Hartmann et al. (2004). Separated AccQ-Tag derivatives were detected with a fluorescence detector Jasco FP-920 (Jasco, Groß-Umstadt, Germany) at 395 nm after excitation with 250 nm. Quantification was performed using the Waters LC control- and analysis software Millennium³² (Waters, USA).

2.7.11.3 Determination of thiol metabolites after derivatization with monobromobimane

Low molecular weight thiols were separated and detected after their full reduction and derivatization to a fluorescent conjugate. Thiols were first reduced by mixing 25 μ l of HCl extract (section 2.7.11) with 20 μ l 1M Tris pH 8.3, 190 μ l water, 10 μ l 10 mM DTT and 25 μ l of 0.08 M NaOH in a 1.5 ml amber eppendorf tube. To ensure full reduction, samples were incubated for 1 h at room temperature in the dark. Conjugation to monobromobimane (MBB) (Synchem, Felsberg, Germany) that is specific for reduced sulfhydryl groups containing metabolites was started by adding 25 μ l of 10 mM MBB (stock in acetonitrile), followed by 15 min incubation at room temperature in the dark. The thiol-bimane-derivatives were stabilized by addition of 705 μ l 5 % acetic acid and separated by reverse phase HPLC

(Waters 600E Controller and pump, Waters 717 plus autosampler and NovaPak C18 column 4.6x250mm, 4 µm beads). Thiols were separated using an isocratic run of 91% buffer A (100 mM potassium acetate, pH 5.5, 0.02 % sodium azide) and 9 % methanol for 12.5 min. Next, the column was washed with 100 % methanol for 3 min and re-equilibrated in 91 % buffer A, 9 % methanol for 8 min. Bimane fluorescence was excited at 380 nm and detected at 480 nm using a Jasco FP-920 (Jasco, Groß-Umstadt, Germany) fluorescence detector. Results were analyzed using Millenium³² software (Waters, USA).

2.7.11.4 Determination of leaf chlorophyll contents

Chlorophyll determination was based on the work of (Mackinney, 1941) about the absorption of light by 80% acetone extracts of chlorophyll. Approximately 80 mg FW leaf material from seven weeks soil-grown plants was first potted in liquid nitrogen and then extracted for 15 minutes on ice in 700 µl of 80% acetone. Cell debris were sedimented by centrifugation at 18,000 x g at 4°C for 10 min at 4°C and supernatant was transferred to a new microcentrifuge tube. The pellet was resuspended in the same volume of 80% acetone as before, mixed thoroughly and after sedimentation of the cell debris by centrifugation, the supernatant was combined with first extraction. In a photometer, the OD of the extract (against 80% acetone) was determined at 645 nm and 663 nm. Total chlorophyll in mg/l was determined according to equation 1.

$$\text{Equation 1} \quad C = C_a + C_b \quad \text{or} \quad C = 20.2 \text{ OD}_{645} + 8.02 \text{ OD}_{663}$$

Whereas, C stands for total chlorophyll, C_a means chlorophyll a, and C_b represents chlorophyll b

2.7.11.5 Determination of glucosinolates

Glucosinolates were extracted and measured as described in Brown et al. (2003) from rosette leaves of approximately seven weeks old soil-grown plants and from their mature seeds in collaboration with M. Reichelt and J. Gershenzon (MPI for Chemical Ecology, Jena).

2.7.12.6 Determination of total CNS contents

Total carbon, nitrogen and sulfur contents of the rosette leaves of 9 weeks old soil-grown plants and from their mature seeds were determined in collaboration with Mr. Gerd Schukraft

at the Geographical Institut at Heidelberg University, using a Vario MAX CNS elemental analyzer (Elementar, Hanau). After complete drying of leaves in a 120°C incubator over night, the plant material was ground to fine powder. In the elemental analyzer, a sample of 20 mg dry weight was incinerated. The CO₂, SO₂ and N₂ were separated by adsorption of CO₂ and SO₂ to specific chromatography columns in the elemental analyzer. Desorption of a gas from the chromatography matrix was achieved by heating of the respective column. Helium served as the mobile phase with a flow rate of 140 ml/min. For incineration of the sample, O₂ was added for 50 sec with a flow rate of 60 ml/min. The elements were detected in the forms of CO₂, N₂ and SO₂ by means of their thermal conductivity and quantified according to a standard calibration curve prepared with sulfadiazin.

2.7.12.7 Determination of sulfolipids

For sulfolipids analysis approx. 200 mg fresh leaf material from seven weeks old soil-grown *sir1-1*, Col-0 and *sqd2* lines were homogenized and extracted in 0.4 ml chloroform/methanol/fomic acid (1:1:0.1) for 10 minutes. During this time the samples were vortexed vigorously, and then centrifuged briefly at 18,000 x g at 4°C. The entire supernatant was transferred into a new 1.5 ml tube, followed by the addition of 0.2 ml of 1 M KCl-0.2 M H₃PO₄. After brief centrifugation 50 µl of the lipids containing lower phase was spotted on activated pre-coated TLC-plates SILGUR-25 (Macherey-Nagel GmbH & Co, Düren, Germany). For this purpose the plates were first soaked for 30 minutes in 0.15 M ammonium sulfate, followed by complete drying at room temperature. After complete drying plates were heated at 120°C for 2.5 hours. For separation of the lipids 100 ml of acetone/toluene/water (90:30:8) was used. After separation plates were dried at room temperature and then sprayed with 50% H₂SO₄ followed by heating at 160°C for 10-15 minutes to visualize the lipids.

2.7.12.8 Determination of total sulfur and selenium through Inductively Coupled Plasma Emission Spectroscopy

For determination of total S and Se approx. 10 mg leaf material (DW) of the seven weeks old hydroponically-grown Col-0, SAT, and SMT overexpressor, and their respective empty vector control line was digested in 2.5 ml 65 % HNO₃. The samples were allowed to stand at room

temperature for two days under the fume hood, and then heated for 1 h at 95°C in a heating block. Afterwards, samples were further heated for additional 3 h at 105°C. Samples were mixed occasionally and contents of the tubes were monitored after short intervals. In case of any reduction to less than 0.5 ml, 0.5 to 2 ml HNO₃ was added to each tube after cooling down the tubes. At the end the contents of each tube were filled to a total of 10 ml with ultrapure water and closed with a lid. The samples were transported and analyzed in collaboration with Ute Krämer (Bioquant, University of Heidelberg).

2.8 Physiological methods

2.8.1 Analysis of metabolic fluxes

2.8.1.1 Incorporation of ³⁵S into thiols and protein from ³⁵SO₄²⁻

Incorporation rates of radioactively labeled sulfur into thiols and protein fraction of the *sir1-1* and Col-0 were determined by incubating their leaf pieces on ³⁵SO₄²⁻ solution, followed by the appearance of the label in the respective fractions. Leaf pieces (approx. 30 mg) of comparable sizes were cut out from the leaves of seven weeks old soil-grown plants, and floated for 15 min on the ³⁵S labeling solution (½ Hoagland medium (section 2.5.2.3) with a total of 0.502 mM sulfate containing 125 nM H₂³⁵SO₄ (1.5 mCi nmol⁻¹)) on a horizontal shaker with 60 rpm in the light (17 μE). The leaf pieces were washed twice with the non-radioactive ½ Hoagland medium, followed by direct harvest for one set of sample (time point 15 min) and a further incubation for another 30 min (time point 45 min) on the non-radioactive ½ Hoagland medium under the same shaking and light conditions. After the two washing steps both set of samples were dried on a plastic-coated paper towel and frozen in liquid nitrogen.

2.8.1.2 Incorporation of ³H into OAS, thiols and protein from ³H-serine

In order to monitor the flux of the pathway providing the carbon skeleton OAS for cysteine synthesis, tritium-labeled serine (³H-serine) was fed to leaf pieces and appearance of the label in the OAS, cysteine, GSH and protein fractions was determined. Like the ³⁵SO₄²⁻

feeding experiments, leaf pieces of (approx. 20 mg) of comparable sizes were floated for 15 min and 30 min on ^3H labeling solution ($\frac{1}{2}$ Hoagland medium (section 2.5.2.3) containing $2.5 \mu\text{M}$ of ^3H -serine ($185; 20 \text{ Ci mmol}^{-1}$)) under the same conditions as described in section 2.8.1.1. Unlike the $^{35}\text{SO}_4^{2-}$ feeding experiments; where one set of sample was given a 30 min chase on the non-radioactive $\frac{1}{2}$ Hoagland medium after 15min of incubation, all set of samples in this experiment were incubated only on ^3H labeling solution. After 15 and 30 min of incubation leaf pieces were washed twice with normal half-strength Hoagland medium followed by drying (on a plastic-coated paper towel) and freezing in liquid nitrogen.

2.8.1.3 Isolation of radiolabeled metabolites

Metabolites were extracted in a volume of 0.3 ml 1 M HCl as described in section 2.7.11. Homogenization of the radiolabeled samples was performed using the Bio101 ThermoSavant Fast Prep system (Qbiogene) according to the manufacturer's instructions.

2.8.1.3.1 Isolation of OAS and thiol metabolites

Isolation of OAS and the thiols (cysteine and GSH) from the radiolabeled metabolite extract (section 2.8.1.3) was achieved by liquid chromatography as described in sections 2.7.11.2 and 2.7.11.3 with the following modifications:

Derivatization of OAS was upscaled to utilize $50 \mu\text{l}$ metabolite extract for derivatization in a total volume of $100 \mu\text{l}$. This was achieved by addition of $30 \mu\text{l}$ 1 M borate buffer pH 8.8 and $20 \mu\text{l}$ 3 mg/ml AccQ-TagTM solution (in acetonitrile) to the reaction mixture. $40 \mu\text{l}$ of the derivatized sample was injected for separation by reversed phase LC. A fraction collector was connected in series with the LC separation for this application and the OAS-containing fraction was collected.

32-fold upscaling of thiol-derivatization in comparison with the standard protocol was achieved by the following procedure: In a total volume of $295 \mu\text{l}$ with 68 mM Tris pH 8.3, 0.34 mM DTT and 0.85 mM monobromobimane, $100 \mu\text{l}$ of the metabolite extract were subjected to derivatization. Therefore, $100 \mu\text{l}$ of 0.08 M NaOH were used in the assay for neutralization of the hydrochloric extract. As in the standard procedure, derivatization was allowed for 15 min. The thiol-bimane-derivatives were stabilized by the addition of $205 \mu\text{l}$ of

20% acetic acid. 40 μ l of the derivatized sample was injected for separation by HPLC. Cystein and GSH containing fractions were collected after elution from the column using a fraction collector in line with the HPLC. The collected metabolite fractions were subjected to liquid scintillation counting (section 2.8.1.4).

2.8.1.3.2 Isolation of the protein fraction after radiolabel feeding experiments

Protein fractions from the radioactively fed leaf pieces were isolated from the pellets of the 0.1 M HCl extract (section 2.8.1.3). 900 μ l 8 M urea was added to the pellet containing 100 μ l of residual HCl extract, mixed thoroughly and incubated at 37°C over night. After mixing again, samples were centrifuged at 16,000 x g for 5 min at room temperature. 50 μ l of the resulting supernatant was used for precipitation of proteins using the 2-D-Quant Kit according to the manufacturer's instructions. After precipitation, 100 μ l copper solution (supplied with the Kit) and 400 μ l H₂O was used to dissolve the pellet. The entire protein fraction was used for liquid scintillation counting (section 2.8.1.4).

2.8.1.4 Determination of incorporated radioactivity by liquid scintillation counting

Liquid samples of the fractions containing the individual metabolites or proteins (sections 2.8.1.3.1 and 2.8.1.3.2) were mixed each with 10 ml of Ultima Gold liquid scintillation amplifier in a 20 ml scintillation vial. The incorporated radioactivity of the samples was determined for 10 min using standard settings for ³⁵S and accordingly ³H with the liquid scintillation counter LS6000SC. After calibration with a solution containing a defined activity of either ³⁵S or ³H and using the specifications of the supplier regarding the activity correspondence to molarity, the cpm or dpm values of the samples were converted to the corresponding molar content of the respective isotope.

2.9 Cloning

2.9.1 Vectors

The following cloning and expression vectors were used:

pBinAR vector Höfgen and Willmitzer, (1990) for stable expression in plants under

35SCaMV promoter, T-DNA carries a kanamycin resistance gene

pET-28 vector (Novagen, Merck, Darmstadt, Germany) for over expression of recombinant *AtSiR* protein in *E. coli*, kanamycin resistance

pDONR201 gateway vector (Invitrogen, www.invitrogen.com/vector) for BP recombination reaction

pB2GW7 gateway vector (Invitrogen, www.invitrogen.com/vector) for LR recombination reaction.

2.9.2 PCR for cloning

High fidelity Phusion DNA polymerase (Finnzymes, New England Biolabs) was used for cloning purposes. All PCR reactions and programmes were set up according to the manufacturer's protocol, using 50 µl reaction volume as a standard. The PCR reactions when necessary, were optimized by using a different buffer, DMSO or adjusting the magnesium concentration according to the guidelines mentioned in the manual. When necessary the annealing temperature was optimized by gradient PCR.

2.9.3 DNA digestion with restriction enzymes

Restriction endonucleases along with their suitable buffers, used for DNA digestion, were mainly from New England Biolabs, Promega or Roche. Each 20 µl reaction consisted of 5 µl plasmid DNA, 2 µl respective buffer and 0.5 µl of the enzyme.

2.9.4 Constructs

2.9.4.1 Construct for genetic complementation and overexpression of *SiR*

For genetic complementation of sulfite reductase mutants, the *AtSiR* ORF along with its plastidic transient peptide was amplified from a cDNA clone (ABRC, clone S45; Genbank accession AF325027) using specially designed Gateway primers (primer 740 & 741, section 2.9.5.4) with *attB* recombination sites. BP recombination reaction between an *attB*-flanked DNA fragment and an *attP*-containing donor vector (pDONRTM201) was carried out according to the supplier's instructions (Invitrogen, www.invitrogen.com/vector) to generate

an entry clone. Afterwards, 1.5 µl of the reaction mixture, termed as BP exchange reaction, was transformed into electrocompetent XL1-B cells (section 2.4.1), and appropriate antibiotic-resistant entry clones were selected. The antibiotic-resistant entry clones were additionally screened by restriction analysis. Positive clones were sequenced to ensure that no amplification errors occurred. Afterwards, LR recombination reaction was performed between an *attL*-containing entry clone (pDONRTM201_*AtSiR*) and an *attR*-containing Gateway^(R) destination vector (pB2GW7.0) according to the supplier's instructions to generate an expression clone. Subsequently, 3 µl of the LR reaction mixture was transformed into electrocompetent XL1-B cells, and appropriate antibiotic-resistant expression clones were selected. Positive expression clones (pB2GW7.0_*AtSiR*) were screened through restriction analysis and subsequently sent out for sequencing to check for the errors.

2.9.4.2 Construct for the overexpression of recombinant *AtSiR* in *E. coli*

The full length open reading frame of *AtSiR* was amplified from a cDNA library of Arabidopsis leaves with the primers 379 & 380 (section 2.9.5.4), which contained an *NdeI* and *XhoI* restriction endonuclease site, respectively. The resulting PCR fragment was cloned via *NdeI* and *XhoI* in the pET-28a vector (Novagen, Germany) and sequenced to confirm the identity of the amplified *AtSiR* sequence. The resulting vector was termed pET-28*AtSiR* and used for the expression of recombinant *AtSiR* protein in fusion with a 6x histidine Tag in *E. coli* host HMS 174 (section 2.4.1).

2.9.5 Primers and oligonucleotides

All primers and oligonucleotides were ordered from MWG (Ebersberg, Germany). Lyophilised oligonucleotides were resuspended in a sterile, ddH₂O to a final concentration of 100 pmol/µl and stored at -20°C.

2.9.5.1 Primers used for sequencing

Primer name	Sequence
605(P1)	5'-TCTTTGATTAAGCATGAAACATTG -3'
606(P2)	5'-AGGCGATTCAAAAAGCATCTC -3'
432(P3)	5'-CCCATTTGGACGTGAATGTAGACAC -3'
639(P7)	5'-GTGGATTGATGTGATATCTCC -3'

1037(P4) 5'-ATATTGACCATCATACTCATTGC -3'

2.9.5.2 Primers used for genotyping and characterization of the T-DNA borders

Primer name	Sequence
605(P1)	5'-TCTTTGATTAAGCATGAAACATTG -3'
606(P2)	5'-AGGCGATTCAAAAAGCATCTC -3'
432(P3)	5'-CCCATTTGGACGTGAATGTAGACAC -3'
1037(P4)	5'-ATATTGACCATCATACTCATTGC -3'
1038(P5)	5'-TAGCACCAGCAAAAACACATAC -3'
638(P6)	5'-CGCCAGGGTTTTCCAGTCACGACG -3'
639(P7)	5'-GTGGATTGATGTGATATCTCC -3'

2.9.5.3 Primers used for RT-PCR analysis

Primer name	Sequence
364	5'-CAACCGGTATTGTGCTCGATTG -3'
365	5'-GAGTGAGTCTGTGAGATCCCG -3'
569	5'-ATCGACGTTTCGAGCTCCGG -3'
570	5'-GCAGGAGTGGAGACGGCTT -3'

2.9.5.4 Primers used for cloning

Primer name	Sequence
379	5'-CATATGATGTCATCGACGTTTCGAGC -3'
380	5'-CTCGAGTCATTGAGAACTCCTTTG -3'
740	5'-AAAAAGCAGGCTATGTCATCGACGTTTCGA -3'
741	5'-AGAAAGCTGGGTTTCATTGAGAACTCCTTT -3'

2.10 Statistical analyses

Comparison of means from different data sets were analyzed for statistical significance with the unpaired t test. Constant variance and normal distribution of data were checked with SigmaStat 3.0 prior to statistical analysis. Significance limits are indicated by asterisks: **, P < 0.001; *, P < 0.005.

3. Results

3.1. Isolation and characterization of the T-DNA insertion line *sir1-1*

Sulfite reductase (SiR) is encoded by a single-copy gene (At5g04590) in *Arabidopsis* consisting of eight exons separated by seven introns (Bork et al., 1998) (Figure 3). Its transcription start site is predicted 272 bp upstream of the translation start site (Bork et al., 1998). An *Arabidopsis* line containing a T-DNA insertion in *AtSiR* was identified and obtained from the GABI-Kat T-DNA collection (550A09). According to the sequence data (<http://www.gabi-kat.de/db/showseq.php?line=550A09&gene=At5g04590>) found in the database the insertion in this line was predicted in the promoter region of *AtSiR* (Fig. 3). This line was in the Col-0 background and was further annotated as *sir1-1*. Homozygous plants for this insertion were isolated through genomic DNA PCR screening using two gene-specific primers binding up and downstream of the predicted insertion in combination with a primer binding to the left border region of the T-DNA. PCR analysis and subsequent sequencing of the PCR amplified fragment (section 3.1.1) revealed that the T-DNA in *sir1-1* was in reverse orientation.

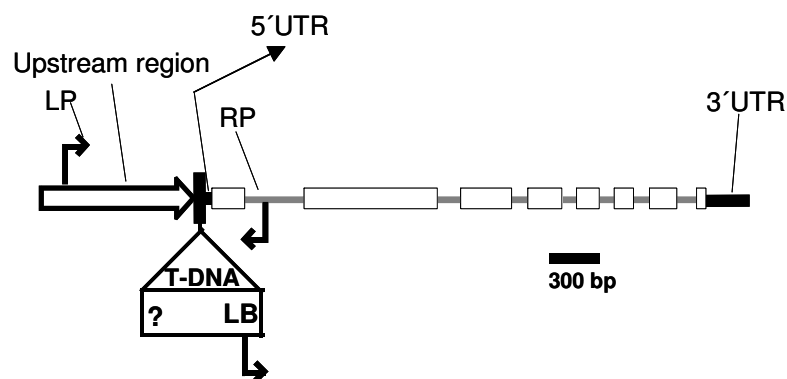


Fig. 3 Structure of *AtSiR* gene with the predicted T-DNA insertion site in *sir1-1*

Exons are indicated in white boxes, untranslated regions by black boxes, and primers for the genetic characterization by small arrows. The putative promoter is marked by a white arrow.

3.1.1 Characterization of T-DNA insertion site in *sir1-1*

Flanking sequences of the T-DNA were PCR amplified and sequenced to thoroughly characterize the insertion sites in the *sir1-1* line. Sequence analysis of a 600 bp PCR product (Fig. 4), obtained with primers P2 and P3 (section 2.9.5.2) showed exact position of the

beginning of the left border (LB) of the insertion in the promoter region of *AtSiR* gene. Alignment of the PCR amplified sequence with the genomic sequence of the sulfite reductase gene revealed the beginning of the left border of insertion 73 bp before the ATG start codon in the genomic sequence (Supplemental data 1).

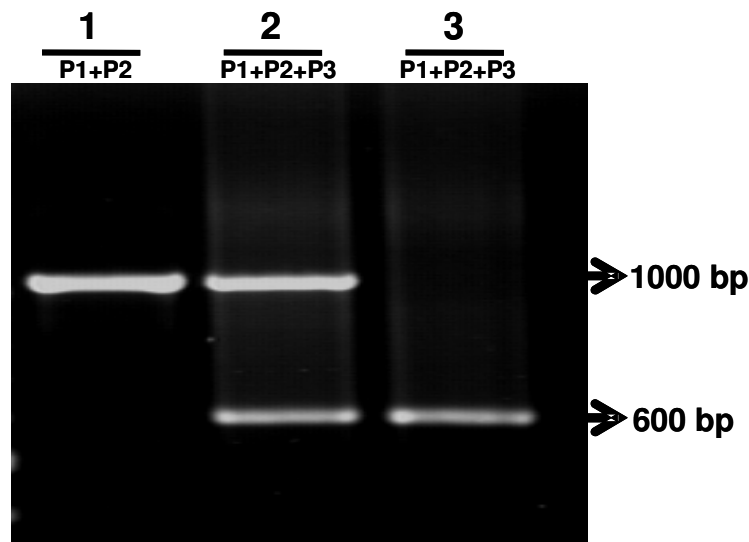


Fig. 4 Genomic characterization of *sir1-1* plants.

Genomic DNA was extracted from wild-type (1), heterozygous (2), and homozygous (3) *sir1-1* plants and tested for the presence of T-DNA insertion allele by PCR. The lack of the wild-type allele specific product in 3 demonstrated that the plant was homozygous for the T-DNA insertion.

3.1.2 *sir1-1* contains a single insertion

In order to screen the seedlings for the presence or absence of the T-DNA, seeds obtained from a PCR verified heterozygous *sir1-1* plant were plated on solid Arabidopsis media (section 2.5.2.4) without any selection marker. Close observation of the seedlings on solid Arabidopsis media revealed two distinct classes of seedlings, (i) wild-type looking seedlings and (ii) severely growth-retarded seedlings. Extraction of the genomic DNA from these seedlings and subsequent PCR analysis (Fig. 4) revealed that the severely growth-retarded seedlings were homozygous for the T-DNA insertion. The question of the single or multiple T-DNA insertions was addressed by plating seeds of PCR verified heterozygous plants on solid Arabidopsis media without any selection marker. The characteristic growth retarded phenotype of the homozygous *sir1-1* seedlings make them easily distinguishable from wild-type (Fig. 5) and heterozygous *sir1-1* seedlings, and therefore, facilitate an easy and rapid

3. Results

screening. Out of 471 seedlings, 119 seedlings were found to have characteristic growth retarded phenotype which fit to the expected 1:3 ratio for a single recessive allele according to Mendelian laws and thus hinting at the absence of a second allele causing a similar phenotype.

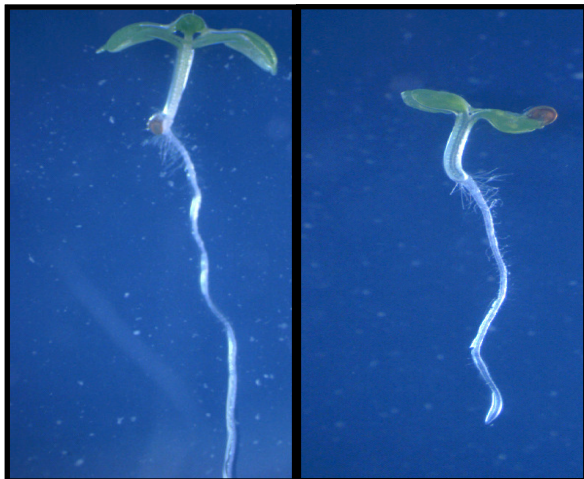


Fig. 5 Growth phenotype of homozygous *sir1-1* seedlings.

Seedlings were grown on solid Arabidopsis medium for 10-days. The homozygous *sir1-1* seedlings (right) grow slower and contain only two leaves compared to four leaves of Col-0 (left) 10-days after germination on growth media. The homozygosity of the *sir1-1* seedlings (right) was confirmed through PCR analysis.

3.1.3. Growth phenotype and total biomass of homozygous *sir1-1* plants

The homozygous plants for the T-DNA insertion at this position showed a severe phenotype of growth retardation and losses in the total biomass compared to Col-0 of the same age (Fig. 6).

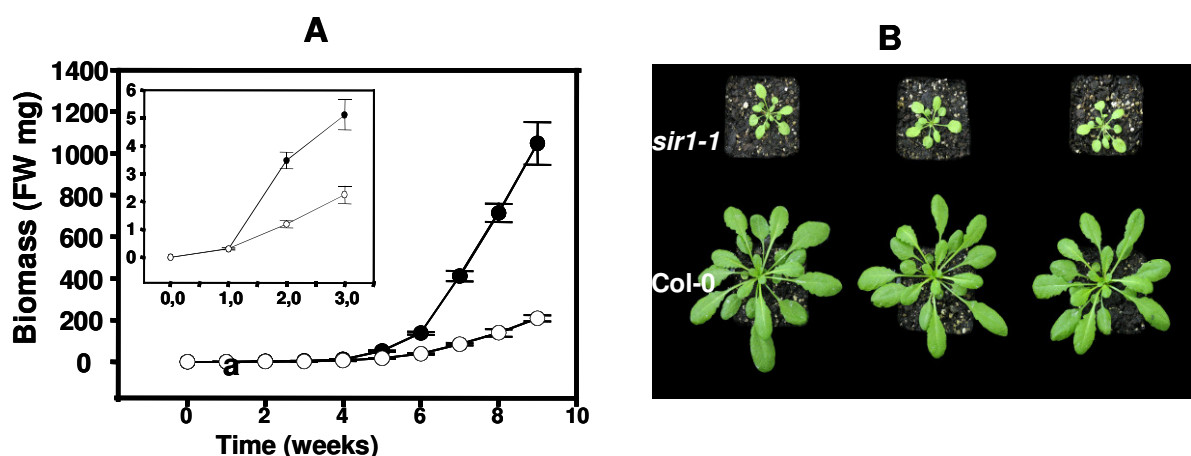


Fig. 6 Growth curve and phenotype of *sir1-1* plants

(A) Top view of the six weeks old *sir1-1* and wild-type plants. (B) Augmentation of fresh weight (FW) of

wild-type (black) and *sir1-1* (white) during vegetative growth. The biomass (aerial parts) of *sir1-1* was statically significant from two weeks on. All plants were grown on soil in a growth chamber under short day conditions.

The differences in the growth phenotype between *sir1-1* and Col-0 plants were significant at a very early stage after germination and became more and more pronounced with time due to slow growth rate of *sir1-1*. An average reduction of approximately 6-7-fold in the total biomass was observed for the seven weeks old soil-grown homozygous *sir1-1* plants compared to Col-0 plants under short day conditions (section 2.5.2.1). Besides slow growth, leaves of homozygous *sir1-1* plants also looked slightly pale yellow in color and smaller in size. However, the number of rosette leaves is approximately the same compared to Col-0 plants of the same age. Flowering in the soil-grown homozygous *sir1-1* plants was delayed approximately by four weeks on the average compared to Col-0 under short day conditions. However, inspite of the severely retarded growth phenotype and delayed flowering, the homozygous *sir1-1* plants were able to set seeds leading to viable offspring in the next generation.

3.1.4. Transcription analysis

As SiR is encoded by a single-copy gene in Arabidopsis, the loss of function for *AtSiR* was therefore, expected to result in a lethal phenotype, based on the assumption that no other gene in Arabidopsis can complement or take over the role of SiR in Arabidopsis. The viability of homozygous *sir1-1* plants would mean that either the expression of SiR in this mutant is leaky or, alternatively, some other unknown factor(s) can partially contribute towards sulfite reduction in Arabidopsis. To address this question, transcription analysis of the seven weeks old soil-grown homozygous *sir1-1* and Col-0 plants were therefore carried out, using gene specific primers for wild-type *SiR* (*AtSiR*) and constitutively expressed actin 7 (*AtACT7*) allele as a control (sections 2.6.4 & 2.9.5.3). Semi-quantitative RT-PCR analysis for *AtSiR* revealed residual *SiR* expression (Fig. 7) in the leaves of homozygous *sir1-1*, providing a plausible explanation about viability of this mutant. As *AtSiR* is thought to be not appreciably regulated at the transcript level (Bork et al., 1998), the activity of SiR in the homozygous *sir1-1* associated to the residual *SiR* expression was tested for further characterization.

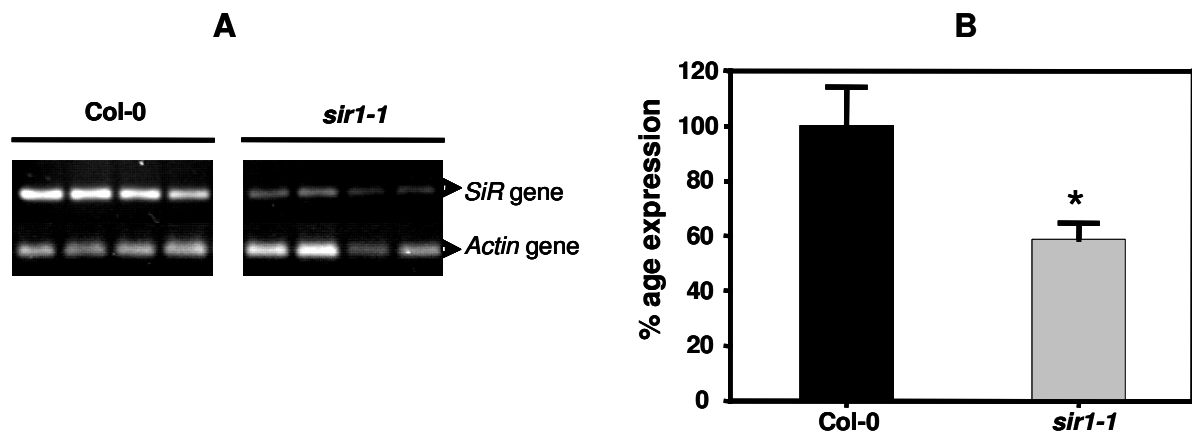


Fig. 7 Semi-quantitative RT-PCR analysis of homozygous *sir1-1* plants

(A) Amplification of *SiR* and *Actin 7* allele through reverse transcription PCR analysis. Amplification of *Actin 7* from the same cDNA preparation was used as a positive control. (B) Quantification of the transcript abundance was done through densitometric analysis. Mean \pm standard deviations are shown. Asterisks indicate statistical significance (**, $P < 0.001$; *, $P < 0.005$)

3.1.5. Enzymatic activity of SiR in *sir1-1* and *Col-0* plants

The issue whether the observed residual expression of *SiR* was sufficient to generate any SiR activity was addressed by establishing an enzymatic assay for the activity of SiR protein. For this purpose total proteins were extracted from the leaves of seven weeks old soil-grown homozygous *sir1-1* and *Col-0* plants (section 2.7.5). The six-electron transfer reduction of sulfite to sulfide catalyzed by plant SiR requires ferredoxin as an electron donor (Nakayama et al., 2000), however in this assay methyl viologen, which can act as electron donor for SiR in bacteria was used instead of ferredoxin. The specific activity of SiR was determined in a coupled assay (0.1 ml) by coupling the product of sulfite reductase reaction, i.e sulfide, with OAS in the presence of excess of purified recombinant OAS-TLC from *Arabidopsis* to form cysteine (section 2.7.7.1). The amount of resulting cysteine in a defined time period therefore reflects the activity of SiR. The activity of SiR in the leaves of homozygous *sir1-1* plants was found to be strongly reduced compared to *Col-0*. Nevertheless, there was still around 30% of the wild-type activity left in the homozygous *sir1-1* plants (Fig. 8). The moderate degree of reduction of the constitutively expressed SiR gene and its association with the severe phenotype of growth retardation was rather surprising, underpinning the critical role of SiR in the reductive assimilation of sulfate in *Arabidopsis thaliana*.

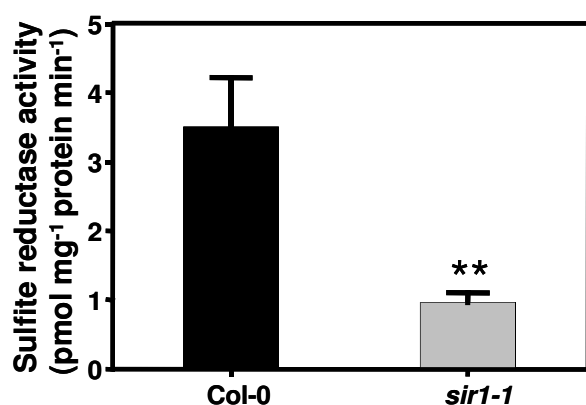


Fig. 8 Activity of SiR in the homozygous *sir1-1* line
The specific activity of SiR was determined in the soluble protein extracts from leaves of seven weeks old soil-grown homozygous *sir1-1* and Col-0 plants (n = 5). Mean \pm standard deviations are shown. Asterisks indicate statistical significance (**, P < 0.001; *, P < 0.005)

3.2 Analysis of sulfur-containing metabolites and related compounds

3.2.1 Analysis of thiol contents

In order to determine the reaction of the primary sulfur metabolism in response to reduced SiR activity, thiol contents in the leaves of seven weeks old soil-grown homozygous *sir1-1* and Col-0 plants were determined (section 2.7.11.3). The limited availability of sulfide due to reduced SiR activity in the *sir1-1* knocked down mutants was expected to result in reduced cysteine and GSH contents. However, the steady-state levels of cysteine in the leaves were rather significantly higher in *sir1-1* compared to wild-type Col-0 (Fig. 9A). GSH contents in the leaves of soil-grown *sir1-1* also tended to higher, however, the increase in this case was not significant in compared to Col-0. An average increase of 100% for the steady-state contents of cysteine was observed in the leaves of *sir1-1* compared to Col-0. For metabolite analysis of the roots, plants were grown hydroponically on modified ½ Hoagland medium (section 2.5.2.3). Cysteine and GSH contents determined in the roots of hydroponically grown *sir1-1* and Col-0 also tended to be higher in *sir1-1* compared to Col-0 (Fig. 9B). However, in contrast to leaves, the ratio of GSH to cysteine was much lower in the roots of both lines compared to leaves. The mean GSH to cysteine ratio in the leaves of *sir1-1* and Col-0 was 16.2 and 27.3, respectively, whereas, for the roots this ratio was 8.9 for *sir1-1* and 12.7 for Col-0. The cysteine and GSH contents in the leaves of hydroponically-grown plants showed a similar trend as observed for the leaves of soil-grown plants (Supplemental Fig. 1A).

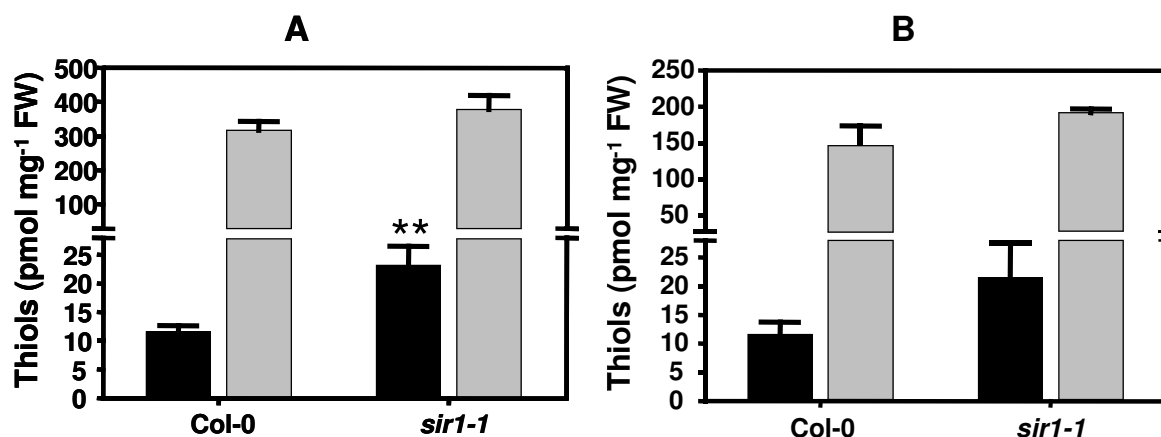


Fig. 9 Impact of reduced SiR activity on the metabolism of *sir1-1* plants

(A) Quantification of cysteine (Cys) and glutathione (GSH) contents by HPLC in the leaves of soil-grown homozygous *sir1-1* and Col-0 plants after extraction of metabolites (n = 5). (B) Quantification of Cys and GSH contents by HPLC in the roots of seven weeks old hydroponically-grown *sir1-1* and Col-0 plants after extraction of metabolites (n = 3). Black bars represent Cys contents whereas, grey bars represent total GSH contents. Mean \pm standard deviations are shown. Asterisks indicate statistical significance (**, P < 0.001; *, P < 0.005)

3.2.2 Analysis of O-acetylserine (OAS) and sulfite contents

OAS is synthesized from serine which serves as acceptor for sulfide in the terminal step of sulfur assimilation, leading to the formation of cysteine. Besides its rate-limiting role in cysteine biosynthetic pathway (Saito et al., 1994), OAS is also regarded as a positive regulatory factor for gene expression (Leustek et al., 2000; Saito, 2000; Leustek, 2002). Limited availability of sulfide due to reduced SiR activity was expected to cause accumulation of OAS. HPLC analysis were carried out (section 2.7.11.2) to determine the amount of OAS present in the leaves of seven weeks old soil-grown *sir1-1* and Col-0 plants. The OAS contents in the leaves of *sir1-1* were significantly increased compared to Col-0 (Fig. 10A). An average increase of more than 2-fold for OAS in the leaves of *sir1-1* compared to Col-0 was observed in this case. The same trend was observed in the roots of hydroponically-grown plants (Fig. 10B). The OAS contents in the leaves of hydroponically-grown were not significantly different from the leaves of Col-0 (Supplemental Fig. 1B).

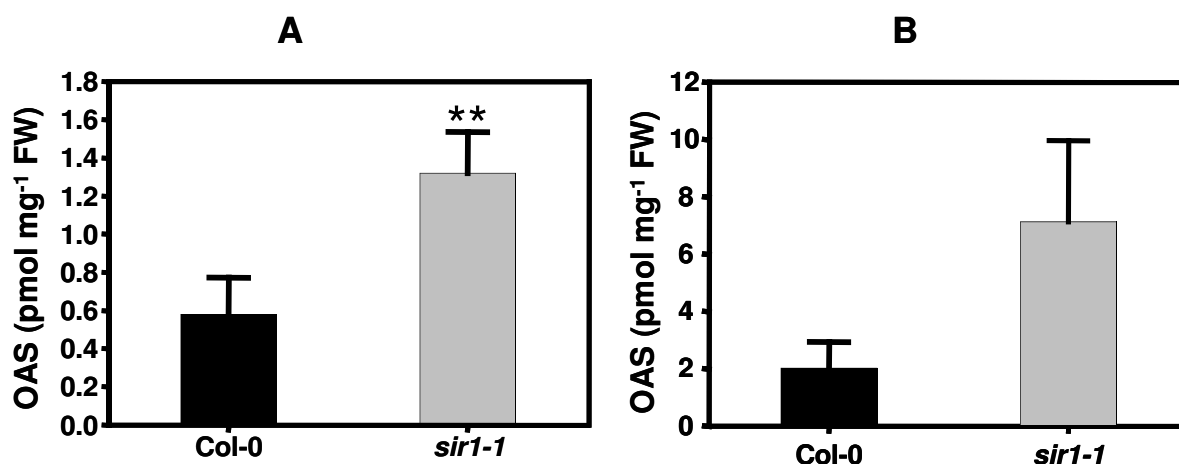


Fig. 10 Impact of reduced sulfide synthesis on OAS contents in *sir1-1* plants

(A) Quantification of *O*-acetylserine (OAS) by HPLC in the leaves of soil-grown homozygous *sir1-1* and Col-0 plants (n = 5) (B) Quantification of OAS by HPLC in the roots of seven weeks old hydroponically-grown homozygous *sir1-1* and Col-0 plants (n = 3). Mean \pm standard deviations are shown. Asterisks indicate statistical significance (**, P < 0.001; *, P < 0.005)

3.2.3 Analysis of sulfite contents

The six electron reduction of sulfite to sulfide in plants is accomplished through the activity of SiR. Ferredoxin serves as the physiological electron donor for SiR during this reaction. The strongly reduced activity of SiR observed in the leaves of *sir1-1* was expected to cause an increase in sulfite contents of *sir1-1* compared to Col-0.

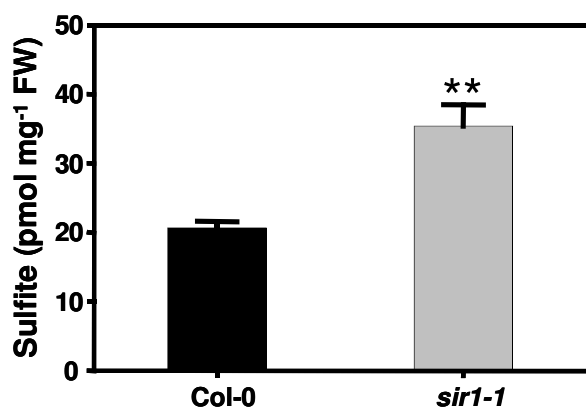


Fig. 11 Impact of reduced SiR activity on sulfite contents

Quantification of sulfite contents by HPLC in the leaves of soil-grown homozygous *sir1-1* and Col-0 plants (n = 5). Asterisks indicate statistical significance (**, P < 0.001; *, P < 0.005)

HPLC analysis (section 2.7.11.2) revealed significantly higher sulfite contents in the leaves of soil-grown *sir1-1* compared to Col-0 plants of the same age (Fig. 11). The elevated sulfite pools in the leaves of *sir1-1* is one of the obvious consequences of reduced SiR activity.

3.2.4 Analysis of inorganic anions

After entering the plants via roots through respective sulfate transporters, sulfate undergoes a number of enzymatic reactions before it is finally reduced to sulfide. Being located upstream of sulfite reductase, a strong reduction in the activity of SiR was therefore, expected to result in the accumulation of sulfate. Analysis of the total sulfate contents in the leaves of *sir1-1* through anion exchange chromatography (section 2.7.11.1) revealed a strong increase in total sulfate contents in *sir1-1* compared to Col-0 (Fig. 12A). Sulfate contents were approximately increased by 9-fold in the leaves of *sir1-1* compared to Col-0 of the same age. In contrast, total nitrate contents were significantly decreased in the leaves of *sir1-1* compared to Col-0 (Fig. 12A).

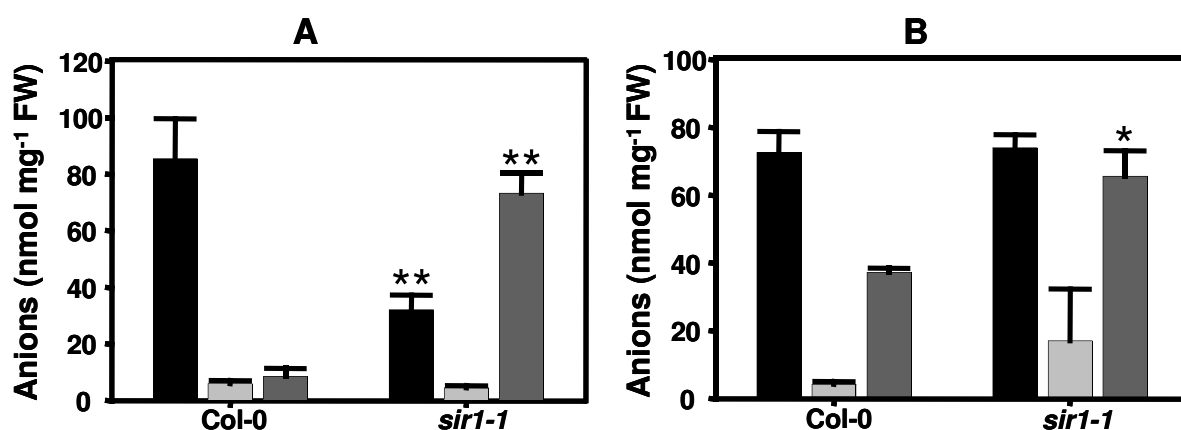


Fig. 12 Impact of reduced sulfide synthesis on the levels of inorganic anions in Arabidopsis

(A) Anions were quantified by HPLC after extraction of metabolites from leaves of seven weeks old soil-grown plants (n = 5). (B) Quantification of anions by HPLC in the roots of hydroponically-grown plants (n = 3). Black bars represent nitrate, light grey bars represent phosphate, and dark grey bars represent sulfate contents. Mean \pm standard deviations are shown. Asterisks indicate statistical significance (**, P < 0.001; *, P < 0.005)

An average reduction of 2.6-fold in the nitrate contents of *sir1-1* leaves was observed compared to Col-0. The huge accumulation of sulfate in the leaves of *sir1-1* showed that these plants were greatly affected in their ability to reduce sulfate in their leaves, where most of sulfate reduction and assimilation is supposed to take place. Analysis of sulfate contents in the roots of hydroponically-grown *sir1-1* plants showed a significant increase compared to the roots of Col-0 plants (Fig. 12B). However, the increase (1.8-fold) in sulfate contents in the roots of *sir1-1* was less pronounced compared to leaves (9-fold). In contrast to leaves, the

total nitrate contents in the roots of hydroponically-grown *sir1-1* plants were not significantly different compared to Col-0 (Fig. 12B). The concentration of anions in the leaves of hydroponically-grown plants was similar to that observed for the leaves of soil-grown plants (Supplemental Fig. 1C).

3.2.5 Analysis of total carbon, nitrogen and sulfur ratio

The retarded growth phenotype of *sir1-1* was further investigated to check whether the dramatic changes observed for most of the sulfur-containing metabolites were eventually leading to any changes in the crucial balance of carbon (C), nitrogen (N), and sulfur (S) in *sir1-1* compared to Col-0.

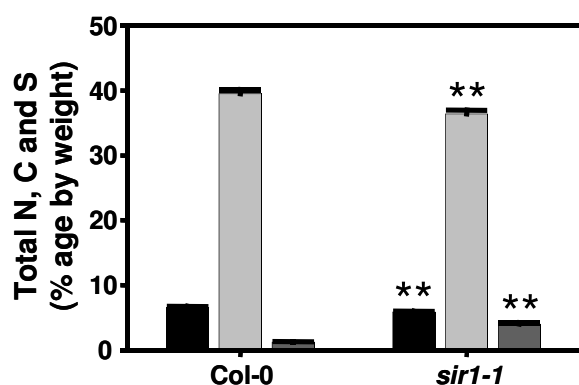


Fig. 13 Impact of reduced sulfide synthesis on total nitrogen (N), carbon (C), and sulfur (S) contents of plants

Comparison of N, C, and S ratio between the leaves of soil-grown *sir1-1* and Col-0 plants (n = 10). Black bars represent N, light grey bars represent C, and dark grey bars represent total S contents. Mean \pm standard deviations are shown. Asterisks indicate statistical significance (**, P < 0.001; *, P < 0.005)

The total CNS (section 2.7.12.6) analysis revealed significant difference for C, N, and S (Fig. 13) in the leaves of soil-grown *sir1-1* compared to Col-0. An average increase of more than 3-fold was observed for total S contents in the *sir1-1* mutant. This increase in the total S contents in the leaves of *sir1-1* was positively correlated to the huge accumulation of sulfate in leaves. In contrast to total S, a significant reduction in the total C (8%) and N (11%) contents was observed in the leaves of *sir1-1* compared to Col-0.

3.2.6 Analysis of glucosinolate contents

Glucosinolates are nitrogen and sulfur-containing natural plant products mainly found in the order Capparales, including the agriculturally important crop plants of Brassicaceae. Their contents in different Brassica species range from 1.7% to 8% of the total sulfur (Fieldsend and Milford, 1994; Blake-Kalff et al., 1998). The contents of different glucosinolates in the

leaves of soil-grown plants were determined in collaboration with M. Reichelt and J. Gershenzon, MPI Jena, to observe the impact of reduced sulfide synthesis on these critical sulfur-containing metabolites. Analysis of the glucosinolate contents in the leaves of *sir1-1* revealed dramatic differences compared to Col-0 of the same age. In fact the entire profile of the different glucosinolates was altered, with significant reduction in the total and most of the individual glucosinolates (Fig. 14) in the leaves of *sir1-1*. Neoglucobrassin was the only glucosinolate which showed an increase in *sir1-1* leaves compared to Col-0.

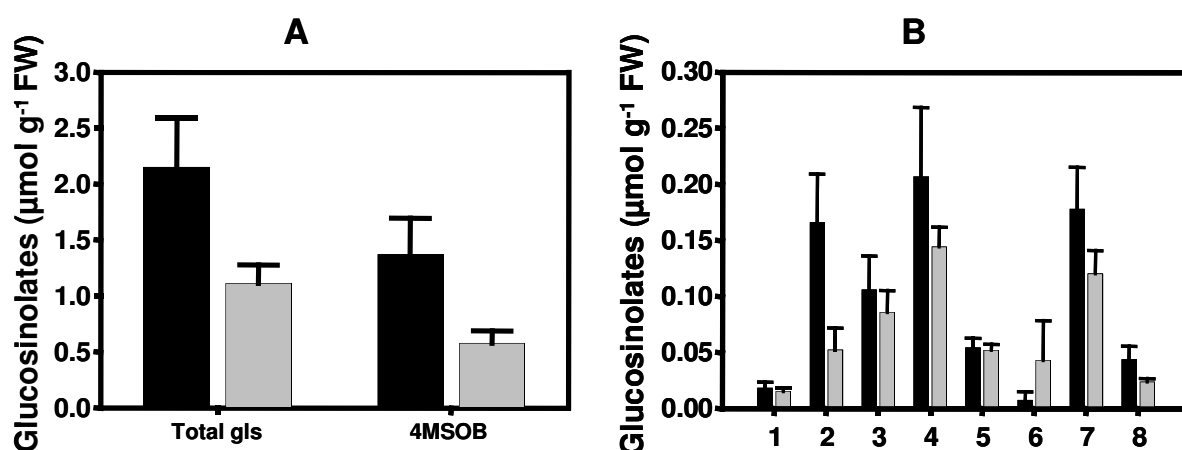


Fig. 14 Impact of reduced SiR activity on the glucosinolates profile in *sir1-1* plants

Comparison of total and individual glucosinolate contents between the leaves of Col-0 and homozygous *sir1-1* soil-grown plants (n = 10). Total gls, total glucosinolates; 4MSOB, glucoraphanin; 1, glucoibarin; 2, glucoerucin; 3, glucohirsutin; 4, glucobrassicin; 5, 4-methoxy-glucobrassicin; 6, neoglucobrassin; 7, glucoiberin; and 8, glucoalyssin. Black bars represent Col-0 and grey bar represents *sir1-1*. Mean \pm standard deviations are shown.

3.2.7 Analysis of sulfolipids contents

In plants sulfite can also be utilized for the biosynthesis of sulfolipids, which is one of the nonphosphorous glycolipids that provide the bulk of the structural lipids in photosynthetic membrane of seed plants. Its biosynthesis proceeds in two steps: in the first step SQD1 protein catalyzes transfer of sulfite to UDP-glucose giving rise to UDP-sulfoquinovose (Sanda et al., 2001), in the second step, SQD2 catalyzes transfer of sulfoquinovose moiety from UDP-sulfoquinovose to diacylglycerol. The elevated sulfite contents of the *sir1-1* (Fig. 11) led us to check whether access of sulfite is channelled for the production of sulfolipids. To this end sulfolipids in the leaves of seven weeks old soil-grown *sir1-1* and Col-0 plants

3. Results

were determined (section 2.7.12.7). Due to the lack of commercially available standard for the determination of sulfolipids, extracts from the leaves of a sulfolipid-deficient Arabidopsis mutant (*sqd2*) was used a marker (Yu et al., 2002). In contrast to *sqd2* mutant which do not contain sulfolipids, wild-type Col-0 Arabidopsis plants contain sulfolipids in their leaves (Fig. 15, black arrow), and by comparing the chromatographs from the extract of Col-0 and *sqd2* leaves, the area of the missing band in the *sqd2* mutant could be identified as the sulfolipids band in Col-0. Analysis of sulfolipids contents in the leaves of *sir1-1* and Col-0 plants did not show any significant difference (Fig. 15), probably due to the strong tendency of the leaves towards maintaining a specific composition of their photosynthetic membranes.

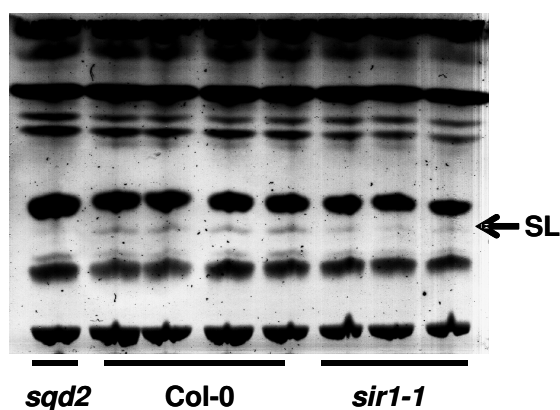


Fig. 15 Impact of reduced SiR activity on sulfolipids composition

Comparison of lipids composition among the leaves of seven weeks soil-grown *sqd2*, Col-0, and *sir1-1* plants via thin layer chromatography. The black arrow points towards sulfolipid (SL) contents.

Moreover, microarray analysis (section 3.7.1) revealed that the expression of *sqd1* and *sqd2* genes which are involved the biosynthesis of sulfolipids were not significantly changed in the leaves of hydroponically-grown *sir1-1* plants compared to Col-0.

3.2.8 Analysis of chlorophyll contents

Total chlorophyll contents in leaves of soil-grown *sir1-1* and Col-0 plants were determined to know whether the paler color of *sir1-1* leaves was associated with any change in the total chlorophyll contents. Analysis of total chlorophyll contents revealed a significant decrease in total chlorophyll contents of *sir1-1* leaves compared to Col-0 (Fig. 16A). These results showed that the decrease in total chlorophyll contents in the leaves of *sir1-1* was mainly due to the strong reduction of chlorophyll a in its leaves, whereas, the difference for chlorophyll b contents in the leaves of *sir1-1* and Col-0 was not significant (Fig. 16B). Decrease in total contents by 13 days of sulfur starvation, a situation comparable to reduced sulfide synthesis

like in *sir1-1*, has been previously reported (Nikiforova et al., 2005). Moreover, microarray analysis revealed that the expression of chlorophyllase 1 (*CLH1*), which are involved in the degradation of chlorophyll, was significantly up-regulated in the leaves of hydroponically-grown *sir1-1* plants compared to Col-0 (Fig. 32A). The degradation of chlorophyll via CHL1 appears to be an important reason for the total chlorophyll reduction.

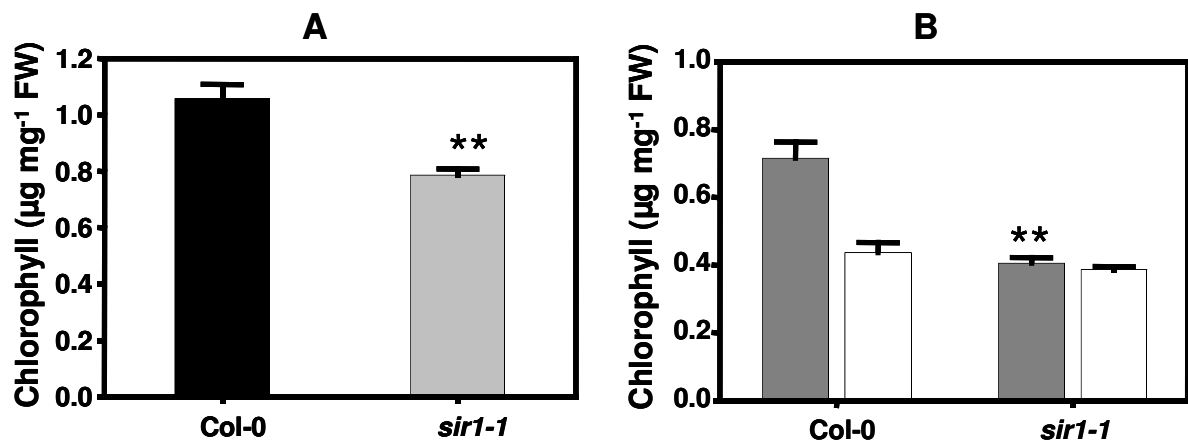


Fig. 16 Impact of reduced sulfide synthesis on chlorophyll contents of *sir1-1* plants (A) Comparison of total chlorophyll contents between the leaves of seven weeks old soil-grown *sir1-1* and Col-0 plants (n = 5). (B) Comparison of chlorophyll a (dark grey bars) and chlorophyll b (white bars) contents between the leaves of seven weeks old soil-grown *sir1-1* and Col-0 plants (n = 5). Mean \pm standard deviations are shown. Asterisks indicate statistical significance (**, P < 0.001; *, P < 0.005)

3.3 Enzymatic assays and protein analysis

3.3.1 Overexpression and purification of AtSiR protein

For the production of antibody against *AtSiR* protein the open reading frame of *AtSiR* was cloned into a bacterial expression vector. The resulting construct was then used for the expression of recombinant *AtSiR* protein in fusion with a 6x histidine tag in *E. coli* host HMS 174 (Fig. 17A). The overexpressed protein was purified under native conditions via nickel affinity chromatography as described in Materials and methods section 2.7.1. Fig. 17B and C show the gel separation of different fractions during purification under native and denaturing conditions, respectively. The concentration of the pure protein fractions obtained under native conditions was however less than the desired concentration due to solubility problems. To overcome this problem the protein was purified under denaturing conditions as

3. Results

described in Material and Methods (section 2.7.2). Sufficiently high concentrations of pure protein were obtained under denaturing conditions. The protein sample that was sent to a commercial antibody producer (Pineda Antibody Service, Germany) for immunization of rabbit is shown in lane 7 (Fig. 17C).

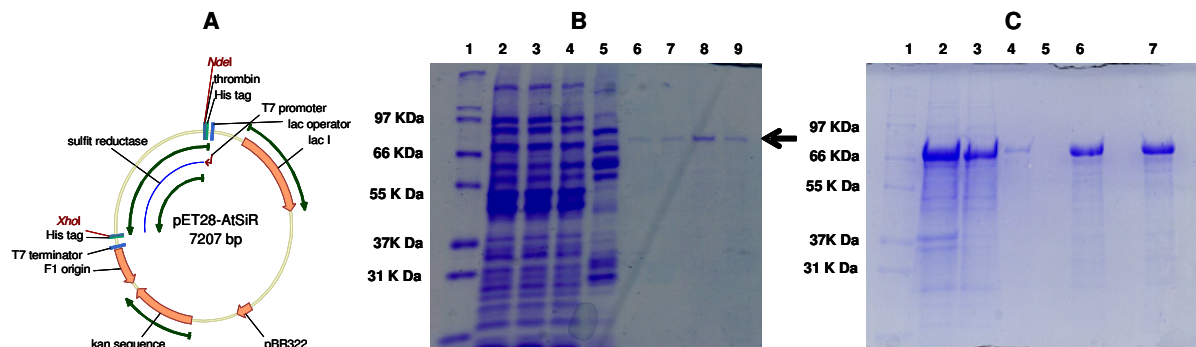


Fig. 17 Overexpression and purification of recombinant *AtSiR* in *E. coli* via Immobilized metal affinity chromatography.

(A) Full length open reading frame of *AtSiR* was overexpressed in fusion with the 6x histidine tag in *E. coli* as described in the materials and methods. (B) Exemplary Coomassie-stained protein gel showing fractions from purification of recombinant *AtSiR* under native conditions in *E. coli*. 1, Marker 12; 2, raw extract; 3, flow through; 4,5,6 and 7, wash fractions; 7, 8, & 9, elution fractions.(C) Exemplary Coomassie-stained protein gel showing fractions from purification of recombinant *AtSiR* under de-natured conditions in *E. coli*. 1. Marker 12; 2, raw extract; 3, flow through; 4 & 5, wash fractions; 7 & 8, elution fractions. Lane 7 (C) shows the final protein fraction that was used for rabbit immunization.

3.3.2 Antibody testing

Samples of the serum along with a preimmune serum obtained (Pineda Antibody Service, Germany) 75 days after immunization were tested for the specificity against *AtSiR*. Different concentrations of the recombinant *AtSiR* were tested against 1:5000 dilutions of the antiserum (Fig. 18A). Similarly, different dilutions of the antiserum were also tested against the same concentration of the same plant extracts. In contrast to preimmune serum, the antiserum reacted against plant extract, thereby giving the expected band of around ~65 KDa (Fig. 18B). After obtaining the antiserum antiserum from the final bleed (100 days after immunization) further tests were carried out for optimization and final confirmation. In all cases specific reaction of the anti-SiR antibody was observed.

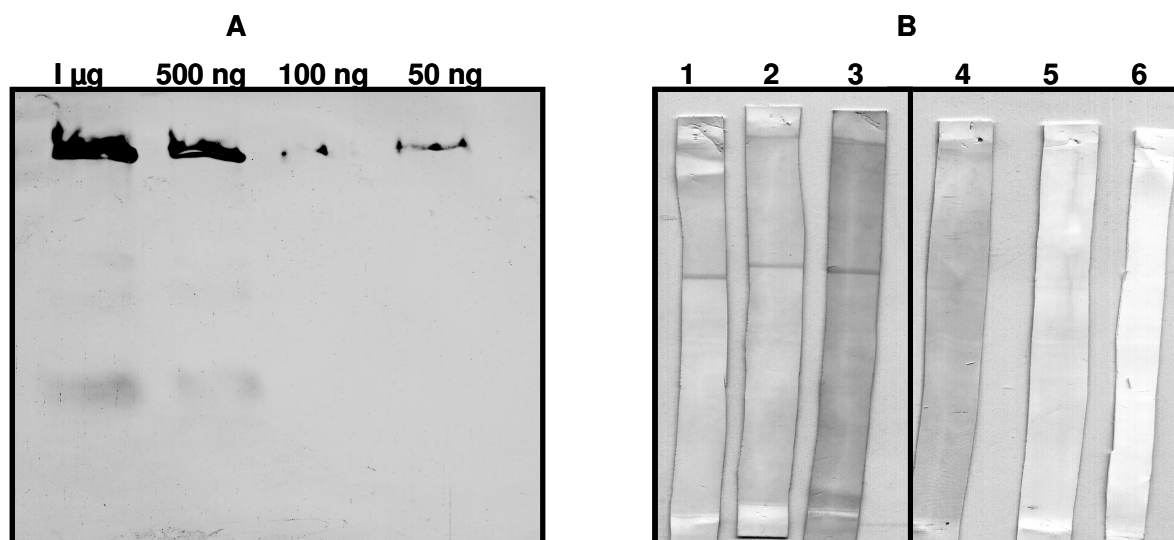


Fig. 18 Immunoblot analysis for the confirmation of the specificity of SiR antiserum

(A) 1:5000 diluted primary antiserum of SiR was tested against different concentrations (50 ng – 1000 ng) of the recombinant AtSiR protein. (B) Different dilutions of the polyclonal antiserum against AtSiR (1-3) and pre-immuneserum (4-6) were tested against the same concentration of the soluble protein extracts from wild-type plants. 1, 1:1000; 2, 1:5000; 3, 1:10,000. The absence of the protein bands in 4,5, and 6 against pre-immuneserum confirm the specificity of the SiR antiserum.

3.3.3 Immunological detection of SiR Protein

A number of similarities exist between sulfite and nitrite reductase, including conserved catalytic architecture designed to guide an essential siroheme cofactor to act as the active center for the six-electrons transfer reduction of sulfite to sulfide (Janick et al., 1983; Crane and Getzoff, 1996; Crane et al., 1997). These similarities suggest that sulfur and nitrogen metabolism may be partially redundant at the point of sulfite/nitrite reduction and/or in the provision of siroheme cofactor, leading to the assumption that the two enzymes may complement each other in sulfite and/or nitrite reduction. The activity of SiR which is based on the formation of the product (sulfide) coupled in the next step through another enzymatic reaction to form cysteine do not fully exclude any contribution of nitrite reductase during this process. Although the residual activity of SiR observed in the leaves of *sir1-1* (Fig. 8) is correlated well to the residual expression of *SiR* in *sir1-1* (Fig. 7), the presence of any residual SiR protein in the *sir1-1* mutant however, more clearly address the issue that the observed residual activity of SiR in *sir1-1* is contributed by residual SiR protein rather than

anything else. Immunological detection of SiR protein carried out on crude protein from the leaves of soil-grown *sir1-1* and Col-0 plants indeed revealed the presence of small amount of SiR protein in *sir1-1* compared to Col-0 when equal amount of proteins were loaded on the gel (Fig. 19) in several independent experiments. Detection of residual SiR protein in *sir1-1* is correlated with the amount of observed expression and activity of SiR in *sir1-1*.

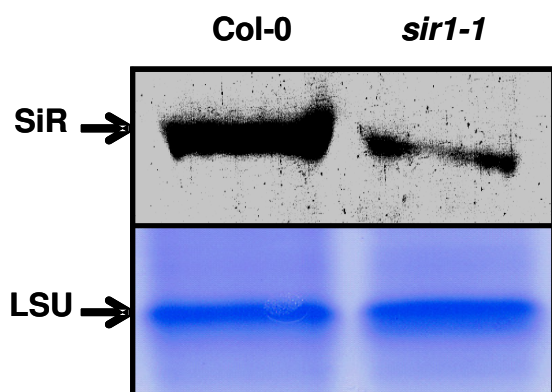


Fig. 19 Abundance of SiR protein in *sir1-1* plants

Immunoblot of soluble leaf proteins from seven weeks old soil-grown *sir1-1* and Col-0 plants with a polyclonal antiserum against SiR from Arabidopsis. Staining intensities of the large subunit of 1,5-bisphosphate carboxylase/oxygenase (LSU) of the same samples confirms equal loading in individual lanes.

3.3.4 Enzymatic activity and immunological detection of SAT and OAS-TL

Serine acetyltransferase (SAT; EC 2.3.1.30) is considered to be the rate-limiting enzyme in the biosynthesis of cysteine. SAT forms the activated thioester OAS from serine and acetyl-coenzyme A. Free sulfide is then incorporated into OAS to yield cysteine and acetate in a reaction catalyzed by *O*-acetylserine(thiol)lyase (OAS-TL; EC 4.2.99.8). To investigate the possible consequences of reduced SiR activity on the downstream enzymes, the activity of SAT and OAS-TL was assayed in *in vitro* assays (section 2.7.7.2 & 2.7.7.2). No significant differences in the activity of SAT and OAS-TL were observed in the leaves of *sir1-1* and Col-0 plants (Fig. 20A & B). Total enzymatic activity under saturating substrate concentrations describe the sum of activities of all isoforms of an enzyme. Immunological detection of SAT-3; which is the major isoform localized into the mitochondria, and of OAS-TL protein were carried out for further investigations using specific antibodies raised against SAT-3 and OAS-TLC. OAS-TLC antibody not only detects OAS-TLC protein but also allow the detection of two other important isoforms of OAS-TL, namely OAS-TLA and OAS-TLB. Like the activity assays, no significant differences were observed in the amount of SAT and OAS-TL proteins present in the leaves of soil grown *sir1-1* and Col-0 plants when equal

amounts of proteins were loaded on the gel (Fig. 20 C & D).

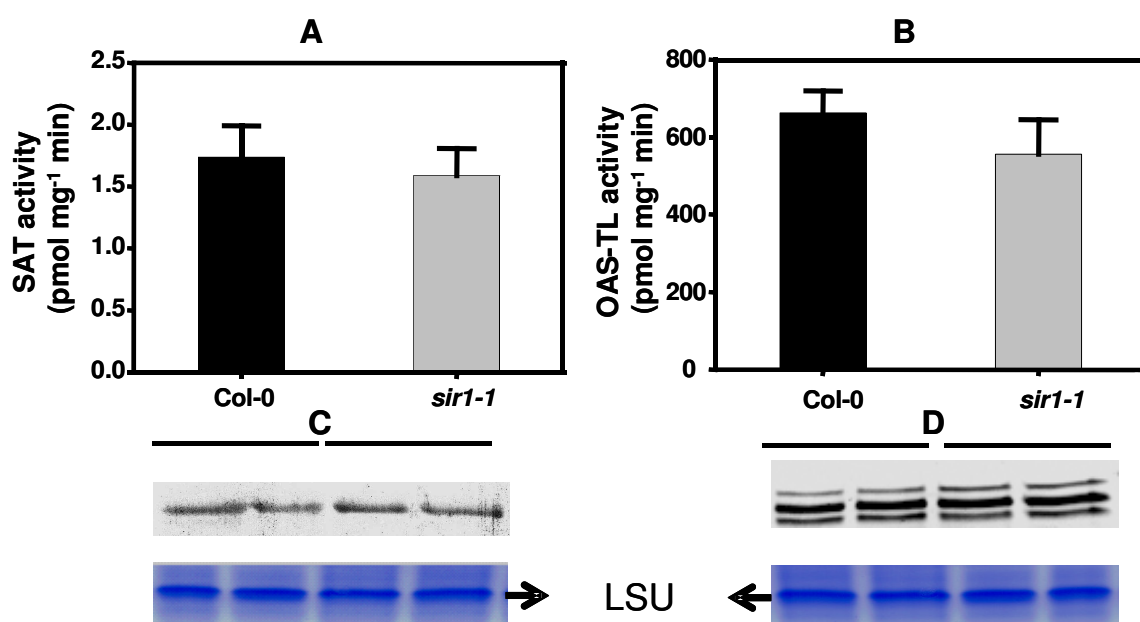


Fig. 20 Abundance and activity of SAT and OAS-TL in *sir1-1* plants

(A & B) Specific activity of SAT (A) and OAS-TL (B) in soluble protein extracts from leaves of seven weeks old soil-grown wild-type and *sir1-1* plants. (C) An immunoblot, loaded with soluble protein from two extractions of the leaves from wild-type and *sir1-1*, was analyzed with an AtSAT3 polyclonal antiserum. (D) Same experimental set up as in C, but a polyclonal antiserum against AtOAS-TLC was used, which also detects OAS-TLA and B via cross reaction. Staining of the large subunit of 1,5-bisphosphate carboxylase/oxygenase (LSU) with Coomassie confirms equal loading in individual lanes.

3.3.5 Enzymatic activity of sulfite oxidase

Sulfite is one of the natural intermediates produced during assimilatory sulfate reduction pathway. Sulfite ions (HSO_3^{1-} and SO_3^{2-}) are strong nucleophiles that can deleteriously react with a wide variety of cellular components affecting human and plant health (Wilson and Murray, 1990). In plants sulfite oxidase (EC; 1.8.3.1) plays an important role thereby oxidizing sulfite to the harmless compound sulfate. This enzyme has been shown to catalyze a two-electron transfer reaction in which the electron from sulfite are transferred via a molybdenum cofactor to molecular oxygen, yielding hydrogen peroxide and sulfate (Eilers et al., 2001; Hänsch et al., 2006). It has been speculated that the activity of sulfite oxidase is required to remove excess sulfite which accumulates under certain circumstances (Hänsch and Mendel, 2005). Under this assumption the significantly higher sulfite contents observed

3. Results

in the leaves of *sir1-1* (Fig. 11) were expected to result in a higher activity of sulfite oxidase. In order to verify this assumption the activity of sulfite oxidase in the leaves of hydroponically-grown plants was assayed in collaboration with R. Hänsch and R. Mendel (Univ. Braunschweig, Germany). As speculated the activity of sulfite oxidase was indeed found to be significantly higher in the leaves of *sir1-1* compared to Col-0 (Fig. 21). A strong increase of 2.4-fold in the activity of sulfite oxidase suggests that it plays an important role in the detoxification of sulfite which accumulates in the leaves of *sir1-1* due to reduced SiR activity.

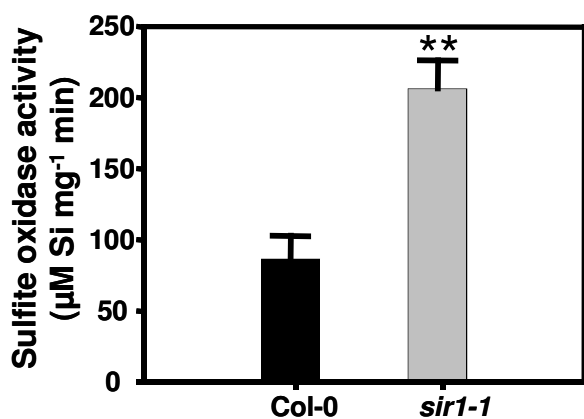


Fig. 21 The impact of reduced SiR activity on the activity of sulfite oxidase
The specific activity of sulfite oxidase was measured in the soluble protein extracts from leaves of hydroponically-grown homozygous *sir1-1* and Col-0 plants (n = 7). Mean ± standard deviations are shown. Asterisks indicate statistical significance (**, P < 0.001; *, P < 0.005)

3.4 impacts of chemical and genetic complementations on *sir1-1*

3.4.1 *sir1-1* can be partially complemented by GSH or sulfide

It has been shown in *Mycobacterium smegmatis* that mutation in the sulfite reductase gene Δ *sirA* makes this strain unable to grow on sulfite, however, replacement of sulfate in the medium by cysteine restored the normal growth with nitrite (Pinto et al., 2007). Following similar lines, the severely retarded-growth phenotype of the homozygous *sir1-1* plants due to reduced SiR activity was chemically complemented by the exogenous supply of the limiting product of SiR reaction, i.e. sulfide at a final concentration of 0.1 mM as Na₂S, in ½ Hoagland medium (section 2.5.2.3). Continuous supply of Na₂S in ½ Hoagland medium substantially, although not entirely, recovered the growth phenotype with significant gains in the total biomass of the homozygous *sir1-1* plants compared to homozygous *sir1-1* grown on the ½ Hoagland medium without Na₂S. Accordingly, glutathione, which represents the major cytoplasmic pool of low molecular weight reduced thiols with a range of metabolic

functions, was also found to result in similar chemical complementation as Na_2S , when exogenously supplied at a final concentration of 1mM GSH in its reduced form through modified $\frac{1}{2}$ Hoagland medium (Fig. 22). Both of these chemical compounds contain reduced S and result in significant recovery in the phenotype and total biomass of the chemically complemented homozygous *sir1-1* plants compared to untreated homozygous *sir1-1* plants.

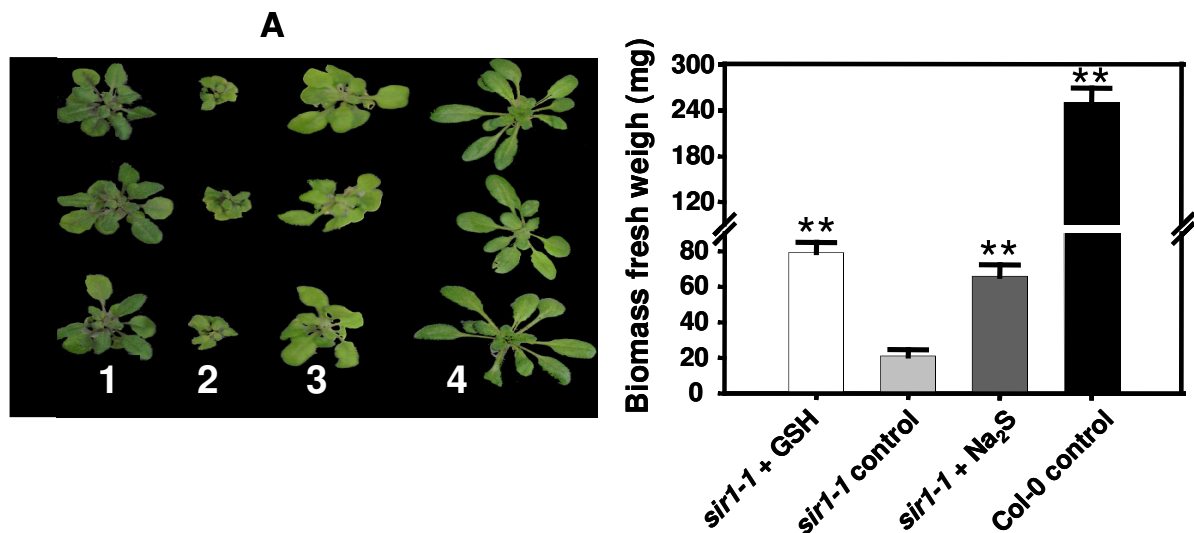


Fig. 22 Chemical complementation of *sir1-1* line

(A) Top view of hydroponically-grown untreated and chemically complemented plants. 1, 1mM GSH treated *sir1-1*; 2, untreated *sir1-1*; 3, 0.1 mM Na_2S treated *sir1-1*; and 4, wild-type plants. (B) Total biomass (FW aerial parts) of untreated Col-0, untreated *sir1-1*, and chemically complemented *sir1-1* plants (n = 5). Mean \pm standard deviations are shown. Asterisks indicate statistical significance (**, P < 0.001; *, P < 0.005)

The total shoot biomass of the homozygous *sir1-1* was increased on the average by approximately of 2- fold for 0.1 mM Na_2S and 2.7-fold for 1mM GSH compared to untreated *sir1-1* of the same age. However, the differences between chemically complemented homozygous *sir1-1* plants and Col-0 control plants were still significant (Fig. 22).

3.4.2 Genetic complementation of homozygous *sir1-1*

In order to provide a more direct proof about the essential role of SiR for the normal growth of the plants, the extremely slow growing *sir1-1* plants were stably transformed with an SiR

overexpression construct (Fig. 23A). The expression of the endogenous *SiR* (*AtSiR*) along with its plastid transit peptide in this construct was driven by the constitutive 35S promoter (section 2.9.4.1).

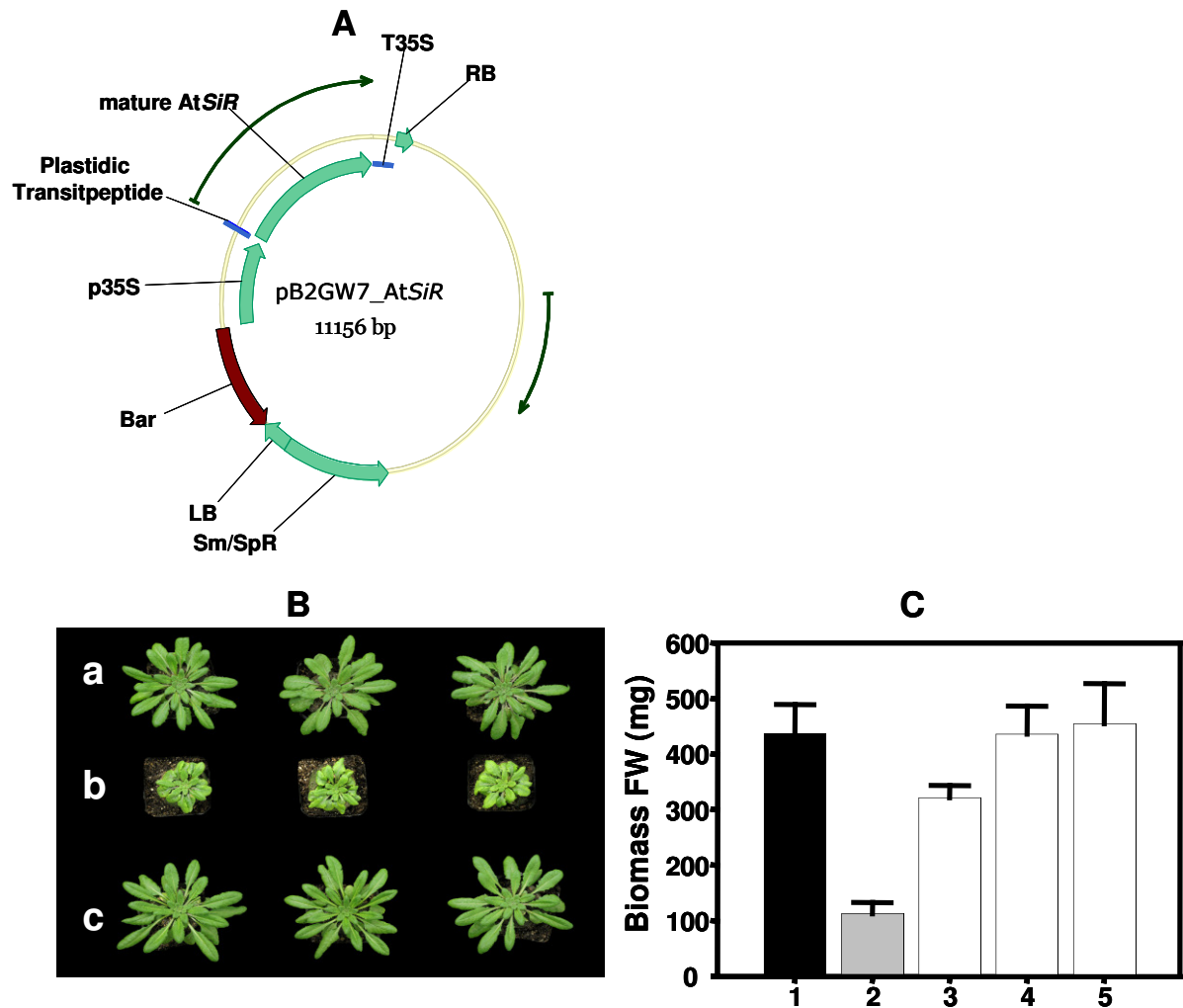


Fig. 23 Genetic complementation of *sir1-1* plants through overexpression of endogenous SiR. (A) The ORF of *AtSiR* along with its plastidic transit peptide was overexpressed under the control of constitutively expressed 35S promoter as described in the materials and methods. (B) Top view of seven weeks old soil-grown wild-type, *sir1-1*, and three independent genetically complemented *sir1-1* lines. (C) Fresh weight of seven weeks old soil-grown wild-type (Black), *sir1-1* (grey), and three independent genetically complemented *sir1-1* lines (white) ($n = 3-5$). Mean \pm standard deviations are shown.

Genetic transformation of homozygous *sir1-1* plants with this construct completely restored the severe phenotype of growth retardation (Fig. 23B). Complementation of *sir1-1* phenotype in the stably transformed independent T2 lines was followed by restoration of total biomass

to approximately the level of wild-type (Fig. 23C), indicating that the highly reduced activity of SiR in the *sir1-1* was the actual cause of the abnormal phenotype of the *sir1-1*. The construct that has been used for the genetic complementation of *sir1-1* was later on used as an overexpression construct for the production of overexpressor lines thereby stably transforming Col-0 plants.

3.4.3 SiR activity in genetically complemented *sir1-1* and SiR overexpressor lines

The activity of SiR in the genetically complemented and overexpressor lines were assayed to provide the evidence that SiR was functional in the stably transformed transgenic lines. A very high activity of SiR in genetically complemented lines (Fig. 24A), was according to expectations due to the construct used for transformation.

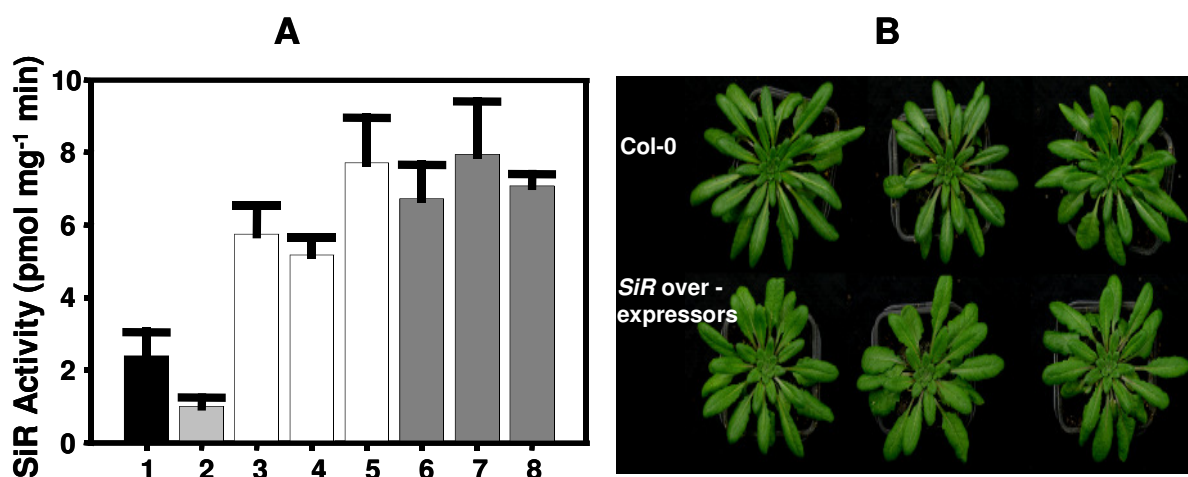


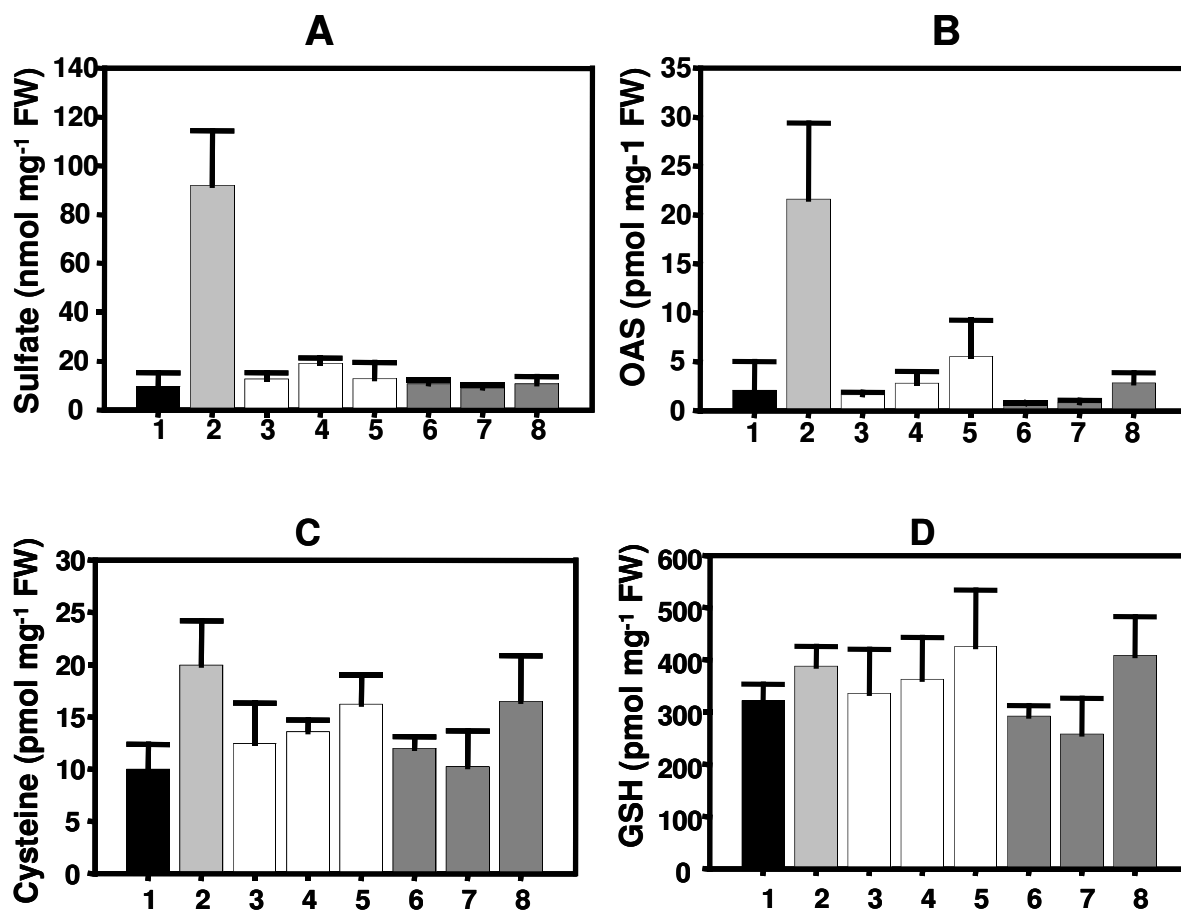
Fig. 24 The impact of overexpression of endogenous *SiR* on the activity of SiR and plant phenotype.

(A) The specific activity of SiR was determined in the soluble protein extracts from leaves of seven weeks old soil-grown plants. Black bar (1) represents Col-0; light grey bar (2) represents *sir1-1*; white bars (3-5) represent three independent genetically complemented *sir1-1* lines; and dark grey bars (6-8) represent three genetically independent *SiR* overexpressor lines ($n = 3-5$). Mean \pm standard deviations are shown. (B) Top view of the seven weeks old soil-grown Col-0 and three genetically independent *SiR* overexpressor lines

The activity of SiR in three independent genetically complemented lines was on the average approx. 2 to 3-fold higher than in Col-0. However, the differences in the activity of SiR between genetically complemented and overexpressor lines were not highly pronounced. Moreover, plants overexpressing SiR did not show any obvious phenotype compared to Col-0 (Fig. 24B).

3.4.4 Metabolite contents in genetically complemented *sir1-1* and *SiR* overexpressor lines

Reduced activity of SiR in the roots and leaves of *sir1-1* lead to an accumulation of sulfate as shown in (Fig. 12A & B). To test the consequences of the higher activity of SiR observed in the leaves of genetically complemented and overexpressor lines, total sulfate contents in the leaves were determined. The steady-state levels of cysteine in genetically complemented and overexpressor lines were found to be comparable to those of Col-0 in most cases as opposed to *sir1-1* which shows significantly higher steady-state levels of cysteine in their leaves (Fig. 25C) compared to Col-0. The pattern for GSH steady-state contents was similar to that observed for cysteine (Fig. 25D).



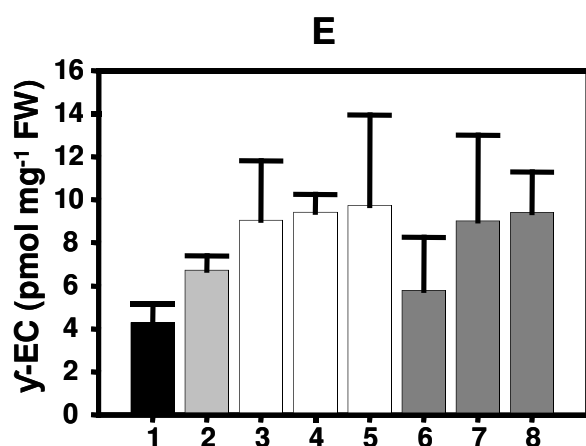


Fig. 25 The impact of reduced and increased SiR activity on the metabolism of plants

(A-E) Metabolites were extracted from leaves of seven weeks old soil-grown plants and quantified by HPLC (n = 3-5). Black bar (1) represents Col-0; light grey bar (2) represents *sir1-1*; white bars (3-5) represent three independent genetically complemented *sir1-1* lines; and dark grey bars (6-8) represent three genetically independent *SiR* overexpressor lines (n = 3-5). Mean \pm standard deviations are shown.

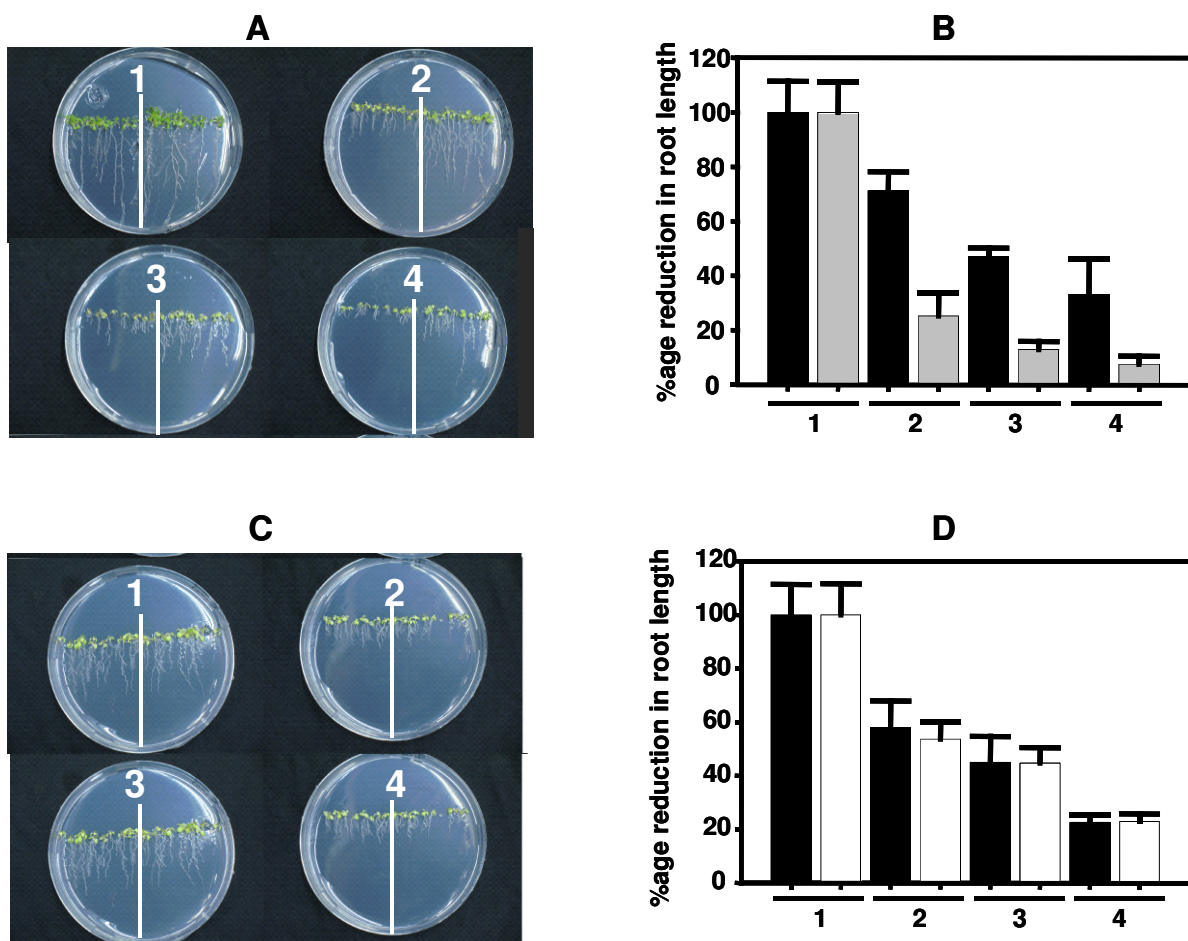
Like cysteine, total GSH contents in some of the overexpressor and genetically complemented lines were also slightly higher compared to Col-0, however on the average no dramatic changes in the steady-state contents of cysteine and GSH were observed. The steady-state levels of γ -EC however, presents a slightly different picture, where the behavior of the genetically complemented and overexpressor lines was more similar to *sir1-1* compared to Col-0 (Fig. 25E). Like the *sir1-1*, genetically complemented *sir1-1* and SiR overexpressor lines, on the average showed significantly elevated γ -EC levels in their leaves compared to Col-0.

3.4.5 Response of *sir1-1*, Col-0, genetically complemented and SiR overexpressor lines towards cadmium exposure

Glutathione takes part in detoxification of heavy metals as an immediate precursor of phytochelatins (PCs). It has been described that in the presence of heavy metal ions PCs are enzymatically synthesized from GSH by cytosolic phytochelatin synthase (Ha et al., 1999). PCs belong to the group of non-protein thiol-rich peptide with a general structure of (γ -Glu-Cys)_n-Gly (n=2-11), and their production is induced by a range of heavy metals, including cadmium (Grill et al., 1989). Reduced GSH has been reported previously to be related to metal stress in higher plants (Schäfer et al., 1998). As shown in the incorporation experiment with ³⁵S, the biosynthesis of GSH in the leaves of *sir1-1* was extremely reduced compared to Col-0 (Fig. 27B), in spite of its relatively higher steady-state levels (Fig. 9A). The highly reduced capacity of the *sir1-1* plants to synthesize GSH was expected to result in a higher sensitivity towards cadmium exposure. To test this hypothesis *sir1-1*, Col-0, genetically

3. Results

complemented *sir1-1* lines, and SiR overexpressor seedlings were exposed to various concentrations of cadmium, ranging from 0-100 μM CdCl_2 for 14 days. After documenting the phenotype of the seedlings, the root length of all these lines was measured. The root length of *sir1-1* seedlings was significantly reduced compared to Col-0 (Fig. 26A and B). The root length of Col-0 seedlings was also reduced upon CdCl_2 exposure, however, the magnitude of this reduction was significantly less compared to *sir1-1*. An average reduction of 75%, 87%, and 92% was observed in the root length of *sir1-1* seedlings upon 14 days exposure to 25 μM , 50 μM , and 100 μM CdCl_2 , respectively when compared to the root length of untreated *sir1-1* seedlings.



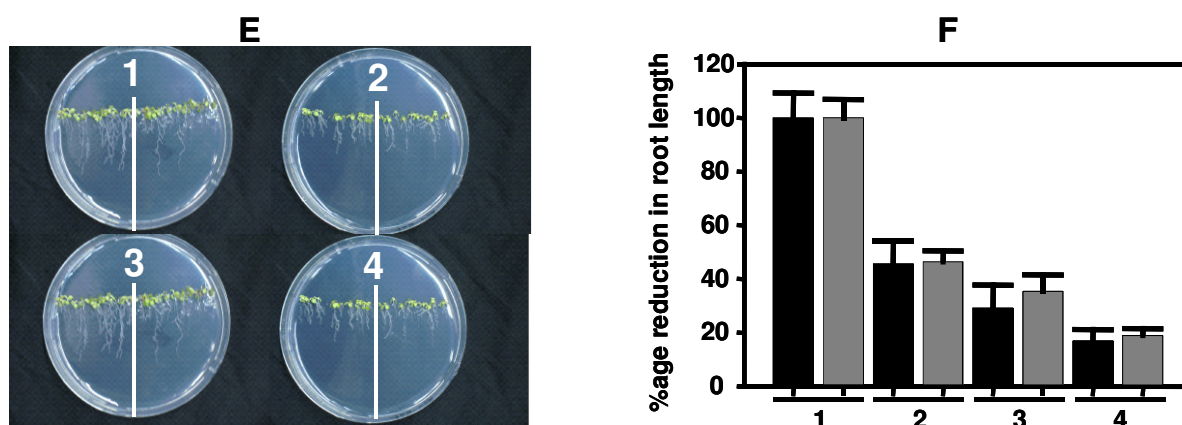


Fig. 26 The impact of reduced and increased SiR activity on the response of Arabidopsis plants towards cadmium stress

(A) *sir1-1* and Col-0 plants; (C) Col-0 and genetically complemented *sir1-1* plants; (E) Col-0 and *SiR* overexpressor plants. 1, untreated plants; 2, 25 μM CdCl₂; 3, 50 μM CdCl₂; 4, 100 μM CdCl₂. Right sides of A, C, and E contain Col-0 seedlings, whereas, left sides of the plates A, C, and E contain seedlings from *sir1-1*, genetically complemented *sir1-1* and *SiR* overexpressor seedlings, respectively. (B) Black bars represent root length of Col-0, whereas, light grey bars represent root length of *sir1-1* seedlings. (D) Black bars represent root length of Col-0, whereas, white bars represent root length of genetically complemented seedlings. (F) Black bars represent root length of Col-0, whereas, dark grey bars represent root length of *SiR* overexpressor seedlings (n = 6-10). Mean ± standard deviations are shown.

Similarly the magnitude of this reduction for Col-0 exposed for 14 days to 25 μM, 50 μM, and 100 μM CdCl₂ was 29%, 53%, and 67%, respectively when compared to the root length of untreated Col-0 seedlings. However, no significant differences in the roots lengths of Col-0, genetically complemented *sir1-1*, and *SiR* overexpressor lines were observed upon exposure to similar concentrations of CdCl₂ (Fig. 26D-F). The severe reduction in the root length of *sir1-1* seedlings underpinned the importance of the optimal SiR activity in carrying out the proper synthesis of thiols, which are then involved in the detoxification of heavy metals like cadmium.

3.5 *In vivo* experiments for determination of incorporation rates

3.5.1 Incorporation of the radioactively labeled sulfate into thiols

The higher steady-state levels of cysteine and GSH (Fig. 9) observed in *in vitro* experiments for the leaves of *sir1-1* compared to Col-0 were rather unexpected due to reduced SiR activity. In order to unravel the underlying fluxes of sulfur for assimilatory sulfate reduction

3. Results

into cysteine and GSH *in vivo*, feeding experiment were performed. In these experiments leaf pieces of similar sizes from the soil-grown Arabidopsis wild-type and homozygous *sir1-1* plants were floated on ½ Hoagland medium supplemented with radioactively labelled sulfate ($^{35}\text{SO}_4^{2-}$) to monitor the incorporation of the radiolabelled sulfate into Cys and GSH (section 2.8.1.1). For the determination of incorporation rates first set of sample was harvested after 15 min of incubation, whereas, the second set of sample was harvested after an additional 30 min chase on the medium without $^{35}\text{SO}_4^{2-}$. After extraction and derivatization, the respective fractions containing Cys and GSH were collected after separation by HPLC to quantify the amount of the incorporated ^{35}S label in these metabolites. Incorporation of the ^{35}S label into Cys and GSH after 15 and 45 min of incubation revealed a strong reduction in the biosynthesis of Cys and GSH in the leaves of homozygous *sir1-1* plants compared to Col-0 (Fig. 27). Taking together these values, an average reduction of approx. 12.4 and 25.6-fold in the incorporation of ^{35}S label into cysteine fraction of *sir1-1* leaves compared to Col-0 was observed after 15 and 45 minutes incubation, respectively, whereas, for GSH the magnitude of this reduction was 16.3 and 32.7-fold after 15 and 45 minutes, respectively. The incorporation rates of ^{35}S label into Cys and GSH in *sir1-1* plants clearly demonstrate the fact that the lack of sufficient SiR activity creates a bottle-neck in sulfate reduction.

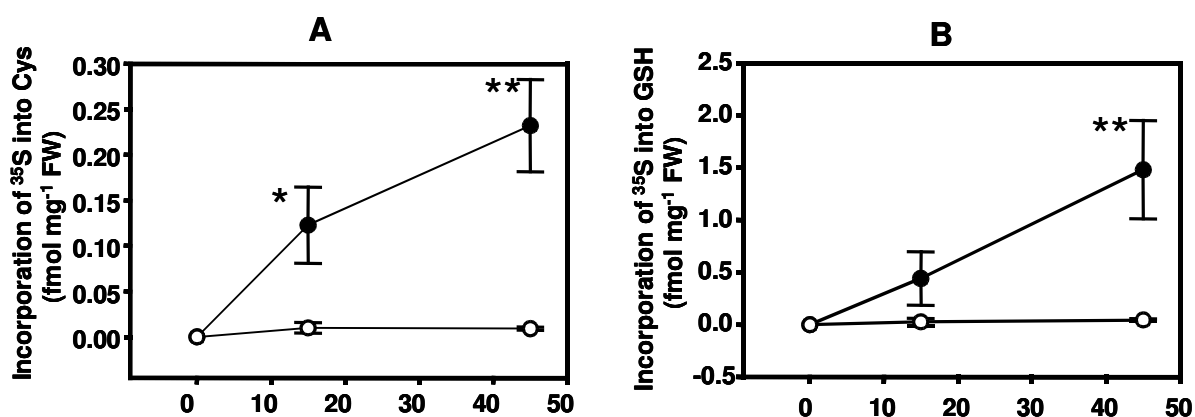


Fig. 27 Incorporation rates of sulfate in wild-type and *sir1-1* plants

Leaf pieces of seven weeks old soil-grown wild-type and *sir1-1* plants were incubated with $^{35}\text{SO}_4^{2-}$ -spiked ½ Hoagland medium for 15 min and subsequently kept on the same medium without radiolabel for 30 min. Samples were taken at indicated time points. (A) cysteine and (B) GSH were extracted and separated by HPLC. The incorporated ^{35}S -label was quantified by scintillation counting. FW, fresh weight. The mean \pm SD from 4 independent extractions of wild-type and *sir1-1* are shown. Asterisks indicate statistical significance

(**, $P < 0.001$; *, $P < 0.005$).

3.5.2 Incorporation of the radioactively labeled sulfate into protein

To know about the portion of the ^{35}S label that goes into the protein fraction, the same procedure for feeding was adopted as described for thiols in section 2.8.1.1, using leaf pieces from hydroponically grown *sir1-1* and Col-0 plants. Protein fractions from the radioactively fed leaf pieces were isolated from the pellets of the 0.1 M HCl extract (section 2.8.1.3). Incorporation of ^{35}S label into the protein fraction also revealed strong reduction in incorporation of the label into proteins of *sir1-1* leaves (Fig. 28). Under these conditions a tiny portion of the ^{35}S label went into protein fraction of *sir1-1* leaves. Taking together, an average reduction of approx. 11.4 and 17.8-fold in the incorporation of ^{35}S label into proteins fractions of *sir1-1* leaves compared to Col-0 was observed after 15 and 45 minutes incubation, respectively.

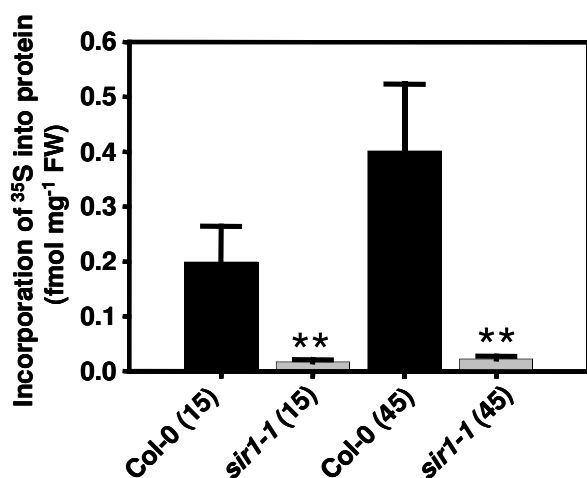


Fig. 28 Incorporation rates of sulfate in the proteins of wild-type and *sir1-1* plants

Leaf pieces of seven weeks old hydroponically-grown wild-type and *sir1-1* plants were incubated with $^{35}\text{SO}_4^{2-}$ -spiked $\frac{1}{2}$ Hoagland medium for 15 min and subsequently kept on the same medium without radiolabel for 30 min. Samples were taken at indicated time points. Proteins were extracted and separated by specific precipitation. The incorporated ^{35}S -label was quantified by scintillation counting. The incorporated ^{35}S -label was quantified by scintillation counting. The mean \pm SD from 4 independent extractions of wild-type and *sir1-1* are shown. Asterisks indicate statistical significance (**, $P < 0.001$; *, $P < 0.005$).

3.5.3 Incorporation of the ^3H serine into OAS and thiols

For this experiment leaf pieces of the seven weeks old hydroponically grown *sir1-1* and Col-0 plants were used. Like the $^{35}\text{SO}_4^{2-}$ feeding experiments, leaf pieces of comparable sizes were floated for 15 min and 30 min on ^3H labeled serine solution. Unlike the $^{35}\text{SO}_4^{2-}$ feeding experiments in which one set of sample was given a 30 min chase on the non-

3. Results

radioactive $\frac{1}{2}$ Hoagland medium after 15min of incubation, all set of samples in this experiment were incubated only on ^3H labelled serine solution. After extraction and derivatization the respective peaks of OAS, Cys and GSH were collected on the HPLC to quantify the amount of the incorporated ^3H label in these metabolites. Incorporation of the ^3H label into GSH after 15 and 45 min of incubation revealed a strong reduction in incorporation of the ^3H label into GSH in the leaves of homozygous *sir1-1* plants compared to Col-0 (Fig. 29). Taking together, an average reduction of approx. 3.4 and 2.3-fold in the incorporation of ^3H label into GSH was observed after 15 and 45 minutes incubation, respectively. After 15 minutes incubation, incorporation of the ^3H into cysteine was less in *sir1-1* compared to Col-0. In contrast to GSH where the steady-state of ^3H label was not reached after 30 minutes, cysteine appeared to have a much higher turnover under these conditions due to fact that the label showed no substantial increase after 15 minutes. Like cysteine, the steady-state of ^3H label into OAS also appeared to have reached after 15 minutes, as the label showed no further increase in Col-0 after this time point. However, in *sir1-1*, which maintains a higher steady-state level of OAS in its leaves (Fig. 10), steady-state of ^3H label into OAS was not reached after 15 minutes. In contrast to Col-0, leaves of *sir1-1* showed approx. 72% increase of the ^3H label into OAS.

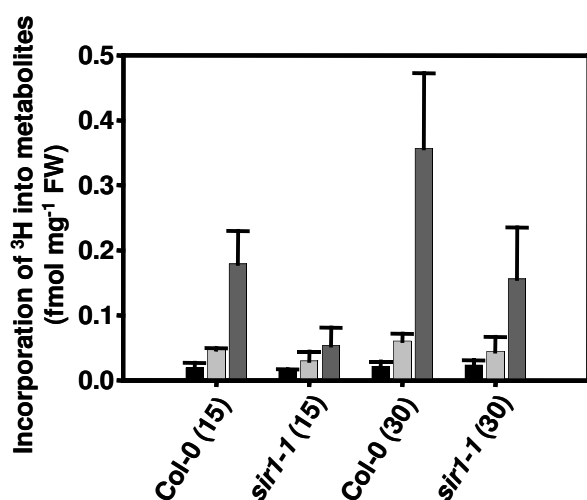


Fig. 29 Incorporation rates of ^3H -labelled serine in wild-type and *sir1-1* plants

Leaf pieces of seven weeks old hydroponically-grown wild-type and *sir1-1* plants were incubated with ^3H -labelled serine-spiked $\frac{1}{2}$ Hoagland medium for 15 or 30 min. Metabolites were extracted and separated by HPLC. The incorporated ^3H -label was quantified by scintillation counting. Black bars represent incorporation of ^3H into OAS, light grey bars represent incorporation of ^3H into cysteine, whereas, dark grey bars represent incorporation of ^3H into GSH fraction. The mean \pm SD from 4 independent extractions of wild-type and *sir1-1* are shown.

The comparable values observed for the incorporation of ^3H label into OAS and cysteine further suggest that *in vivo* the activities of the downstream enzymes, i.e SAT and OAS-TL are not dramatically changed, indicating that a different regulation mechanism might be in place in the downstream part of the pathway. The non-significant differences between *sir1-1*

and Col-0 observed in *in vitro* assays, immunoblot and microarray analysis of the major isoforms of SAT and OAS-TL (Fig. 20 & supplementary data 2) are in line with the current *in vivo* findings.

3.6 Sulfur metabolism in seeds

3.6.1 Determination of total carbon, nitrogen, sulfur and inorganic anions in the seeds

Analysis of the total carbon, nitrogen and sulfur contents in the seeds were carried out to monitor the consequences of reduced sulfide synthesis on the crucial balance of C, N, and S in the seed. As shown (Fig. 13) the C, N and S ratio in the leaves of *sir1-1* was significantly altered compared to Col-0 in a way that the total S was significantly higher in the leaves of *sir1-1* compared to Col-0, whereas, the total N and C was significantly reduced in *sir1-1*. However, analysis of the total total C, N and S contents in the seeds revealed that this does not hold true for the seeds. There were no significant differences in the total C, N, and S contents in the seeds of *sir1-1* and Col-0 (Fig. 30A). Previous data for the total sulfate contents showed accumulation of sulfate in the leaves (approx. 9-fold) of *sir1-1*, compared to Col-0 (Fig. 12A). However, in contrast to leaves, HPLC data showed no significant difference for the total sulfate and nitrate contents between the seeds of *sir1-1* and Col-0 (Fig. 30B).

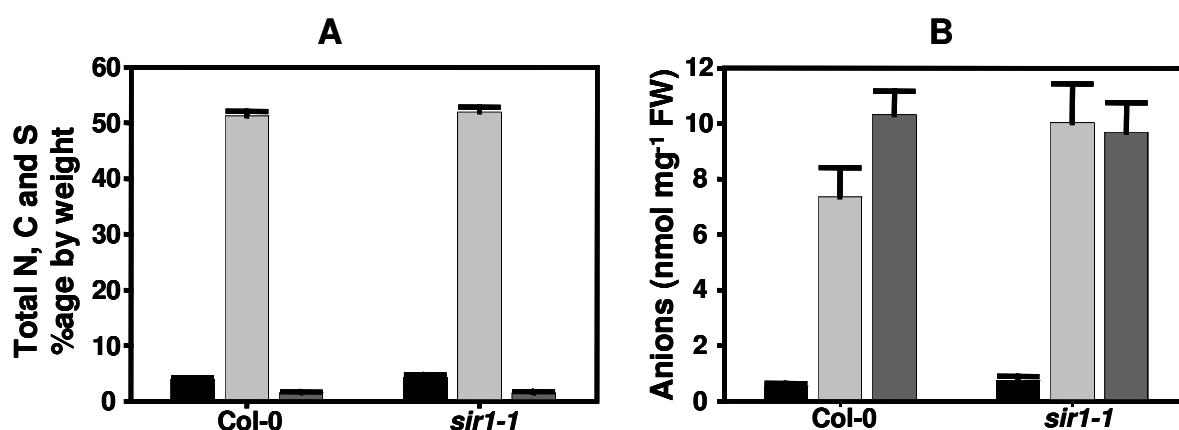


Fig. 30 The impact of reduced SiR activity on the inorganic anions and CNS contents in seeds

(A) Total contents of nitrogen (black bars), carbon (light grey bars), and sulfur (dark grey bars) were determined from mature seeds of soil-grown Col-0 and *sir1-1* plants. (B) Metabolites were extracted and

quantified by HPLC from same sample sets ($n = 5$). (B) Black bars represent nitrate, light grey bars represent phosphate, and dark grey bars represent sulfate. Mean \pm standard deviations are shown.

3.6.2 Glucosinolate, thiols and OAS contents in the seeds

Glucosinolates in mature seeds were determined in cooperation with M. Reichelt and J. Gershenzon, MPI Jena to see whether *sir1-1* and Col-0 show some differences in the leaves and seeds glucosinolate profile. In contrast to glucosinolate profile in the leaves where the *sir1-1* showed a decrease in most of the glucosinolates compared to Col-0 (Fig. 14), most of the glucosinolates in the seeds of *sir1-1* were either significantly higher or tended to be higher compared to Col-0 (Fig. 31A and B). Total glucosinolates in the seeds of *sir1-1* were significantly higher compared to Col-0.

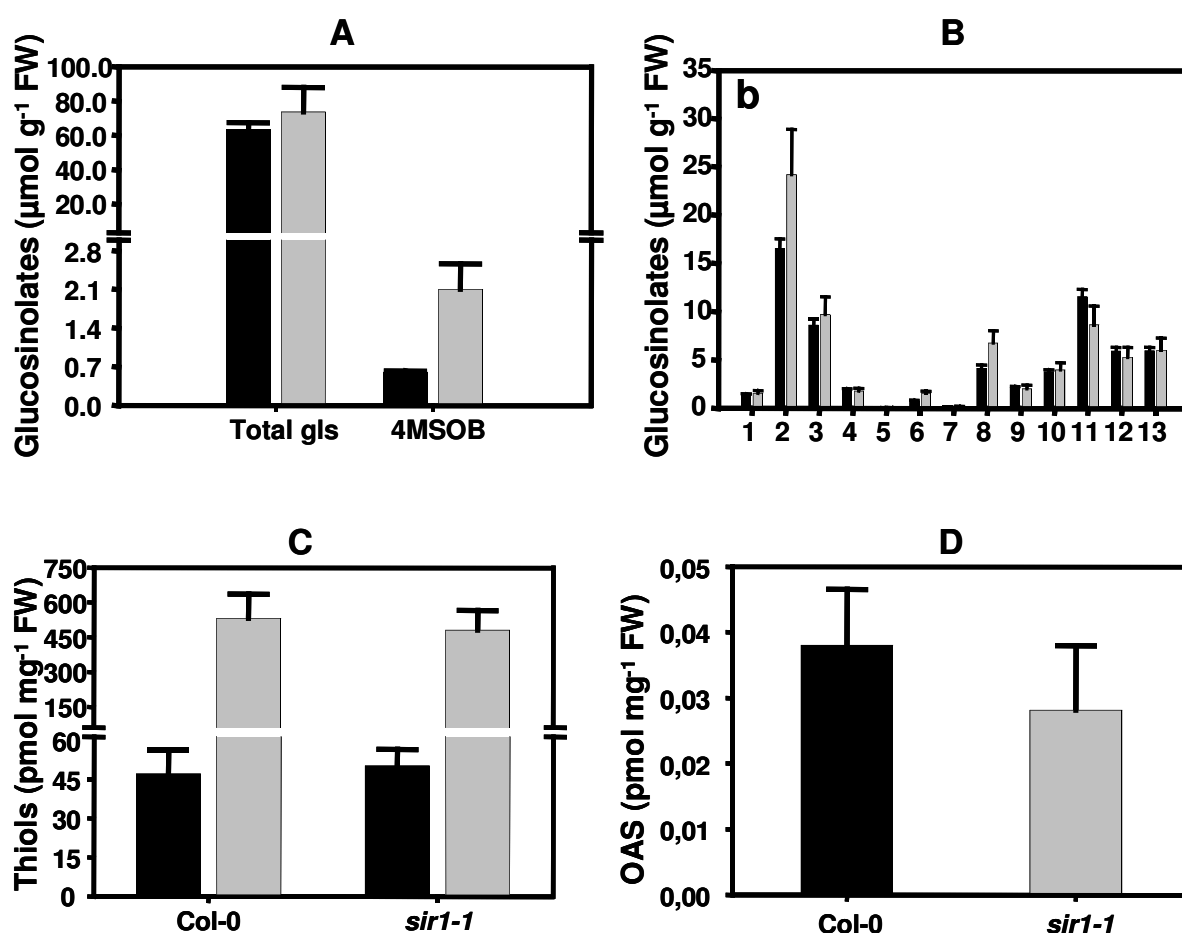


Fig. 31 The impact of reduced SiR activity on the primary and secondary metabolites in seeds

(A & B) Glucosinolates were extracted and quantified as described in the materials and methods from mature

seeds of soil-grown Col-0 and *sir1-1* plants. (C & D) Metabolites were extracted and quantified by HPLC from the same sample set (n = 5). Mean \pm standard deviations are shown. (A & B) Black bars represent glucosinolate contents in seeds of Col-0, whereas, light grey bars represent glucosinolate contents in the seeds of *sir1-1* plants. Total gls, total glucosinolate; 4MSOB, glucoraphanin; 1, glucoibarin; 2, glucoerucin; 3, glucohirsutin; 4, glucobrassicin; 5, glucoiberin; 6, 3-hydroxypropyl glucosinolate; 7, glucoalyssin; 8, 4-hydroxybutyl glucosinolate; 9, glucoberteroin; 10, glucomalcomiin; 11, 4-benzoyloxybutyl glucosinolate; 12, 7-methylthioheptyl glucosinolate; and 13, 8-methylthiooctyl glucosinolate.

Similarly among the individual glucosinolates, glucoraphanin, glucoerucin, 4-hydroxybutyl glucosinolate, and 3-hydroxypropyl glucosinolate were found to be significantly higher in the seeds of *sir1-1* compared to Col-0. Moreover, Arabidopsis seeds were in general quite rich in glucosinolates compared to leaves. The significant perturbations of cysteine and GSH contents in leaves (Fig. 9) of *sir1-1* was a characteristic response towards reduced SiR activity. In addition to that it also shows that the optimal activity of SiR was absolutely necessary for maintaining a proper balance of the primary and secondary metabolites in the leaves. To investigate the role of sulfite reductase in seeds with respect to primary sulfur containing metabolites, total cysteine and GSH contents in the seeds of *sir1-1* and Col-0 were determined. Analysis of the total cysteine and GSH contents revealed no significant difference between the seeds of *sir1-1* and Col-0 plants (Fig. 31C). Moreover, HPLC analysis for determination of OAS contents in the seeds of *sir1-1* and Col-0 revealed no significant difference between Col-0 and *sir1-1* seeds (Fig. 31D).

3.7 Transcriptional analysis of sulfur metabolism related genes in *sir1-1* and Col-0

3.7.1 Impact of reduced sulfide synthesis on the expression of sulfur metabolism related genes in the leaves of *sir1-1*

The impact of reduced SiR activity on the transcription of the selected sulfur metabolism-related genes was investigated with a microarray. The array contains 920 selected genes, designed for detection of even small changes in the mRNA abundance as is often observed with the genes of primary sulfur metabolism. Sixty different genes with different expression intensity by robust constitutive pattern according to Czechowski et al. (2005) were included to optimize the evaluation of all genes. The array contains all the genes of sulfur metabolism and key regulatory genes of other metabolic pathways as well as stress response, redox

3. Results

homeostasis, hormone metabolism and membrane transport were included in the array. In addition, 152 candidate genes, previously reported to be regulated in response to sulfur availability were also included (Hirai et al., 2003; Higashi et al., 2006; Maruyama-Nakashita et al., 2006). Based on three biological repetitions of wild-type and *sir1-1* with four technical replicates, each including dye-swaps for each set, 67 genes were found to be significantly up or Down-regulated in the leaves of hydroponically-grown *sir1-1* plants compared to Col-0 according to p-values of lower than 0.05 (supplemental data 2). Most of the significantly regulated genes (20) were related to redox-homeostasis, whereas, genes of sulfur metabolism (11), pathogen resistance (11), glucosinolate synthesis (10), hormone related (5), GSH transfer activity (4), sulfur induced (3), and amino acid synthesis (3) were also found to be significantly changed in abundance. Microarray analysis of *sir1-1* confirmed the specificity and extent of down-regulation of SiR expression that had been previously observed by semi-quantitative RT-PCR (Fig. 7).

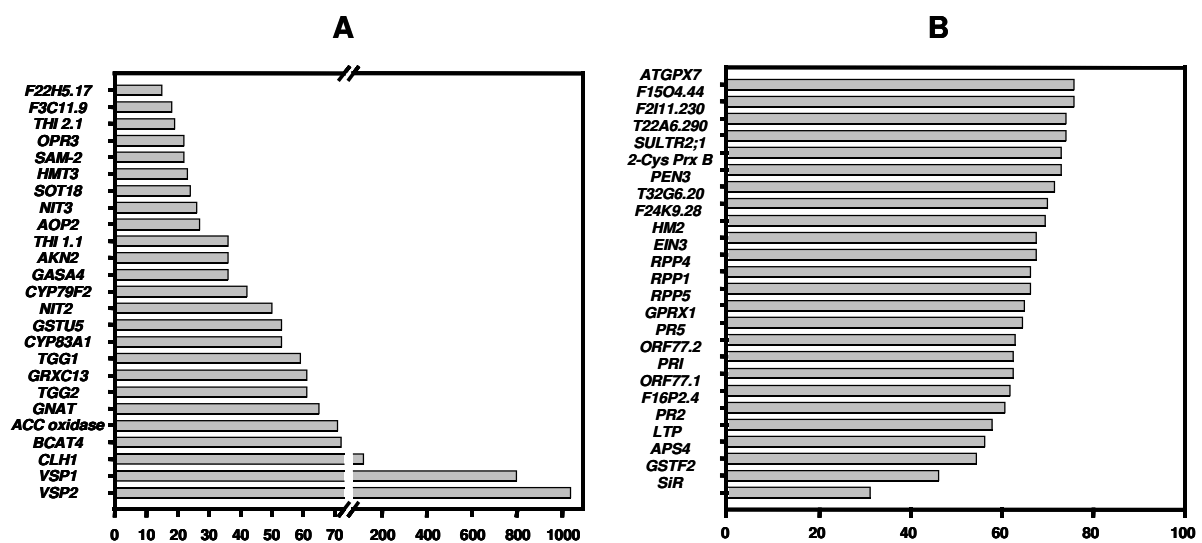


Fig. 32 The impact of reduced SiR activity on the expression of sulfur metabolism-related genes in the leaves

Total mRNA was extracted from the leaves of seven weeks old hydroponically-grown Col-0 and *sir1-1* plants. (A) significantly up-regulated genes ($P < 0.05$). *VSP2*, vegetative storage protein 2; *VSP1*, vegetative storage protein 1; *CLH1*, chlorophyllase 1 or coronatine-induced protein 1; *BCAT4*, branched-chain aminotransferase4; *ACC oxidase*, 1-aminocyclopropane-1-carboxylate oxidase; *GNAT*, GCN5-related N-acetyltransferase family protein; *TGG2*, glucoside glucohydrolase 2 (myrosinase); *GRXC13*, glutaredoxin, *TGG1*, glucoside glucohydrolase 1 (myrosinase); *CYP83A1*, cytochrome P450 83A1; *GSTU5*, *Arabidopsis thaliana* glutathione s-transferase tau 5; *NIT2*, nitrilase 2; *CYP79F2*, cytochrome p450 79f2; *GASA4*, gast1 protein homolog 4; *AKN2*, APS-kinase 2; *THI 1.1*, thionin; *AOP2*, alkenyl hydroxalkyl producing 2; *NIT3*, nitrilase 3; *SOT18*, sulfotransferase 18, *HMT3*, homocysteine S-methyltransferase (HMT3); *SAM-2*, s-adenosylmethionine synthetase 2; *OPR3*, opda reductase 3; *THI 2.1*, thionin 2.1; *F3C11.9*, GDSL-motif lipase/hydrolase family protein; *F22H5.17*, isoflavone reductase. (B) significantly down-regulated genes ($P < 0.05$). *SiR*, sulfite

3. Results

reductase; *GSTF2*, glutathione s-transferase phi 2; *APS4*, ATP sulfurylase 4; *LTP*, similar to lipid transfer protein; *PR2*, pathogenesis-related protein 2; *F16P2.4*, Zinc finger family protein; *ORF77.1*, hypothetical protein of chloroplast genome; *PR1*, pathogenesis-related protein 1; *ORF77.2*, hypothetical protein of chloroplast genome; *PR5*, pathogenesis-related protein 5; *GPRX1*, glutathione peroxidase 1; *RPP5*, recognition of *Peronospora parasitica* 5; *RPP1*, recognition of *Peronospora parasitica* 1; *RPP4*, recognition of *Peronospora parasitica* 4; *EIN3*, ethylene-insensitive 3; *HM2*, chloroplast localized thioredoxin; *F24K9.28*, 2-cys peroxyredoxin; *T32G6.20*, encodes a NADPH thioredoxin reductase; *PEN3*, penetration3; *2-Cys Prx B*, 2-Cysteine peroxiredoxin B; *Sultr2;1*, sulfate transporter 2;1; *T22A6.290*, unknown protein; *F2111.230*, GCN5-related N-acetyltransferase (GNAT) family protein; *F15O4.44*, pseudogene of isochorismate synthase-related; *ATGPX7*, glutathione peroxidase 7

Among the up-regulated genes the expression of two vegetative storage proteins (*VSP1*) genes, i.e. *VSP1* (At5g24780) and *VSP2* (At5g24770), was increased by approximately 9 and 11-fold, respectively in the leaves of *sir1-1* compared to Col-0 (Fig 32A). Currently, VSPs are thought to serve as transient reserve that sequester surplus amino acids during plant development in various vegetative storage organs. The expression of thioglucoside glucohydrolase 1 (*TGG1*) and thioglucoside glucohydrolase 2 (*TGG2*), the two known functional myrosinases in Arabidopsis, was also significantly up-regulated in the leaves of *sir1-1* compared to Col-0. The sulfur starvation inducible nitrilase 3 (*NIT3*) (Kutz et al., 2002), involved in the biosynthesis of indole-3-acetic acid (IAA), was also slightly up-regulated together with nitrilase 2 (*NIT2*) in the leaves of *sir1-1*. The expression of chlorophyllase 1 (*CLH1*), involved in chlorophyll degradation, was also strongly induced in the leaves of *sir1-1* compared to Col-0. Among the significantly regulated genes, the expression of ATP sulfurylase 4 (*APS4*) was significantly down-regulated in the leaves of *sir1-1* (Fig. 32B). In addition the expression of APS reductase 2 (*APR2*) was also found to be slightly down in the leaves of *sir1-1* (Supplemental data 2). Many of the pathogenesis related genes such as pathogenesis-related gene 1 (*PR1*), pathogenesis-related gene 2 (*PR2*), pathogenesis-related gene 5 (*PR5*), recognition of *Peronospora parasitica* 1 (*RPP1*), recognition of *Peronospora parasitica* 4 (*RPP4*), recognition of *Peronospora parasitica* 5 (*RPP5*), ethylene-insensitive 3 (*EIN3*), and penetration 3 (*PEN3*) were significantly down-regulated in the leaves of *sir1-1*. Apart from that a large number (15) of genes related to redox homeostasis were also down-regulated in the leaves of *sir1-1*.

3.7.2 Impact of reduced sulfide synthesis on the expression of sulfur metabolism related genes in the roots of *sir1-1*

The impact of reduced sulfide synthesis on the transcription of the selected sulfur

3. Results

metabolism-related was investigated with the same array as described in previous section. Based on three biological repetitions of wild-type and *sir1-1* with four technical replicates, each including dye-swaps for each set, a large number of genes (180) compared to leaves (67) were significantly up or down-regulated in the roots of *sir1-1* compared to Col-0 (supplemental data 3). The high affinity sulfate transporters, sulfate transporter 1;1 (*SULTR1;1*) and sulfate transporter 1;2 (*SULTR1;2*) were strongly up-regulated in the roots of *sir1-1* compared to Col-0 (Fig. 33A). Moreover, two group 4 sulfate transporters i.e. sulfate transporter 4;1 (*SULTR4;1*) and sulfate transporter 4;2 (*SULTR4;2*) were also significantly up-regulated in the roots of *sir1-1* compared to Col-0. Contrary to the slight down-regulation of *APR2* in the leaves of *sir1-1* (supplemental data 2), the expression of *APR1*, *APR2*, and *APR3* was rather up-regulated in the roots of *sir1-1* compared to Col-0. On the other hand, the expression ATP sulfurylase 1 (*APS1*), ATP sulfurylase 2 (*APS2*), and ATP sulfurylase 4 (*APS4*) was down-regulated in the roots of *sir1-1* (Fig. 33B). Like the leaves, many of the pathogen related genes *PR5*, *RPP1*, *RPP4*, *RPP5*, ethylene-insensitive 3 (*EIN3*), and penetration 3 (*PEN3*) were significantly Down-regulated in the roots of *sir1-1* (Fig 33B & supplemental data 3). Similar to the leaves of *sir1-1*, a large number (31) of genes related to redox homeostasis were also down-regulated in the roots of *sir1-1*.

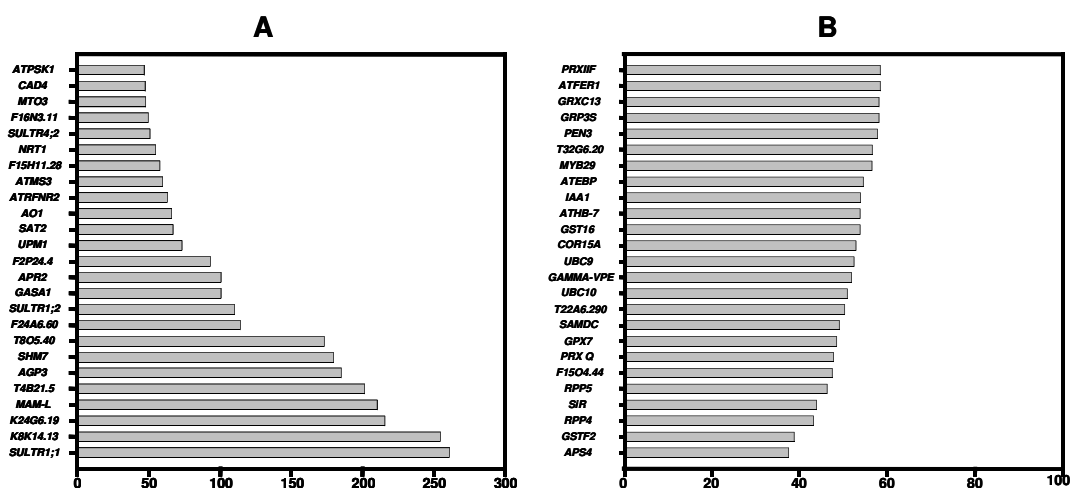


Fig. 33 The impact of reduced SiR activity on the expression of sulfur metabolism-related genes in the roots

Total mRNA was extracted from the roots of seven weeks old hydroponically-grown Col-0 and *sir1-1* plants. (A) significantly up-regulated genes ($P < 0.05$). *SULTR1;1*, sulfate transporter 1;1; *K8K14.13*, peroxidase 73; *K24G6.19*, male sterility MS5 family protein; *MAM-L*, methylthioalkymalate synthase-like; *T4B21.5*, methionine sulfoxide reductase; *AGP3*, arabinogalactan-protein 3; *SHM7*, serine hydroxymethyltransferase 7; *T8O5.40*, methionine sulfoxide reductase domain-containing protein; *F24A6.60*, similar to transporter; *SULTR1;2*, sulfate transporter 1;2; *GASA1*, gast1 protein homolog 1; *APR2*, 5'adenylylphosphosulfate

reductase 2; *F2P24.4*, similar to 1-aminocyclopropane-1-carboxylate oxidase; *UPM1*, uroporphyrin methylase 1; *SAT2*, serine acetyltransferase 2; *AO1*, aldehyde oxidase 1; *ATRFNR2*, root fnr 2; *ATMS3*, methionine synthase 3; *F15H11.28*, Bet v I allergen family protein; *NRT1*, nitrate transporter 1; *SULTR4;2*, sulfate transporter 4;2; *F16N3.11*, similar to glycosyl hydrolase family 1 protein; *MTO3*, methionine over-accumulator 3; *CAD4*, cinnamyl alcohol dehydrogenase 4; *ATPSK1*, phytoalkaline 1 precursor (B) significantly down-regulated genes ($P < 0.05$). *APS4*, ATP sulfurylase 4; *GSTF2*, glutathione s-transferase phi 2; *RPP4*, recognition of peronospora parasitica 4; *SiR*, sulfite reductase; *RPP5*, recognition of peronospora parasitica 5; *F15O4.44*, pseudogene of isochorismate synthase-related; *PRX Q*, periredoxin Q; *GPX7*, glutathione peroxidase 7; *SAMDC*, s-adenosylmethionine decarboxylase; *T22A6.290*, unknown protein; *UBC10*, ubiquitin-conjugating enzyme 10; *GAMMA-VPE*, gamma vacuolar processing enzyme; *UBC9*, ubiquitin-conjugating enzyme 9; *COR15A*, cold-regulated 15A; *GSTI6*, glutathione s-transferase 16; *ATHB-7*, Arabidopsis thaliana homeobox 7; *IAA1*, indole-3-acetic acid inducible; *ATEBP*, ethylene-responsive element binding protein; *MYB29*, myb domain protein 29; *T32G6.20*, encodes a NADPH thioredoxin reductase; *PEN3*, penetration3; *GRP3S*, glycine-rich protein 3 short isoform; *GRXC13*, glutaredoxin; *ATFER1*, encodes a ferritin protein; *PRXIIIF*, peroxiredoxin IIF

3.8 Sulfur and selenium (Se) uneven twins in plant metabolism

3.8.1 Selenite and selenate treatment increase total sulfur contents in Arabidopsis

Selenium is a group (V1A) element with chemical properties similar to sulfur (Broadley et al., 2006; White et al., 2007). Due to similar chemical properties selenium and sulfur are thought to share the initial steps for uptake and assimilation. Keeping into account this consideration, SeO_4^{2-} , which enter roots cells through high affinity sulfate transporters (White et al., 2004), is therefore expected to compete with sulfate for the initial steps of uptake and assimilation. Serine acetyltransferase (SAT) and selenocysteine methyltransferase (SMT) overexpressor lines along with their respective empty vector control line, tested in these experiments, were kindly provided by Professor David Salt, Purdue University, West Lafayette, USA. Selenium hyperaccumulation in eight *Astragalus* species with varying abilities to accumulate selenium, has been found to positively correlate to the level of SMT enzymatic activity (Sors et al., 2005b). Overexpression of SAT in transgenic *Arabidopsis thaliana* has been shown to cause a slight increase in selenate reduction to organic forms (Sors et al., 2005b).

The response of different *Arabidopsis* lines towards selenium fertilization was determined by exposing six weeks old hydroponically-grown plants to 50 μM sodium selenite or sodium selenate for one week. ICP analysis carried out in collaboration with Ute Krämer (Bioquant, University of Heidelberg), revealed a significant increase in the total sulfur contents in the leaves of *Arabidopsis* plants upon selenate treatment compared to untreated plants (Fig. 34).

Apart from the empty vector control line selenite treatment tend to increase total sulfur contents in the leaves of all other tested Arabidopsis lines.

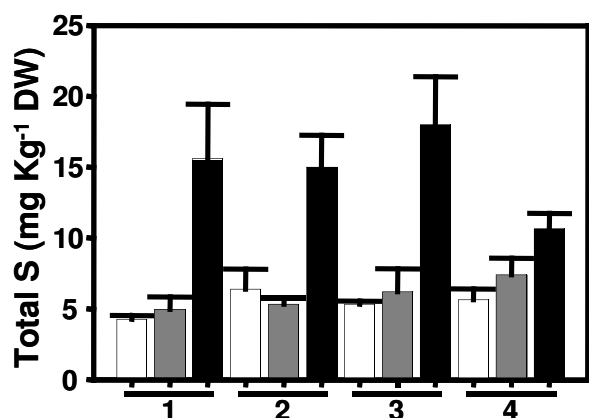


Fig. 34 The response of different Arabidopsis lines towards selenium fertilization

Total sulfur (S) contents in the leaves of seven weeks old hydroponically-grown plants were determined by ICP analysis. 1, Col-0; 2, Empty vector control line for SAT and SMT overexpressor lines; 3, SAT overexpressor line; and 4, SMT overexpressor line. White bars represent control (untreated) plants of respective lines, grey bars represent plants treated with 50 μM SeO₃, and black bars represent plants treated with 50 μM SeO₄. The mean ± SD from 4 independent biological samples are shown.

3.8.2 Selenite and selenate treatment increase total selenium contents in Arabidopsis

The response of the same Arabidopsis lines towards selenium fertilization in terms of total Se contents was determined in 50 μM sodium selenite or sodium selenate treated plants as described in previous section. ICP analysis revealed a significant increase in the total Se contents in the leaves of Arabidopsis plants upon selenate treatment compared to untreated plants (Fig. 35). Like the total S contents the increase in total Se contents of the selenite treated plants was not highly pronounced compared to selenate treated plants. The strong increase in Se in selenate treated plants compared to untreated plants is presumably due higher selenate contents in these plants, since selenate treatment in the same Arabidopsis lines has previously been shown to result in sulfate accumulation in their leaves (Peter, 2007). An up-regulation of the high affinity root sulfate transporters would therefore, not only increase the uptake of sulfate but also of selenate, thereby, causing an increase in the total S and Se. However, unexpectedly plants of the SMT overexpressor line did not show any increase in total Se contents upon selenite or selenate treatment. This might be explained if Se is assumed to be present only or mainly in its organic form, which might represent a small fraction of the total Se pool in the leaves of SMT overexpressor plants.

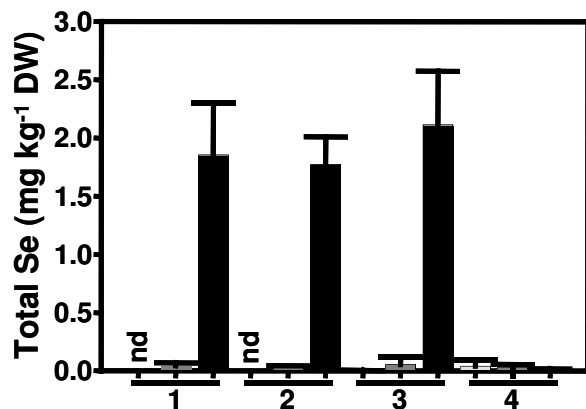


Fig. 35 The response of different *Arabidopsis* lines towards selenium fertilization

Total selenium (Se) contents in the leaves of seven weeks old hydroponically-grown plants were determined by ICP analysis. 1, Col-0; 2, Empty vector control line for SAT and SMT overexpressor lines; 3, SAT overexpressor line; 4, SMT overexpressor line; and nd, not detectable. White bars represent control (untreated) plants of respective lines, grey bars represent plants treated with 50 μM SeO₃, black bars represent plants treated with 50 μM SeO₄, and nd means not detectable. The mean ± SD from 4 independent biological samples are shown.

3.9 Isolation and characterization of a 2nd T-DNA insertion line for *SiR*

A second T-DNA *Arabidopsis* line containing a T-DNA insertion in *AtSiR* became available during the last part of PhD project in the GABI-Kat T-DNA collection (727B08). According to the sequence data found in the database (<http://www.gabi-kat.de/db/showseq.php?line=727B08&gene=At5g04590>) the insertion in this line was predicted in the promoter region of *AtSiR* (Fig. 36). This line was also in the Col-0 background and was further annotated as *sir1-2*. Homozygous plants for this insertion were isolated through genomic DNA PCR screening using two gene-specific primers binding up and downstream of the predicted insertion in combination with a primer binding to the left border region of the T-DNA (Fig. 37)

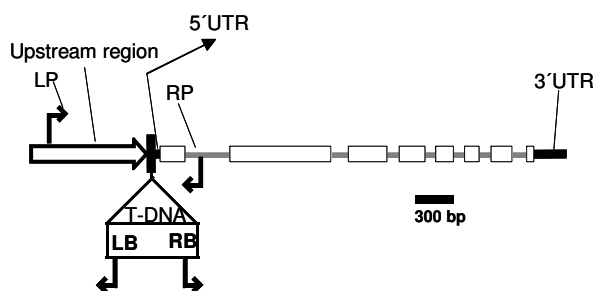


Fig. 36 Structure of *AtSiR* gene with the predicted T-DNA insertion site in *sir1-2*

Exons are indicated in white boxes, untranslated regions by black boxes, and primers for the genetic characterization by small arrows. The putative promoter is marked by a white arrow.

3.9.1 Characterization of T-DNA insertion in *sir1-2*

Flanking sequences of the T-DNA were PCR amplified and sequenced to thoroughly characterize the insertion sites in the *sir1-1* line. Sequence analysis of a 600 bps PCR

product, obtained with primers P1 and P4 (Fig. 37) showed exact position of the beginning of the left border (LB) of the insertion in the promoter region of *AtSiR* gene. To characterize the right border (RB) of the T-DNA, PCR reaction was performed using T-DNA specific RB-primer (P7) in combination with a downstream primer binding to *SiR* gene (P2). Alignment of the PCR amplified sequences with the genomic sequence of the sulfite reductase gene revealed the beginning of the left and right border of insertion at position -54 bp and -53 bp, respectively before translational start (ATG) codon in the genomic sequence of *SiR* gene. Sequence alignment data of the T-DNA and gene specific primers with the genomic sequence of *SiR*, showing the exact position of the T-DNA insertion in *sir1-2* is shown in supplemental data 4 A and B.

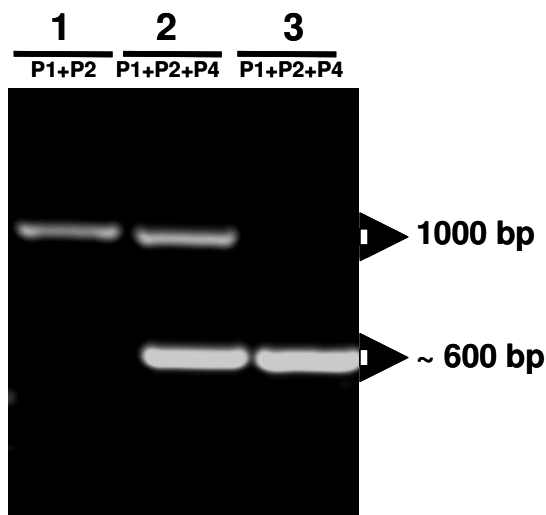


Fig. 37 Genomic characterization of *sir1-2* plants.

Genomic DNA was extracted from wild-type (1), heterozygous (2), and homozygous (3) *sir1-2* seedlings and tested for the presence of T-DNA insertion allele by PCR. The lack of the wild-type allele specific product in 3 demonstrated that the seedlings were homozygous for the T-DNA insertion.

3.9.2 *sir1-2* contains a single insertion

In order to screen the seedlings for the presence or absence of the T-DNA, seeds obtained from PCR verified heterozygous *sir1-2* plants were plated on solid Arabidopsis media (section 2.5.2.4) without any selection marker. Growth observation of the seedlings on solid Arabidopsis media revealed two distinct classes of seedlings, (i) wild-type seedlings and (ii) bleached seedlings that died 2-3 weeks after germination. Extraction of the genomic DNA from these seedlings and subsequent PCR analysis (Fig. 37) revealed that the bleached seedlings that died soon after germination were homozygous for the T-DNA insertion. The question of the single or multiple T-DNA insertions was addressed by plating seeds of PCR verified heterozygous plants on solid Arabidopsis media without any selection marker. The

seedlings lethal phenotype of the homozygous *sir1-2* seedlings make them easily distinguishable from wild-type and heterozygous *sir1-2* seedlings (Fig. 38), and facilitated an easy and rapid screening. Like *sir1-1* mutant, approximately $\frac{1}{4}$ (132/533) of the seedlings were found to be lethal which according to Mendelian laws fit to the expected 1:3 ratio of self-fertilized heterozygous plant's progeny with a single recessive allele, hinting at the absence of a second allele causing a similar phenotype.

3.9.3 Phenotype of homozygous *sir1-2* seedlings

The homozygous plants for the T-DNA insertion at this position were seedlings lethal (Figure 38). Homozygous seeds were able to germinate and develop seedlings, however, these seedlings were not able to grow further and therefore, bleached and died at 2-leaf stage 2-3 weeks after germination. None of homozygous seedlings was able to develop into a four-leaves or multiple-leaves stage when grown on the standard Arabidopsis media.

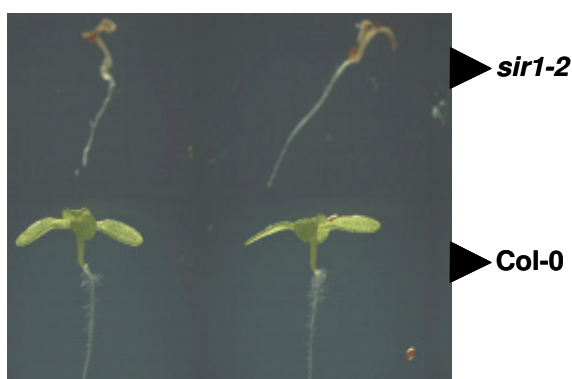


Fig. 38 Growth phenotype of homozygous *sir1-2* seedlings.

Seedlings were grown on solid Arabidopsis medium for 4 weeks. The homozygous *sir1-2* seedlings die 2-3 weeks after germination. The homozygosity of the dying *sir1-2* seedlings was confirmed through PCR analysis.

3.9.4 Transcription analysis

As SiR is encoded by a single-copy gene in Arabidopsis, seedlings lethal phenotype of the of the homozygous *sir1-2* was therefore, expected to have no expression of *SiR* wild-type gene. However, quite surprisingly, transcription analysis of homozygous *sir1-2* and Col-0 seedlings, using gene specific primers for wild-type *SiR* (*AtSiR*) gene expression and primers for constitutively expressed actin 7 (*AtACT7*) as a control, revealed residual *SiR* expression for homozygous *sir1-2* (Fig. 39). However, unlike *sir1-1* the residual expression of *SiR* in *sir1-2* was not able to result viable plants when germinated on standard Arabidopsis media.

In contrast to *sir1-1*, the extent of activity derived from residual expression of *SiR* in homozygous *sir1-2* seedlings seems to be insufficient to rescue them. It is also possible that the encoded *SiR* protein might not be functional at all for unknown reasons.

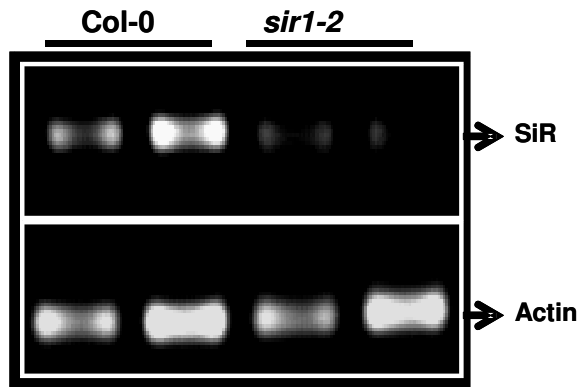


Fig. 39 Semi-quantitative RT-PCR analysis of homozygous *sir1-2* plants. Amplification of *SiR* and *Actin 7* allele through reverse transcription PCR analysis. Amplification of *Actin 7* from the same cDNA preparation was used as a positive control.

3.9.5 *sir1-2* can be partially complemented by GSH or sulfide

Several attempts were made to rescue the lethal phenotype of homozygous *sir1-2* seedlings, including chemical complementation by the exogenous supply of either sulfide, cysteine at a final concentration of 0.1 mM as Na_2S , or GSH at a final concentration of 1mM GSH in standard Arabidopsis media. However, unlike *sir1-1* seedlings, none of these attempts proved successful to rescue the seedlings lethal phenotype of homozygous *sir1-2* seedlings even though these chemicals tended to prolong the green period of the homozygous *sir1-2* seedlings compared to the untreated homozygous *sir1-2* seedlings which were bleached soon after germination (Fig. 40A). Like the untreated homozygous *sir1-2* seedlings, the chemically complemented homozygous *sir1-2* seedlings on the normal Arabidopsis media were also unable to develop into four or multiple-leaves stage from two-leaves stage and eventually died later on (Fig. 40A). Accumulation of sulfite to the level of extreme toxicity was considered as a possible cause of the lethality of homozygous *sir1-2* seedlings. To avoid excessive accumulation of sulfite, sulfate in the Arabidopsis media was replaced by the same concentration of MgCl_2 , and seedlings were then grown on this modified Arabidopsis medium. Homozygous *sir1-2* seedlings were then again complemented with either sulfide at a final concentration of 0.1 mM Na_2S or GSH at a final concentration of 1 mM GSH. Chemically complemented homozygous *sir1-2* seedlings on media without sulfate not only

remained green but were also able to develop into multiple-leaves stage (Fig. 40B). The homozygosity of the suspected *sir1-2* seedlings was confirmed through PCR analysis.

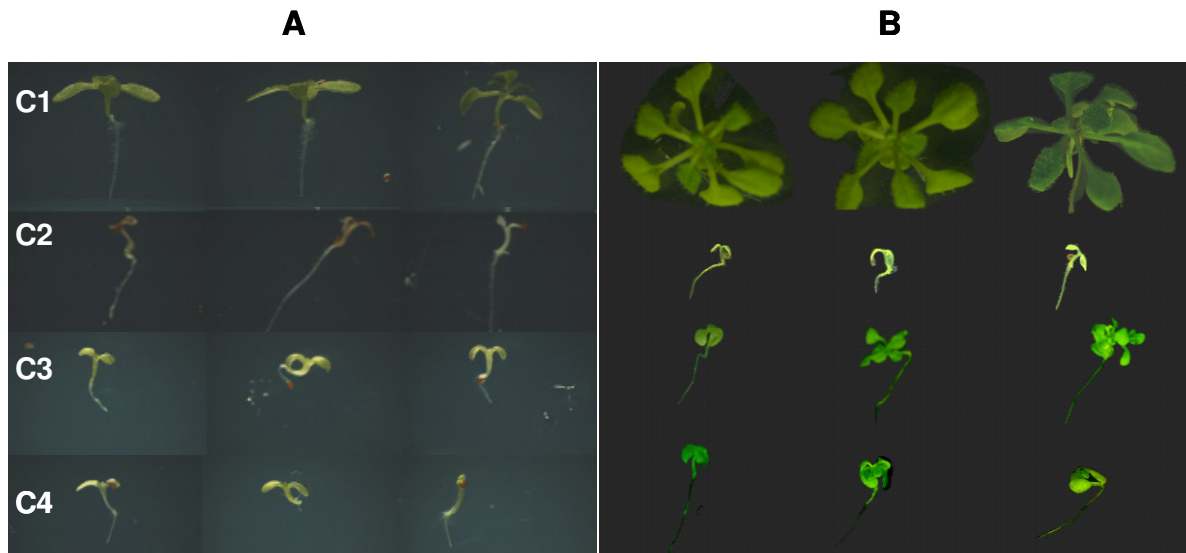


Fig. 40 Chemical complementation of *sir1-2* seedlings.

Wild-type (C1) and homozygous *sir1-2* seedlings (C2) were grown in the presence (A) or absence (B) of sulfate for 4 and 6 weeks, respectively. In both cases *sir1-2* seedlings die after expansion of cotyledons. Only in the absence of oxidized sulfur source (sulfate), the seedling lethal phenotype of *sir1-2* was partially rescued by the exogenous supply of 0.1 mM Na_2S (C3) or 1 mM GSH (C4).

4 Discussion

4.1 Arabidopsis *sir1-1* is severely affected in growth

The selected T-DNA insertion line for SiR, termed as *sir1-1*, from the GABI-Kat collection was found to be a knock-down mutant as indicated by the evaluation of SiR transcript levels through semi-quantitative reverse transcription RT-PCR analysis. The mRNA levels in the leaves of homozygous *sir1-1* plants was reduced to about 50% of wild-type level. Microarray analysis confirmed the RT-PCR results, showing a down-regulation of approximately the same extent. Consequently, the abundance and activity of SiR in leaves of *sir1-1* was reduced in the same manner, suggesting the absence of post-transcriptional and post-translational compensatory regulation.

The moderate degree of reduction of the constitutively expressed *SiR* gene (Bork et al., 1998) and its association with the severe phenotype of growth retardation was one of important discovery of the current work. The viability of the knock-down mutant of SiR provided a powerful tool to address many questions regarding the exact role of SiR *in vivo* and to investigate flux through the entire pathway. Detailed analysis to thoroughly characterize the insertion sites in the *sir1-1* line revealed the beginning of the left border of the T-DNA insertion 73 bp before the ATG start codon in the genomic sequence of *AtSiR* gene. Additionally, according to the available sequence informations of the inserted T-DNA in *sir1-1*, the T-DNA in *sir1-1* was found to be in reverse orientation as shown by the PCR analysis and subsequent sequencing of the PCR amplified fragment. Genomic DNA PCR screening revealed that the T-DNA specific primer, which binds to the left border region of the T-DNA, was unexpectedly giving a product in combination with a gene specific primer binding downstream instead of upstream of the predicted insertion. This result suggested the reverse orientation of the T-DNA in *sir1-1*. Segregation of the severely growth-retarded phenotype agreed with the expected 1:3 (mutant : wild-type) ratio for a single recessive allele. Heterozygous *sir1-1* plants and seedlings did not show any phenotype and looked completely like the wild-type control lines, suggesting that the expression of SiR driven by one allele is sufficient to maintain the normal growth and development of Arabidopsis plants. However, homozygous *sir1-1* plants showed a severe phenotype of growth-retardation and losses in the total biomass compared to Col-0 of the same age. Homozygous *sir1-1* plants

flowered and set viable seeds, albeit later than wild-type plants grown under short day conditions. Besides slow growth, leaves of homozygous *sir1-1* plants looked slightly pale yellow in color and smaller in size. The pale yellow color of the homozygous *sir1-1* leaves was associated to the total chlorophyll contents which were significantly decreased in the leaves of *sir1-1* compared to Col-0. The isolation of a second mutant termed as *sir1-2* from the GABI-Kat T-DNA collection which has a T-DNA insertion site very similar to that of *sir1-1*, but about 19 base pairs closer to the transcription start site, has added further insight about the role SiR in primary sulfur metabolism. The preliminary results strongly indicate that this second mutant allele causes early seedling lethality. Accumulation of the excessive amounts of the toxic sulfite seems to be at least one probable reason of the lethality of these seedlings as indicated by the partial complementation of the seedling lethal phenotype by reduced sulfur compounds in sulfate deprived growth media. This would allow to provide final evidence to answer a fundamental question in primary sulfur metabolism: is sulfite reductase the only enzyme that provides sulfide or is there a hidden second pathway (Hell, 1997)?

4.2 Consequences of the T-DNA insertion for the plant's metabolism

The homozygous *sir1-1* mutant showed significant differences in most sulfur-containing metabolites compared to the wild-type. A block/reduction in the activity of SiR was expected to cause an increase in the concentration of metabolites upstream and a decrease in the concentration of metabolites downstream of SiR in the assimilatory sulfate reduction pathway in the absence of any exceptional unknown regulatory mechanisms. Based on this assumption, the cysteine and thiol contents in the homozygous *sir1-1* plants were expected to be lower compared to wild-type. However, HPLC analysis revealed that the total cysteine contents in the leaves of soil-grown *sir1-1* plants were rather significantly higher compared to Col-0, whereas the GSH contents also tended to be higher in the same samples (Fig. 9A). The same trend for cysteine and GSH was observed in the roots of hydroponically grown *sir1-1* plants, albeit the values were non-significant due to less number of biological replicates. Cysteine thiol residues are both exceptionally useful in terms of structural and regulatory aspects for cells (Meyer and Hell, 2005). As the protein bound cysteine that might be used for redox-signaling and regulation of protein activity is not sufficient to maintain the

cellular redox balance (Meyer and Hell, 2005), the maintenance of certain steady-state levels of cysteine and GSH, specially in plants exposed to oxidative stress become more important to protect cells against oxidative damage. The down-regulation of a large number redox homeostasis-related genes in the *sir1-1* suggested an increased oxidative stress. The tendency of maintaining higher steady-state levels of cysteine and GSH in the leaves *sir1-1* inspite of reduced flux, therefore seemed to be a response of the *sir1-1* towards oxidative stress.

The HPLC analysis for the determination of OAS contents revealed an average increase of more than 2-fold in the leaves of *sir1-1* plants compared to Col-0. The accumulation of OAS in the leaves of *sir1-1* was a consequence of the reduced sulfide availability rather than increased SAT activity as indicated by the non-significant differences in the activity of SAT in the leaves of Col-0 and *sir1-1* plants. Western blot analysis using specific antibodies raised against SAT3 revealed no change in the abundance of SAT3 protein between the the leaves of Col-0 and *sir1-1*. An increase in OAS concentration has been reported in the siliques and old-rosette leaves of sulfur-starved Arabidopsis and sulfur-starved cultured cotyledons of soybean (Kim et al., 1999; Awazuhara et al., 2000). Sulfate, positioned upstream of SiR in the pathway, was expected to accumulate in response to reduced SiR activity. However, besides reduced capacity for reduction of sulfate, the dramatic increase of sulfate contents observed in the leaves of *sir1-1* was also strongly associated to the up-regulation of sulfate transporters. Microarray analysis had revealed that the high affinity sulfate transporters, sulfate transporter 1;1 (*SULTR 1;1*) and sulfate transporter 1;2 (*SULTR 1;2*) (Smith et al., 1995; Smith et al., 1997; Hawkesford and De Kok, 2006) were strongly up-regulated in the roots of *sir1-1* compared to Col-0 (Fig. 33A).

The significantly higher sulfite contents in the leaves of *sir1-1* could be directly associated to the inability of the plants to efficiently reduce sulfite. Since sulfite could be toxic for the plants in high doses, the question arises how does the plant cope with excessive sulfite? Sulfite oxidase, catalyzing the oxidation of sulfite to sulfate, has been recently reported in plants (Eilers et al., 2001). It catalyzes a two-electron transfer reaction in which the electron from sulfite are transferred via a molybdenum cofactor to molecular oxygen, yielding hydrogen peroxide and sulfate (Eilers et al., 2001; Hänsch et al., 2006). It has been speculated that the activity of sulfite oxidase is required to remove excess sulfite which accumulates under certain circumstances (Hänsch and Mendel, 2005). In fact it has been

shown that by modulating the level of sulfite oxidase, Arabidopsis and tomato plants can be rendered resistant or susceptible to SO₂/sulfite (Brychkova et al., 2007). In order to check the possible role of sulfite oxidase in plants impaired in sulfite reduction, the activity of sulfite oxidase was assayed in the leaves of *sir1-1* plant. Interestingly, the activity of sulfite oxidase was found to be significantly increased (2.4-fold) in the leaves of *sir1-1*, suggesting an important role of sulfite oxidase in the detoxification of sulfite which accumulate in the leaves of *sir1-1* due reduced SiR activity. The accumulation of sulfate therefore, could be attributed to the following factors : (i) the inability of the plants to efficiently reduce sulfate, (ii) up-regulation of the high affinity sulfate transporters, and (iii) increased oxidation of sulfite to sulfate due to higher activity of sulfite oxidase.

The significant changes in the contents of total carbon, nitrogen, and sulfur in the leaves of *sir1-1* were indicative of the strong perturbation in entire metabolism of the plants. If elevated sulfate forms a signal for repression of sulfate transporters, this was overruled by the downstream demand for reduced sulfur, leading to increased expression of sulfate transporters. The significantly higher sulfur contents in the leaves of *sir1-1* could be directly linked to the accumulation of sulfate which constitute a considerable portion of the total sulfur present in the cell. A significant decrease in the contents of total glucosinolates in the leaves of *sir1-1* showed that unlike the primary sulfur containing metabolites cysteine and glutathione, the steady-state contents of these secondary sulfur-containing metabolites were flexible. In contrast to leaves, the glucosinolate contents in the seeds of *sir1-1* were not reduced. In fact, the total glucosinolates and as well as many of the individual glucosinolates in the seeds of *sir1-1* were significantly higher compared to Col-0. The seeds, in general contained higher concentrations of glucosinolates. The presence of an import system in this tissue has been suggested by the fact that the high accumulation of glucosinolates in the seeds does not have a correspondingly high level of associated biosynthesis (Du and Halkier, 1998). The higher glucosinolate contents in the seeds of *sir1-1* inspite of its reduced capacity for the synthesis of sulfide, and hence the downstream sulfur containing-compounds including glucosinolates, also supported the presence of such an import system rather than *de novo* synthesis in the seeds. Analysis of total CNS and important sulfur-containing metabolites in seeds of *sir1-1* revealed interesting differences in the metabolism of sulfur between seeds and leaves. The non-significant differences between the total CNS, sulfate and

nitrate contents of *sir1-1* and Col-0 seeds suggested that like glucosinolates, Arabidopsis seemed to have a special import system to meet the demands of different metabolites and elements in the seeds .

4.3 SiR activity creates a bottleneck in sulfate reduction

The assimilatory reduction of sulfate to sulfide is an essential requirement for the production of organic compounds containing reduced sulfur. The role of ATP sulfurylase and APR in the assimilatory sulfate reduction pathway has been discussed in several reports (Logan et al., 1996; Lappartient et al., 1999). The activity and steady-state mRNA level of ATP sulfurylase have been reported to increase upon sulfur starvation and decrease when reduced forms of sulfur were fed to the plants. However, these changes were of relatively small magnitude, i.e. approximately 2-fold or even less (Leustek and Saito, 1999). APR has been suggest to play a regulatory role in the assimilatory sulfate reduction pathway (Brunold and Rennenberg, 1997). The activity and steady-state mRNA level of APR increased markedly and coordinately under sulfur-starvation (Takahashi et al., 1997; Yamaguchi et al., 1999), oxidative stress (Leustek et al., 2000), or heavy metal stress (Heiss et al., 1999). The role of APR in the control of flux of the pathway has also been demonstrated in $^{35}\text{SO}_4^{2-}$ feeding experiments (Vauclare et al., 2002). The activity and transcript levels of APR were decreased if cysteine and GSH were fed in excess. From these tracer experiments with $^{35}\text{SO}_4^{2-}$, performed in the presence of 0.5 mM L-cysteine or glutathione, Vauclare et al. (2002) suggested that APR plays a critical role in the control of flux of the pathway. However, as the uptake of sulfate in these experiments was even more inhibited by glutathione than APS reduction, it therefore implies that APR share the control of flux with sulfate uptake system. The individual contributions of APR and the uptake system in the control of flux of the pathway is still not entirely clear.

In comparison to ATP sulfurylase and APR, catalyzing the first two steps in the assimilatory reduction of sulfate, little attention has been paid to SiR. In order to find out the *in vivo* role of SiR in the control of flux of the pathway, tracer experiments with $^{35}\text{SO}_4^{2-}$ were performed (section 3.5.1 & 3.5.2) in the absence of any other reduced sulfur compounds. In these experiments leaf pieces of similar sizes from the soil-grown Arabidopsis wild-type and homozygous *sir1-1* plants were floated for a defined time on $\frac{1}{2}$ Hoagland medium

supplemented with radioactively labelled sulfate ($^{35}\text{SO}_4^{2-}$) to monitor the incorporation of the radiolabelled sulfate into Cys and GSH. Incorporation of the ^{35}S label into Cys and GSH after 15 and 45 min of incubation revealed a strong reduction in the rate of biosynthesis of Cys and GSH in the leaves of homozygous *sir1-1* plants compared to Col-0 (Fig. 27). After 45 minutes, *sir1-1* leaves in comparison to the wild-type control showed a strong reduction of approximately 25.6-fold and 32.7-fold in the incorporation of ^{35}S label into cysteine and GSH, respectively. These experiments performed in the absence of added cysteine or GSH, therefore, demonstrated the decisive contribution of SiR in controlling the flux over the entire assimilatory sulfate reduction pathway.

Incorporation of ^{35}S label into the protein fraction also revealed strong reduction in incorporation of the label into proteins of *sir1-1* leaves (Fig. 28). The dramatic reduction of approximately 17.8-fold in the incorporation of ^{35}S label into proteins of *sir1-1* leaves compared to Col-0 after 45 minutes incubation further demonstrate that the activity SiR creates a bottle-neck in sulfate reduction. The insight gained through these experiments adds useful information to the existing knowledge of the assimilatory sulfate reduction in higher plants. The exact role of SiR in reductive assimilation of sulfate seemed to have been overlooked (Hell, 1997; Saito, 1998; Leustek et al., 2000; Kopriva, 2006), and therefore needs to be revisited.

4.4 The activity of SiR is crucial in the response of plants towards cadmium exposure

GSH plays an important role in the detoxification of heavy metals as an immediate precursor of phytochelatins (PCs). In the presence of heavy metal ions PCs are enzymatically synthesized from GSH by cytosolic phytochelatin synthase (Ha et al., 1999). PCs have a high affinity for binding with heavy metals, particularly Cd and Cu. These metal-PC complexes are then transported into the vacuole thus sequestering the metals away from sensitive enzymes (Rauser et al., 1991). PCs may accumulate to levels 10-fold higher than wild-type GSH concentration causing a decrease in GSH contents. This mechanism is particularly critical for cadmium detoxification as demonstrated by the isolation of GSH-deficient *cad2* and PC-deficient *cad1* (Howden et al., 1995; Cobbett et al., 1998). As shown in the metabolite analysis, the steady-state contents for cysteine and GSH in the leaves of *sir1-1*

were higher compared to Col-0 (Fig. 9A). However, the tracer experiments with ^{35}S revealed that the rate of biosynthesis of cysteine and GSH in the leaves of *sir1-1* was extremely reduced compared to Col-0 (Fig. 27B). Here, the question arises whether the existing steady-state pools for thiols, which were already higher in the leaves of *sir1-1* compared to Col-0, were sufficient for detoxification of heavy metals like cadmium or do plants need to produce more thiols *de novo*? Moreover, if *de novo* synthesis of thiols is necessary for the detoxification of heavy metals, then how do the plants with reduced capacity for the synthesis of sulfide and subsequently thiols cope with the challenge of heavy metals stress such as cadmium? In order to find answers to these questions, *sir1-1* and Col-0 seedlings were exposed to various concentrations of cadmium, ranging from 0-100 μM CdCl_2 for 14 days. A significant reduction in the root length of *sir1-1* seedlings was observed compared to Col-0 (Fig. 26A and B). The root length of Col-0 seedlings was also reduced upon CdCl_2 exposure, however, the magnitude of this reduction was significantly less compared to *sir1-1*. An average reduction of 75%, 87%, and 92% was observed in the root length of *sir1-1* seedlings upon 14 days exposure to 25 μM , 50 μM , and 100 μM CdCl_2 , respectively compared to the root length of untreated *sir1-1* seedlings. However, the reduction in the root length of Col-0 seedlings exposed for 14 days to same concentrations of CdCl_2 compared to the root length of untreated Col-0 seedlings, were of smaller magnitude. These results implied that exposure of seedlings to CdCl_2 creates a demand for the synthesis of low molecular weight thiols, which, due to the reduced rate of biosynthesis of thiols in *sir1-1* seedlings, could not be efficiently met, thus leading to a higher sensitivity of the *sir1-1* seedlings towards CdCl_2 compared to Col-0. These results are in good agreement to the previous reports where Arabidopsis plants with low glutathione levels were shown to be hypersensitive to cadmium due to the limited capacity of these plants to make phytochelatins (Howden et al., 1995; Cobbett et al., 1998). These authors have reported that silencing of γ -glutamylcysteine synthetase (GSH1), which led to decreased GSH levels, in parallel caused cadmium sensitivity (Howden et al., 1995; Cobbett et al., 1998).

Moreover, an increase in thiol contents followed by increased resistance to cadmium was observed in *Brassica juncea* overexpressing bacterial GSH1 in plastids (Zhu et al., 1999). These observations led us to check the impact of increased SiR activity on the response of Arabidopsis seedlings towards cadmium stress. Exposure of Col-0, genetically

complemented *sir1-1*, and *SiR* overexpressor seedlings to various concentrations of cadmium, ranging from 0-100 μM CdCl_2 however, did not show significant differences in their root lengths. These results suggested that an increase in the activity of SiR beyond wild-type level did not further increase the rate of biosynthesis of thiols, as indicated by the non-significant differences in the cysteine and GSH contents in the leaves of Col-0, genetically complemented *sir1-1*, and *SiR* overexpressor lines (Fig. 25C and D).

4.5 The impact of reduced sulfide synthesis on the expression of sulfur metabolism-related genes

The response of different genes related to sulfur metabolism towards reduced sulfide synthesis, investigated through microarray analysis, added a wealth of information about *in vivo* regulatory processes. Out of 920 selected genes, 67 genes were found to be significantly up- or down-regulated in the leaves of hydroponically-grown *sir1-1* plants compared to Col-0 according to p-values of lower than 0.05. Among the strongly up-regulated genes, the transcript levels of two vegetative storage protein genes, i.e. *VSP1* and *VSP2* was found to increase by approximately 9 and 11-fold, respectively in the leaves of *sir1-1* compared to Col-0. The dramatic up-regulation of two *VSP* genes i.e. *VSP1* (At5g24780) and *VSP2* (At5g24770) provided a clue towards the critical role of vegetative storage proteins in fulfilling the nutrient demands, specially that of reduced sulfur under limited sulfur supply in Arabidopsis seeds. It has been hypothesized that the stored VSPs, presumably serving as transient reserve that sequester unused amino acids during plant development in various vegetative storage organs, play a role in making nitrogen and other nutrients available for seed development at the beginning of seed production (Liu et al., 2005). The non-significant differences in the seeds of *sir1-1* for most of the sulfur-containing compounds, contrary to the significant differences in the leaves of *sir1-1* compared to Col-0, might be linked to the increased expression of *VSP1* and *VSP2* in *sir1-1* leaves. However, VSPs may also served, other functions beyond source-sink interaction as suggested by the up-regulation of VSPs by methyl jasmonate (Berger et al., 1995) and anti-insect acid phosphatase activity of At*VSP2* (Liu et al., 2005). Up-regulation of the *VSP2* in Arabidopsis upon application of methyl jasmonate has been reported (Berger et al., 1995).

The expression of *TGG1* and *TGG2*, the two known functional myrosinases in Arabidopsis, was also significantly up-regulated in the leaves of *sir1-1* compared to Col-0. It has been

suggested that overexpression of thioglucosidases may force degradation of glucosinolates and generates unstable aglycons, spontaneously releasing sulfate (Wittstock and Halkier, 2002). This catabolic cycle of glucosinolates may generate considerable amounts of sulfate for cysteine synthesis. The sulfur starvation inducible nitrilase 3 (*NIT3*) (Kutz et al., 2002), involved in the biosynthesis of indole-3-acetic acid (IAA), was also up-regulated together with nitrilase 2 (*NIT2*) in the leaves of *sir1-1*. Induction of nitrilase under sulfur starvation conditions suggested interaction of glucosinolates and auxin synthesis in *Arabidopsis* (Kutz et al., 2002). Degradation of indole glucosinolates during catabolism generates indole-3-acetonitril, the precursor of indole-3-acetic acid. It has been suggested that induction of *NIT3* during sulfur deficiency (Kutz et al., 2002) considerably participate in converting indole-3-acetonitril to auxin and affects root growth.

Nutrient deprivation often leads to a reduction in the pigments associated with photosynthetic function. *Synechococcus* sp. PCC 7942 has been reported to lose most of its photosynthetic pigments, which include phycocyanin, allophycocyanin and chlorophyll, during nitrogen or sulfur deprivation (Collier and Grossman, 1992, 1994). Decrease in total chlorophyll contents by 13 days of sulfur starvation (Nikiforova et al., 2005) suggested a similar phenomenon. The strong induction of chlorophyllase 1 (*CLH1*), in the leaves of *sir1-1* indicated that the impact of reduced sulfide synthesis in *Arabidopsis* is similar to the above mentioned responses of different organisms under nitrogen or sulfur deprivation. Moreover, the up-regulation of *CLH1* in the leaves of *sir1-1* compared to Col-0 was also inversely correlated to the chlorophyll contents of *sir1-1* leaves, which were significantly lower in the leaves of *sir1-1* compared to Col-0.

The significant down-regulation of *APS4* and *APR2*, encoding the enzymes for the first two steps of the assimilatory sulfate reduction pathway up-stream of *SiR*, suggested that the entire reduction pathway up-stream of *SiR* was down-regulated in the leaves of *sir1-1* in response to reduced *SiR* activity. A decrease in the transcript levels of *APR2* by OAS treatment has previously been reported (Hirai et al., 2003). Interestingly, the transcript levels of many of the pathogenesis related genes, including *PR1*, *PR2*, *PR5*, *RPP1*, *RPP4*, *RPP5*, *EIN3*, and *PEN3* were significantly decreased in the leaves of *sir1-1* compared to wild-type control. Apart from that a large number (15) of genes related to redox homeostasis were also down-regulated in the leaves of *sir1-1*. The down-regulation of many of the pathogen and redox-

related genes in the *sir1-1* leaves pointed towards the inability of Arabidopsis plants to cope with a variety of biotic and abiotic stresses under long term inadequate sulfur supply.

In comparison to leaves (67), a large number of genes (180) were significantly up or Down-regulated in the roots of *sir1-1* compared to Col-0. In this work, the high affinity sulfate transporters, *SULTR 1;1* and *SULTR 1;2* were strongly up-regulated in the roots of *sir1-1* compared to Col-0 (Fig. 33A). Moreover, two group 4 sulfate transporters, *SULTR 4;1* and *SULTR 4;2* were also significantly up-regulated in the roots of *sir1-1* compared to Col-0. The expression of *SULTR1;1* is known to be up-regulated in the roots under sulfur deficiency (Takahashi et al., 2000; Vidmar et al., 2000; Maruyama-Nakashita et al., 2003). Similarly the expression of *SULTR 1;2* is also known to be up-regulated under starved conditions (Hirai et al., 2003). Group 4 sulfate transporters, localised in the tonoplast membrane and thought to be involved in vacuolar sulfate efflux, were induced by S-deprivation with a complex pattern (Parmar et al., 2007). An increase in the transcript levels of *SULTR4;1* and *SULTR4;2* upon sulfur deficiency in *Brassica napus* L. has been reported by these authors. The role *SULTR4;1* and *SULTR4;2* in sulfate accumulation by controlling transport across the tonoplast has been suggested (Kataoka et al., 2004). The up-regulation of sulfate transporters in the *sir1-1* roots provides an other plausible explanation for the observed sulfate accumulation in the leaves and roots of *sir1-1* apart from reduced SiR activity. Up-regulation of sulfate transporters is assumed to be an important step that may enhance the capacities of the primary sulfate uptake under limited supply of reduced sulfur. Contrary to the slight down-regulation of *APR2* in the leaves of *sir1-1*, the expression of *APR1*, *APR2*, and *APR3* was rather up-regulated in the roots of *sir1-1* compared to Col-0. Hirai et al. (2003) reported that the transcript levels of *APR2* was decreased by OAS treatment only in leaves. Moreover, (Koprivova et al., 2000) reported that OAS treatment led to a slight increase in *APR2* mRNA levels only in roots of nitrogen starved Arabidopsis. In this respect our results are consistent with the above mentioned reports in the point that both of these reports have confirmed that OAS application has different effects on *APR2* expression in leaves and roots. On the other hand, the expression of *APS1*, *APS2*, and *APS4* was Down-regulated in the roots of *sir1-1*. The down-regulation of three major isoforms of ATP sulfurylases, catalyzing the sole entry step of the reductive assimilatory pathway suggest that most of the sulfate taken up by the roots in *sir1-1* stays in the inert form. Since the activation of sulfate by ATP sulfurylases is a

prerequisite for further assimilation, only a small amount of sulfate is therefore available for the plants to be assimilated. The impact of reduced SiR activity on the expression of the genes involved in primary sulfur metabolism in leaves and roots is presented in Fig. 41.

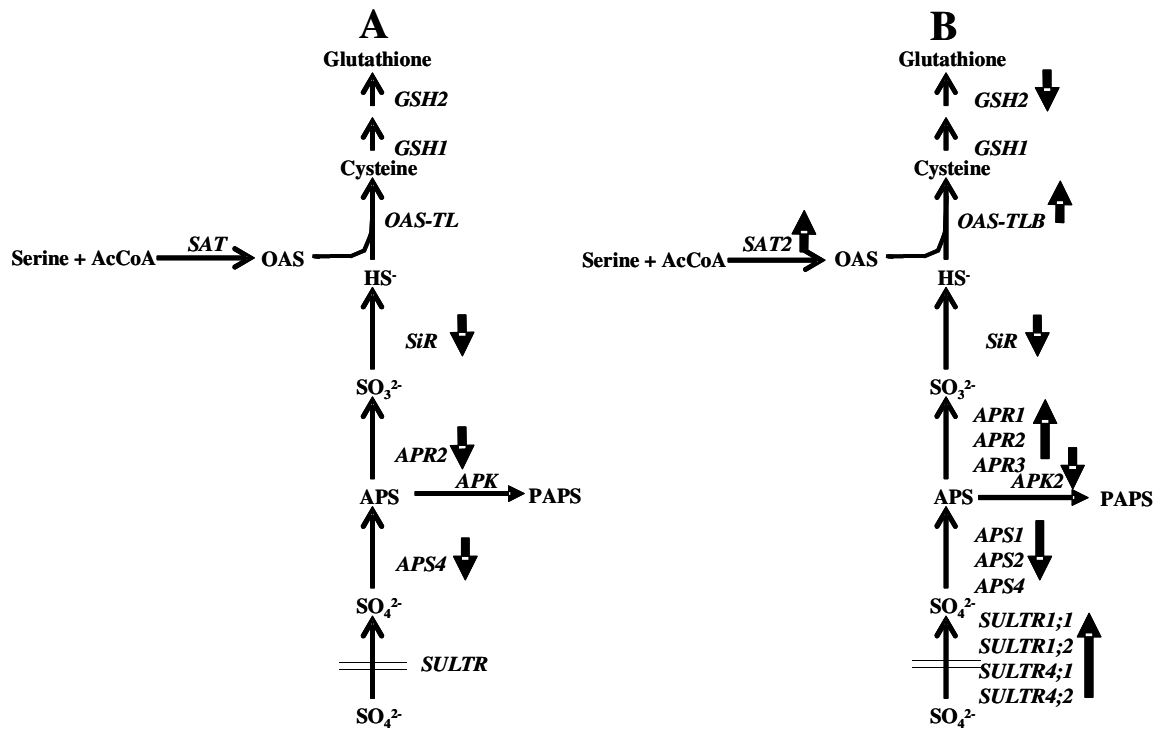


Fig. 41 The Impact of reduced SiR activity on the expression of the primary sulfur metabolism-related genes in Arabidopsis

Differential expression of the genes is indicated by the arrows pointing up or downward. The arrows pointing upward represent genes that were significantly up-regulated, whereas the arrows pointing downward represent genes that were significantly down-regulated in the leaves (A) or roots (B) of *sir1-1* compared to Col-0. *SULTR*, sulfate transporters; *APS*, ATP sulfurylase; *APK*, APS kinase; *APR*, APS reductase; *SiR*, sulfite reductase; *SAT*, serine acetyltransferase; *OAS-TL*, O-acetylcysteine(thiol)lyase; *GSH1*, γ -glutamylcysteine synthetase, and *GSH2*, glutathione synthetase.

4.6 Response of Arabidopsis lines towards selenium fertilization

Due to similar chemical properties selenium and sulfur are thought to share the initial steps for uptake and assimilation. As SeO_4^{2-} is believed to enter roots cells through high affinity sulfate transporters (White et al., 2004), its presence in the growth media is therefore expected to compete with sulfate for the initial steps of uptake and assimilation. *SAT* overexpressor line, which in transgenic *Arabidopsis thaliana* has been shown to cause a slight increase in selenate reduction to organic forms (Sors et al., 2005b), was included in the

current study. As Se hyperaccumulation in different *Astragalus species* has been found to positively correlate to the level of SMT enzymatic activity (Sors et al., 2005b), therefore an SMT overexpressor line was also included in this study. The primary objective of including both these lines in the current work was to achieve maximum reduction of selenate or selenite in Arabidopsis. ICP analysis of the hydroponically-grown Arabidopsis plants, exposed to 50 μM sodium selenite or sodium selenate for one week, revealed a significant increase in the total sulfur contents of the plants compared to untreated plants. Due to the structural similarity of selenate to sulfate, it has been suggested that selenium (as selenate) competes for access to membrane sulfate transporters and to enzymes of the sulfur assimilation pathway, leading to the reduction and assimilation of selenate to the selenium analogs of Cys and Met, seleno-Cys and seleno-Met, in plants (Terry et al., 2000; Sors et al., 2005a). Based on these assumptions, selenium treatment of the plants was expected to lower total sulfur contents. However, Se fertilization, specially selenate and not selenite treatment, in the same Arabidopsis lines has been shown to result in sulfate accumulation in their leaves (Peter, 2007), which probably suggest an up-regulation of the high affinity root sulfate transporters. Since sulfate constitute a major portion of the total sulfur present inside the cell, its accumulation therefore leads to an increase in the total sulfur contents in the cell.

ICP analysis also revealed a significant increase in the total Se contents in the leaves of Arabidopsis plants upon selenate treatment compared to untreated plants. The huge increase in Se in selenate treated plants compared to untreated plants is presumably due to higher selenate contents in these plants. Since selenate treatment in the same Arabidopsis lines has previously been shown to result in sulfate accumulation in their leaves (Peter, 2007), it is therefore reasonable to assume the same scenario for selenate. The higher sulfate/selenate contents seemed to be the result of the up-regulation of the high affinity root sulfate transporters, ultimately causing an increase in the total S and Se. However, quite unexpectedly plants of the SMT overexpressor line did not show any increase in total Se contents upon selenite or selenate treatment. This might be explained if Se is assumed to be present only or mainly in its organic form, which might represent a small fraction of the total Se pool in the leaves of SMT overexpressor plants. It can be concluded from these experiments that selenium, specially selenate treatment seemed to create a situation similar to that of sulfur starvation situation. Such situation in the leaves of Arabidopsis, therefore

causes an up-regulation of the high affinity sulfate transporters, leading to higher sulfate/selenate pools in the plants. As sulfate/selenate constitute a major portion of the total sulfur or selenium present in the plants, an increase in total sulfur or selenium, therefore might be the consequences of the higher sulfate/selenate pools.

References

- Akashi, T., Matsumura, T., Ideguchi, T., Iwakiri, K., Kawakatsu, T., Taniguchi, I., and Hase, T.** (1999). Comparison of the electrostatic binding sites on the surface of ferredoxin for two ferredoxin-dependent enzymes, ferredoxin-NADP⁺ reductase and sulfite reductase. *J Biol Chem* **274**, 29399-29405.
- Asher, C.J., Butler, G.W., and Peterson, P.J.** (1977). Selenium Transport in Root Systems of Tomato. *J Exp Bot* **28**, 279-291.
- Awazuhara, M., Hirai, M.Y., Hayashi, H., Chino, M., Naito, S., and Fujiwara, T.** (2000). *O*-Acetyl-L-serine content in rosette leaves of *Arabidopsis thaliana* affected by S and N nutrition. In: Sulfur Nutrition and Sulfur Assimilation in Higher Plants, C. Brunold, H. Renneberg, L.J. De Kok, I. Stulen, and J.-C. Davidian, eds (Bern: P. Haupt), pp. 331-333.
- Beckett, G.J., and Arthur, J.R.** (2005). Selenium and endocrine systems. *J Endocrinol* **184**, 455-465.
- Berger, S., Bell, E., Sadka, A., and Mullet, J.** (1995). *Arabidopsis thaliana Atvsp* is homologous to soybean *VspA* and *VspB*, genes encoding vegetative storage protein acid phosphatases, and is regulated similarly by methyl jasmonate, wounding, sugars, light and phosphate. *Plant Mol Biol* **27**, 933-942.
- Berken, A., Mulholland, M.M., and LeDuc, D.L.T., N.** (2002). Genetic engineering of plants to enhance selenium phytoremediation. *Crit Rev Plant Sci* **21**, 567-582.
- Bick, J.A., Setterdahl, A.T., Knaff, D.B., Chen, Y., Pitcher, L.H., Zilinskas, B.A., and Leustek, T.** (2001). Regulation of the plant-type 5'-adenylyl sulfate reductase by oxidative stress. *Biochem* **40**, 9040-9048.
- Blake-Kalff, M.M., Harrison, K.R., Hawkesford, M.J., Zhao, F.J., and McGrath, S.P.** (1998). Distribution of sulfur within oilseed rape leaves in response to sulfur deficiency during vegetative growth. *Plant Physiol* **118**, 1337-1344.
- Bork, C., Schwenn, J.D., and Hell, R.** (1998). Isolation and characterization of a gene for assimilatory sulfite reductase from *Arabidopsis thaliana*. *Gene* **212**, 147-153.
- Bradford, M.M.** (1976). A rapid and sensitive method for the quantitation of microgram quantities of protein utilizing the principle of protein-dye binding. *Anal Biochem* **72**, 248-254.
- Broadley, M.R., White, P.J., Bryson, R.J., Meacham, M.C., Bowen, H.C., Johnson, S.E., Hawkesford, M.J., McGrath, S.P., Zhao, F.J., Breward, N., Harriman, M., and Tucker, M.** (2006). Biofortification of UK food crops with selenium. *Proc Nutr Soc* **65**, 169-181.
- Brown, L., Scholefield, D., Jewkes, E.C., Preedy, N., Wadge, K., and Butler, M.** (2000). The effect of sulphur application on the efficiency of nitrogen use in two contrasting grassland soils. *J Agric Sci* **135**: 31-138.
- Brown, P., Tokuhisa, J., Reichelt, M., and Gershenzon, J.** (2003). Variation of glucosinolate accumulation among different organs and developmental stages of *Arabidopsis thaliana*. *Phytochem* **62**, 471-481.

- Brunold, C., and Suter, M.** (1984). Regulation of sulfate assimilation by nitrogen nutrition in the Duckweed *Lemna minor* L. . Plant Physiol **76**, 579-583.
- Cannon, G., Ward, L., Case, C., and Heinhorst, S.** (1999). The 68 kDa DNA compacting nucleoid protein from soybean chloroplasts inhibits DNA synthesis *in vitro*. Plant Mol Biol **39**, 835-845.
- Charron, C., Kopsell, D., Randle, W., and Sams, C.** (2001). Sodium selenate fertilisation increases selenium accumulation and decreases glucosinolate concentration in rapid-cycling *Brassica oleracea*. J Sci Food Agric **81**, 962–966.
- Clough, S.J., and Bent, A.F.** (1998). Floral dip: a simplified method for Agrobacterium-mediated transformation of *Arabidopsis thaliana*. Plant J **16**, 735-743.
- Cobbett, C.S., May, M.J., Howden, R., and Rolls, B.** (1998). The glutathione-deficient, cadmium-sensitive mutant, *cad2-1*, of *Arabidopsis thaliana* is deficient in γ -glutamylcysteine synthetase. Plant J **16**, 73-78.
- Collier, J.L., and Grossman, A.R.** (1992). Chlorosis induced by nutrient deprivation in *Synechococcus* sp. strain PCC 7942: not all bleaching is the same. J Bacteriol **174**, 4718-4726.
- Collier, J.L., and Grossman, A.R.** (1994). A small polypeptide triggers complete degradation of light-harvesting phycobiliproteins in nutrient-deprived cyanobacteria. Embo J **13**, 1039-1047.
- Combs, G., and Gray, W.** (1998). Chemopreventive agents: selenium. Pharmacol Ther **79**, 179-192.
- Crane, B., and Getzoff, E.** (1996). The relationship between structure and function for the sulfite reductases. Curr Opin Struct Biol **6**, 744-756.
- Crane, B., Siegel, L., and Getzoff, E.** (1997). Structures of the siroheme- and Fe₄S₄-containing active center of sulfite reductase in different states of oxidation: heme activation via reduction-gated exogenous ligand exchange. Biochem **36**, 12101-12119.
- Crane, B.R., Siegel, L.M., and Getzoff, E.D.** (1995). Sulfite reductase structure at 1.6 Å: evolution and catalysis for reduction of inorganic anions. Science **270**, 59-67.
- Czechowski, T., Stitt, M., Altmann, T., Udvardi, M.K., and Scheible, W.R.** (2005). Genome-wide identification and testing of superior reference genes for transcript normalization in Arabidopsis. Plant Physiol **139**, 5-17.
- Dhillon, K., and Dhillon, S.** (2003). Distribution and management of seleniferous soils. Adv Agron **79**, 119-184.
- Dobermann, A., Cassman, K.G., Mamaril, C.P., and Sheehy, J.E.** (1998). Management of phosphorus, potassium, and sulfur in intensive, irrigated lowland rice. Field Crops Res. **56**, 113-138.
- Edwards, K., Johnstone, C., and Thompson, C.** (1991). A simple and rapid method for the preparation of plant genomic DNA for PCR analysis. Nuc Aci Res **19**, 1349-.
- Eilers, T., Schwarz, G., Brinkmann, H., Witt, C., Richter, T., Nieder, J., Koch, B., Hille, R., Hansch, R., and Mendel, R.R.** (2001). Identification and biochemical characterization of

- Arabidopsis thaliana* sulfite oxidase. A new player in plant sulfur metabolism. *J Biol Chem* **276**, 46989-46994.
- Ellis, D., and Salt, D.** (2003). Plants, selenium and human health. *Curr Opin Plant Biol* **6**, 273-279.
- Fieldsend, J., and Milford, G.F.J.** (1994). Changes in glucosinolates during crop development in single- and double-low genotypes of winter oilseed rape (*Brassica napus*). I: Production and distribution in vegetative tissues and developing pods during development and potential role in the recycling of sulfur within the crop. *Ann Appl Biol* **124**, 531-542.
- Finley, J.** (2003). Reduction of cancer risk by consumption of selenium-enriched plants: enrichment of broccoli with selenium increases the anticarcinogenic properties of broccoli. *J Med Food* **6**, 19-26.
- Finley, J.W., Davis, C.D., and Feng, Y.** (2000). Selenium from High Selenium Broccoli Protects Rats from Colon Cancer. *J Nutr* **130**, 2384-2389.
- Gaitonde, M.K.** (1967). A spectrophotometric method for the direct determination of cysteine in the presence of other naturally occurring amino acids. *Biochem J* **104**, 627-633.
- Gamet-Payraastre, L., Li, P., Lumeau, S., Cassar, G., Dupont, M.A., Chevolleau, S., Gasc, N., Tulliez, J., and Terce, F.** (2000). Sulforaphane, a Naturally Occurring Isothiocyanate, Induces Cell Cycle Arrest and Apoptosis in HT29 Human Colon Cancer Cells. *Cancer Res* **60**, 1426-1433.
- Ganther, H., and Lawrence, J.** (1997). Chemical transformations of selenium in living organisms. Improved forms of selenium for cancer prevention. *Tetrahedron* **53**, 12229.
- Ganther, H.E.** (1999). Selenium metabolism, selenoproteins and mechanisms of cancer prevention: complexities with thioredoxin reductase. *Carcinogenesis* **20**, 1657-1666.
- Graser, G., Oldham, N., Brown, P., Temp, U., and Gershenzon, J.** (2001). The biosynthesis of benzoic acid glucosinolate esters in *Arabidopsis thaliana*. *Phytochem* **57**, 23-32.
- Grill, E., Löffler, S., Winnacker, E.-L., and Zenk, M.H.** (1989). Phytochelatins, the heavy-metal-binding peptides of plants, are synthesized from glutathione by a specific γ -glutamylcysteine dipeptidyl transpeptidase (phytochelatin synthase). *Proc Natl Acad Sci USA* **86**, 6838-6842.
- Gutierrez-Marcos, J.F., Roberts, M.A., Campbell, E.I., and Wray, J.L.** (1996). Three members of a novel small gene-family from *Arabidopsis thaliana* able to complement functionally an *Escherichia coli* mutant defective in PAPS reductase activity encode proteins with a thioredoxin-like domain and "APS reductase" activity. *Proc Natl Acad Sci USA* **93**, 13377-13382.
- Ha, S.B., Smith, A.P., Howden, R., Dietrich, W.M., Bugg, S., O'Connell, M.J., Goldsbrough, P.B., and Cobbett, C.S.** (1999). Phytochelatin synthase genes from *Arabidopsis* and the Yeast *Schizosaccharomyces pombe*. *Plant Cell* **11**, 1153-1164.
- Haas, F; H., Heeg, C., Queiroz, R., Bauer, A., Wirtz, M., and Hell, R.** (2008). Mitochondrial serine acetyltransferase functions as a pacemaker of cysteine synthesis in plant cells. *Plant Physiol* **148**, 1055-1067.

- Hänsch, R., and Mendel, R.** (2005). Sulfite oxidation in plant peroxisomes. *Photosynth Res* **86**, 337-342.
- Hänsch, R., Lang, C., Riebeseel, E., Lindigkeit, R., Gessler, A., Rennenberg, H., and Mendel, R.R.** (2006). Plant sulfite oxidase as novel producer of H₂O₂: Combination of enzyme catalysis with a subsequent non-enzymatic reaction step. *J Biol Chem* **281**, 6884-6888.
- Hartmann, T., Honicke, P., Wirtz, M., Hell, R., Rennenberg, H., and Kopriva, S.** (2004). Regulation of sulphate assimilation by glutathione in poplars (*Populus tremula* x *P. alba*) of wild type and overexpressing γ -glutamylcysteine synthetase in the cytosol. *J Exp Bot* **55**, 837-845.
- Hatzfeld, Y., Cathala, N., Grignon, C., and Davidian, J.C.** (1998). Effect of ATP sulfurylase overexpression in bright yellow 2 Tobacco cells . Regulation of ATP sulfurylase and SO₄²⁻ transport activities. *Plant Physiol* **116**, 1307-1313.
- Hatzfeld, Y., Lee, S., Lee, M., Leustek, T., and Saito, K.** (2000). Functional characterization of a gene encoding a fourth ATP sulfurylase isoform from *Arabidopsis thaliana*. *Gene* **248**, 51-58.
- Haughn, G.W., and Somerville, C.** (1986). Sulfonylurea-resistant mutants of *Arabidopsis thaliana*. *Mol Gen Genet* **204**, 430-434.
- Hawkesford, M.J.** (2003). Transporter gene families in plants: the sulphate transporter gene family redundancy or specialization? *Physiol Plant* **117**, 155-163.
- Hawkesford, M.J.** (2008). Uptake, distribution and subcellular transport of sulfate. In: *Sulfur metabolism in phototrophic organisms*, R. Hell, C. Dahl, and T. Leustek, eds (Dordrecht, The Netherlands: Springer), pp. 17-32.
- Hawkesford, M.J., and Wray, J.L.** (2000). Molecular genetics of sulphate assimilation. *Adv Bot Res* **33**, 159-223.
- Hawkesford, M.J., and De Kok, L.J.** (2006). Managing sulphur metabolism in plants. *Plant Cell Environ* **29**, 382-395.
- Heiss, S., Schafer, H.J., Haag-Kerwer, A., and Rausch, T.** (1999). Cloning sulfur assimilation genes of *Brassica juncea* L.: cadmium differentially affects the expression of a putative low-affinity sulfate transporter and isoforms of ATP sulfurylase and APS reductase. *Plant Mol Biol* **39**, 847-857.
- Hell, R., Jost, R., Berkowitz, O., and Wirtz, M.** (2002). Molecular and biochemical analysis of the enzymes of cysteine biosynthesis in the plant *Arabidopsis thaliana*. *Amino Acids* **22**, 245-257.
- Higashi, Y., Hirai, M.Y., Fujiwara, T., Naito, S., Noji, M., and Saito, K.** (2006). Proteomic and transcriptomic analysis of *Arabidopsis* seeds: molecular evidence for successive processing of seed proteins and its implication in the stress response to sulfur nutrition. *Plant J* **48**, 557-571.
- Hirai, M., Fujiwara, T., Awazuhara, M., Kimura, T., Noji, M., and Saito, K.** (2003). Global expression profiling of sulfur-starved *Arabidopsis* by DNA macroarray reveals the role of *O*-acetyl-L-serine as a general regulator of gene expression in response to sulfur

nutrition. *Plant J* **33**, 651-663.

Höfgen, R., and Willmitzer, L. (1990). Biochemical and genetic analysis of different patatin isoforms expressed in various organs of potato (*Solanum tuberosum* L.). *Plant Sci* **99**, 221-230.

Howden, R., Goldsbrough, P.B., Andersen, C.R., and Cobbett, C.S. (1995). Cadmium-sensitive, *cad1* mutants of *Arabidopsis thaliana* are phytochelatin deficient. *Plant Physiol* **107**, 1059-1066.

Ihnat, M. (1989). Plants and agricultural materials. p. 33-104. In: Ihnat M, ed. Occurrence and distribution of selenium. Boca Raton, Florida: CRC Press,.

Ip, C. (1998). Lessons from basic research in selenium and cancer prevention. *J Nutr* **128**, 1845-1854.

Ip, C., and Ganther, H.E. (1991). Combination of blocking agents and suppressing agents in cancer prevention. *Carcinogenesis* **12**, 365-367.

Ip, C., Hayes, C., Budnick, R.M., and Ganther, H.E. (1991). Chemical form of selenium, critical metabolites, and cancer prevention. *Cancer Res* **51**, 595-600.

Janick, P., Rueger, D., Krueger, R., Barber, M., and Siegel, L. (1983). Characterization of complexes between *Escherichia coli* sulfite reductase hemoprotein subunit and its substrates sulfite and nitrite. *Biochem* **22**, 396-408.

Jost, R., Altschmied, L., Bloem, E., Bogs, J., Gershenzon, J., Hähnel, U., Hänsch, R., Hartmann, T., Kopriva, S., Kruse, C., Mendel, R., Papenbrock, J., Reichelt, M., Rennenberg, H., Schnug, E., Schmidt, A., Textor, S., Tokuhsa, J., Wachter, A., Wirtz, M., Rausch, T., and Hell, R. (2005). Expression profiling of metabolic genes in response to methyl jasmonate reveals regulation of genes of primary and secondary sulfur-related pathways in *Arabidopsis thaliana*. *Photosynth Res* **86**, 491-508.

Kataoka, T., Watanabe-Takahashi, A., Hayashi, N., Ohnishi, M., Mimura, T., Buchner, P., Hawkesford, M.J., Yamaya, T., and Takahashi, H. (2004). Vacuolar sulfate transporters are essential determinants controlling internal distribution of sulfate in *Arabidopsis*. *Plant Cell* **16**, 2693-2704.

Kim, H., Hirai, M.Y., Hayashi, H., Chino, M., Naito, S., and Fujiwara, T. (1999). Role of *O*-acetyl-L-serine in the coordinated regulation of the expression of a soybean seed storage-protein gene by sulfur and nitrogen nutrition. *Planta* **209**, 282-289.

Klein, M., and Papenbrock, J. (2004). The multi-protein family of *Arabidopsis* sulphotransferases and their relatives in other plant species. *J Exp Bot* **55**, 1809-1820.

Kopriva, S., and Koprivova, A. (2004). Plant adenosine 5'-phosphosulphate reductase: the past, the present, and the future. *J Exp Bot* **55**, 1775-1783.

Kopriva, S., Patron, N., Keeling, P., and Leustek, T. (2008). Phylogenetic analysis of sulfate assimilation and cysteine biosynthesis in phototrophic organisms. In: Sulfur metabolism in phototrophic organisms, R. Hell, C. Dahl, and T. Leustek, eds (Dordrecht, The Netherlands: Springer), pp. 33-60.

Koprivova, A., Suter, M., den Camp, R.O., Brunold, C., and Kopriva, S. (2000). Regulation of sulfate assimilation by nitrogen in *Arabidopsis*. *Plant Physiol* **122**, 737-746.

- Kryukov, G.V., Castellano, S., Novoselov, S.V., Lobanov, A.V., Zehtab, O., Guigo, R., and Gladyshev, V.N.** (2003). Characterization of mammalian selenoproteomes. *Science* **300**, 1439-1443.
- Kuroiwa, T.** (1991). The replication, differentiation, and inheritance of plastids with emphasis on the concept of organelle nuclei. *Int Rev Cytol* **128**, 1-62.
- Kutz, A., Muller, A., Hennig, P., Kaiser, W.M., Piotrowski, M., and Weiler, E.W.** (2002). A role for nitrilase 3 in the regulation of root morphology in sulphur-starving *Arabidopsis thaliana*. *Plant J* **30**, 95-106.
- Laemmli, U.K.** (1970). Cleavage of structural proteins during the assembly of the head of bacteriophage T4. *Nature* **227**, 680-685.
- Lappartient, A.G., Vidmar, J.J., Leustek, T., Glass, A.D., and Touraine, B.** (1999). Inter-organ signaling in plants: regulation of ATP sulfurylase and sulfate transporter genes expression in roots mediated by phloem-translocated compound. *Plant J* **18**, 89-95.
- LeDuc, D., AbdelSamie, M., Montes-Bayon, M., Wu, C., Reisinger, S., and Terry, N.** (2006). Overexpressing both ATP sulfurylase and selenocysteine methyltransferase enhances selenium phyto remediation traits in Indian mustard. *Environ Pollut* **144**, 70-76.
- LeDuc, D.L., Tarun, A.S., Montes-Bayon, M., Meija, J., Malit, M.F., Wu, C.P., AbdelSamie, M., Chiang, C.-Y., Tagmount, A., deSouza, M., Neuhierl, B., Bock, A., Caruso, J., and Terry, N.** (2004). Overexpression of selenocysteine methyltransferase in *Arabidopsis* and Indian mustard increases selenium tolerance and accumulation. *Plant Physiol.* **135**, 377-383.
- Lee, S., and Thomas Leustek.** (1999). The affect of cadmium on sulfate assimilation enzymes in *Brassica juncea*. *Plant Sci* **141**, Pages 201-207.
- Leustek, T.** (2002). Sulfate metabolism. *The Arabidopsis Book*, 1-16.
- Leustek, T., and Saito, K.** (1999). Sulfate transport and assimilation in plants. *Plant Physiol* **120**, 637-644.
- Leustek, T., Martin, M.N., Bick, J.-A., and Davies, J.P.** (2000). Pathways and regulation of sulfur metabolism revealed through molecular and genetic studies. *Ann Rev Plant Physiol Plant Mol Biol* **51**, 141-165.
- Liu, Y., Ahn, J.-E., Datta, S., Salzman, R.A., Moon, J., Huyghues-Despointes, B., Pittendrigh, B., Murdock, L.L., Koiwa, H., and Zhu-Salzman, K.** (2005). *Arabidopsis* vegetative storage protein is an anti-insect acid phosphatase. *Plant Physiol* **139**, 1545-1556.
- Logan, H.M., Cathala, N., Grignon, C., and Davidian, J.C.** (1996). Cloning of a cDNA encoded by a member of the *Arabidopsis thaliana* ATP sulfurylase multigene family. Expression studies in yeast and in relation to plant sulfur nutrition. *J Biol Chem* **271**, 12227-12233.
- Mackinney, G.** (1941). Absorption of light by chlorophyll solutions. *J Biol Chem* **140**, 315-322.
- Malhi, S.S., Schoenau, J.J., and Grant, C.A.** (2005). A review of sulphur fertilizer management for optimum yield and quality of canola in the Canadian Great Plains. *Can J Plant Sci* **85**, 297-307.

- Maruyama-Nakashita, A., Inoue, E., Watanabe-Takahashi, A., Yamaya, T., and Takahashi, H.** (2003). Transcriptome profiling of sulfur-responsive genes in *Arabidopsis* reveals global effects of sulfur nutrition on multiple metabolic pathways. *Plant Physiol* **132**, 597-605.
- Maruyama-Nakashita, A., Nakamura, Y., Tohge, T., Saito, K., and Takahashi, H.** (2006). *Arabidopsis* SLIM1 is a central transcriptional regulator of plant sulfur response and metabolism. *Plant Cell* **18**, 3235-3251.
- McGrath, S.P., Zhao, F.J., and Blake-Kalff, M.M.A.** (2002). History and outlook for sulphur fertilisers in Europe. Proceedings No. 497. Int Fert Soc York.
- Mikkelsen, M., Petersen, B., Olsen, C., and Halkier, B.** (2002). Biosynthesis and metabolic engineering of glucosinolates. *Amino Acids* **22**, 279-295.
- Nakamura, K., Hayama, A., Masada, M., Fukushima, K., and Tamura, G.** (1987). Measurement of serine acetyltransferase activity in crude plant extracts by a coupled assay system using cysteine synthase. *Plant Cell Physiol*. **28**, 885-891.
- Nakayama, M., Akashi, T., and Hase, T.** (2000). Plant sulfite reductase: molecular structure, catalytic function and interaction with ferredoxin. *J Inorg Biochem* **82**, 27-32.
- Nikiforova, V.J., Kopka, J., Tolstikov, V., Fiehn, O., Hopkins, L., Hawkesford, M.J., Hesse, H., and Hoefgen, R.** (2005). Systems rebalancing of metabolism in response to sulfur deprivation, as revealed by metabolome analysis of *Arabidopsis* plants. *Plant Physiol* **138**, 304-318.
- Orser, C.S., Salt, D.E., Pickering, I.J., Prince, R., Epstein, A., and Ensley, B.D.** (1999). Brassica plants to provide enhanced human mineral nutrition: selenium phytoenrichment and metabolic transformation. *J Med Food* **1**, 253-261.
- Parmar, S., Buchner, P., and Hawkesford, M.J.** (2007). Leaf developmental stage affects sulfate depletion and specific sulfate transporter expression during sulfur deprivation in *Brassica napus* L. *Plant Biol (Stuttg)* **9**, 647-653.
- Peter, M.** (2007). Untersuchungen zum Schwefel- und Selenmetabolismus in *Arabidopsis thaliana*. Master thesis submitted to Faculty of Bio Sciences, University of Heidelberg, Germany.
- Pilon-Smits, E.A.H., Hwang, S., Mel Lytle, C., Zhu, Y., Tai, J.C., Bravo, R.C., Chen, Y., Leustek, T., and Terry, N.** (1999). Overexpression of ATP sulfurylase in Indian mustard leads to increased selenate uptake, reduction, and tolerance. *Plant Physiol* **119**, 123-132.
- Pinto, R., Harrison, J.S., Hsu, T., Jacobs, W.R., Jr., and Leyh, T.S.** (2007). Sulfite reduction in mycobacteria. *J Bacteriol* **189**, 6714-6722.
- Rauser, W.E., Robert Schupp, and Rennenberg, H.** (1991). Cysteine, γ -glutamylcysteine, and glutathione levels in maize seedlings. Distribution and translocation in normal and cadmium-exposed plants. *Plant Physiol* **97**, 128-138.
- Reichelt, M., Brown, P., Schneider, B., Oldham, N., Stauber, E., Tokuhisa, J., Kliebenstein, D., Mitchell-Olds, T., and Gershenzon, J.** (2002). Benzoic acid glucosinolate esters and other glucosinolates from *Arabidopsis thaliana*. *Phytochem* **59**, 663-671.
- Reid, M.E., Duffield-Lillico, J., A., Garland, L., Turnbull, B.W., Clark, L.C., and**

- Marshall, J.R.** (2002). Selenium supplementation and lung cancer incidence: An update of the nutritional prevention of cancer trial. *Cancer Epidemiol Biomarkers Prev* **11**, 1285-1291.
- Rotte, C., and Leustek, T.** (2000). Differential subcellular localization and expression of ATP sulfurylase and 5'-adenylylsulfate reductase during ontogenesis of Arabidopsis leaves indicates that cytosolic and plastid forms of ATP sulfurylase may have specialized functions. *Plant Physiol* **124**, 715-724.
- Saito, K.** (2000). Regulation of sulfate transport and synthesis of sulfur-containing amino acids. *Curr Opin Plant Biol* **3**, 188-195.
- Saito, K.** (2004). Sulfur assimilatory metabolism. The long and smelling road. *Plant Physiol* **136**, 2443-2450.
- Saito, K., Kurosawa, M., Tatsuguchi, K., Takagi, Y., and Murakoshi, I.** (1994). Modulation of cysteine biosynthesis in chloroplasts of transgenic tobacco overexpressing cysteine synthase [O-acetylserine(thiol)-lyase]. *Plant Physiol* **106**, 887-895.
- Saitoh, T., Ikegami, T., Nakayama, M., Teshima, K., Akutsu, H., and Hase, T.** (2006). NMR study of the electron transfer complex of plant ferredoxin and sulfite reductase: Mapping the interaction sites of ferredoxin. *J Biol Chem* **281**, 10482-10488.
- Sambrook, J., Fritsch, E.F., and Maniatis, T.** (1989). *Molecular cloning: a laboratory manual*. New York: Cold Spring Harbour Laboratory Press.
- Sanda, S., Leustek, T., Theisen, M.J., Garavito, R.M., and Benning, C.** (2001). Recombinant Arabidopsis SQD1 converts UDP-glucose and sulfite to the sulfolipid head group precursor UDP-sulfoquinovose *in vitro*. *J Biol Chem* **276**, 3941-3946.
- Schäfer, H.J., Haag-Kerwer, A., and Rausch, T.** (1998). cDNA cloning and expression analysis of genes encoding GSH synthesis in roots of the heavy-metal accumulator *Brassica juncea* L.: evidence for Cd-induction of a putative mitochondrial γ -glutamylcysteine synthetase isoform. *Plant Mol Biol* **37**, 87-97.
- Sekine, K., Hase, T., and Sato, N.** (2002). Reversible DNA compaction by sulfite reductase regulates transcriptional activity of chloroplast nucleoids. *J Biol Chem* **277**, 24399-24404.
- Sekine, K., Fujiwara, M., Nakayama, M., Takao, T., Hase, T., and Sato, N.** (2007). DNA binding and partial nucleoid localization of the chloroplast stromal enzyme ferredoxin:sulfite reductase. *FEBS J* **274**, 2054-2069.
- Sors, T.G., Ellis, D.R., and Salt, D.E.** (2005a). Selenium uptake, translocation, assimilation and metabolic fate in plants. *Photosynth Res* **86**, 373-389.
- Sors, T.G., Ellis, D.R., Na, G.N., Lahner, B., Lee, S., Leustek, T., Pickering, I.J., and Salt, D.E.** (2005b). Analysis of sulfur and selenium assimilation in Astragalus plants with varying capacities to accumulate selenium. *Plant J* **42**, 785-797.
- Takahashi, H., Watanabe-Takahashi, A., Smith, F.W., Blake-Kalff, M., Hawkesford, M.J., and Saito, K.** (2000). The roles of three functional sulphate transporters involved in uptake and translocation of sulphate in *Arabidopsis thaliana*. *Plant J* **23**, 171-182.
- Takahashi, H., Yamazaki, M., Sasakura, N., Watanabe, A., Leustek, T., Engler, J.A., Engler, G., Van Montagu, M., and Saito, K.** (1997). Regulation of sulfur assimilation in higher plants: a sulfate transporter induced in sulfate-starved roots plays a central role in

- Arabidopsis thaliana*. Proc Natl Acad Sci USA **94**, 11102-11107.
- Talalay, P., and Fahey, J.W.** (2001). Phytochemicals from cruciferous plants protect against cancer by modulating carcinogen metabolism. J Nutr **131**, 3027S-3033.
- Terry, N., Zayed, A.M., De Souza, M.P., and Tarun, A.S.** (2000). Selenium in higher plants. Annu Rev Plant Physiol Plant Mol Biol **51**, 401-432.
- Tocquin, P., Corbesier, L., Havelange, A., Pieltain, A., Kurtem, E., Bernier, G., and Perilleux, C.** (2003). A novel high efficiency, low maintenance, hydroponic system for synchronous growth and flowering of *Arabidopsis thaliana*. BMC Plant Biol **3**, 2.
- Tomatsu, H., Takano, J., Takahashi, H., Watanabe-Takahashi, A., Shibagaki, N., and Fujiwara, T.** (2007). An *Arabidopsis thaliana* high-affinity molybdate transporter required for efficient uptake of molybdate from soil. Proc Natl Acad Sci USA **104**, 18807-18812.
- Towbin, H., Staehelin, T., and Gordon, J.** (1979). Electrophoretic transfer of proteins from polyacrylamide gels to nitrocellulose sheets: Procedure and some applications. Proc Natl Acad Sci USA **76**, 4350-4354.
- Vauclare, P., Kopriva, S., Fell, D., Suter, M., Sticher, L., von Ballmoos, P., Krahenbuhl, U., den Camp, R.O., and Brunold, C.** (2002). Flux control of sulphate assimilation in *Arabidopsis thaliana*: adenosine 5'-phosphosulphate reductase is more susceptible than ATP sulphurylase to negative control by thiols. Plant J **31**, 729-740.
- Vidmar, J.J., Tagmount, A., Cathala, N., Touraine, B., and Davidian, J.E.** (2000). Cloning and characterization of a root specific high-affinity sulfate transporter from *Arabidopsis thaliana*. FEBS Lett **475**, 65-69.
- Vinceti, M., Wei, E., Malagoli, C., Bergomi, M., and Vivoli, G.** (2001). Adverse health effects of selenium in humans. Rev Environ Health **16**, 233-251.
- Whanger, P.** (2004). Selenium and its relationship to cancer: an update dagger. Br J Nutr **91**, 11-28.
- Whanger, P.D.** (2002). Selenocompounds in Plants and Animals and their Biological Significance. J Am Coll Nutr **21**, 223-232.
- White, P.J., Bowen, H.C., Marshall, B., and Broadley, M.R.** (2007). Extraordinarily high leaf selenium to sulfur ratios define 'Se-accumulator' plants. Ann Bot **100**, 111-118.
- White, P.J., Bowen, H.C., Parmaguru, P., Fritz, M., Spracklen, W.P., Spiby, R.E., Meacham, M.C., Mead, A., Harriman, M., Trueman, L.J., Smith, B.M., Thomas, B., and Broadley, M.R.** (2004). Interactions between selenium and sulphur nutrition in *Arabidopsis thaliana*. J Exp Bot **55**, 1927-1937.
- Wilson, S., and Murray, F.** (1990). SO₂-induced growth reductions and sulphur accumulation in wheat. Environ. Pollut. **66**, 179-191.
- Wittstock, U., and Halkier, B.A.** (2002). Glucosinolate research in the *Arabidopsis* era. Trends Plant Sci **7**, 263-270.
- Wu, L.** (1998). Selenium accumulation and uptake by crop and grassland plant species. In: Frankenberger WT, Engberg RA, eds. Environmental chemistry of selenium. (Marcel Dekker, New York), pp. 657-686.

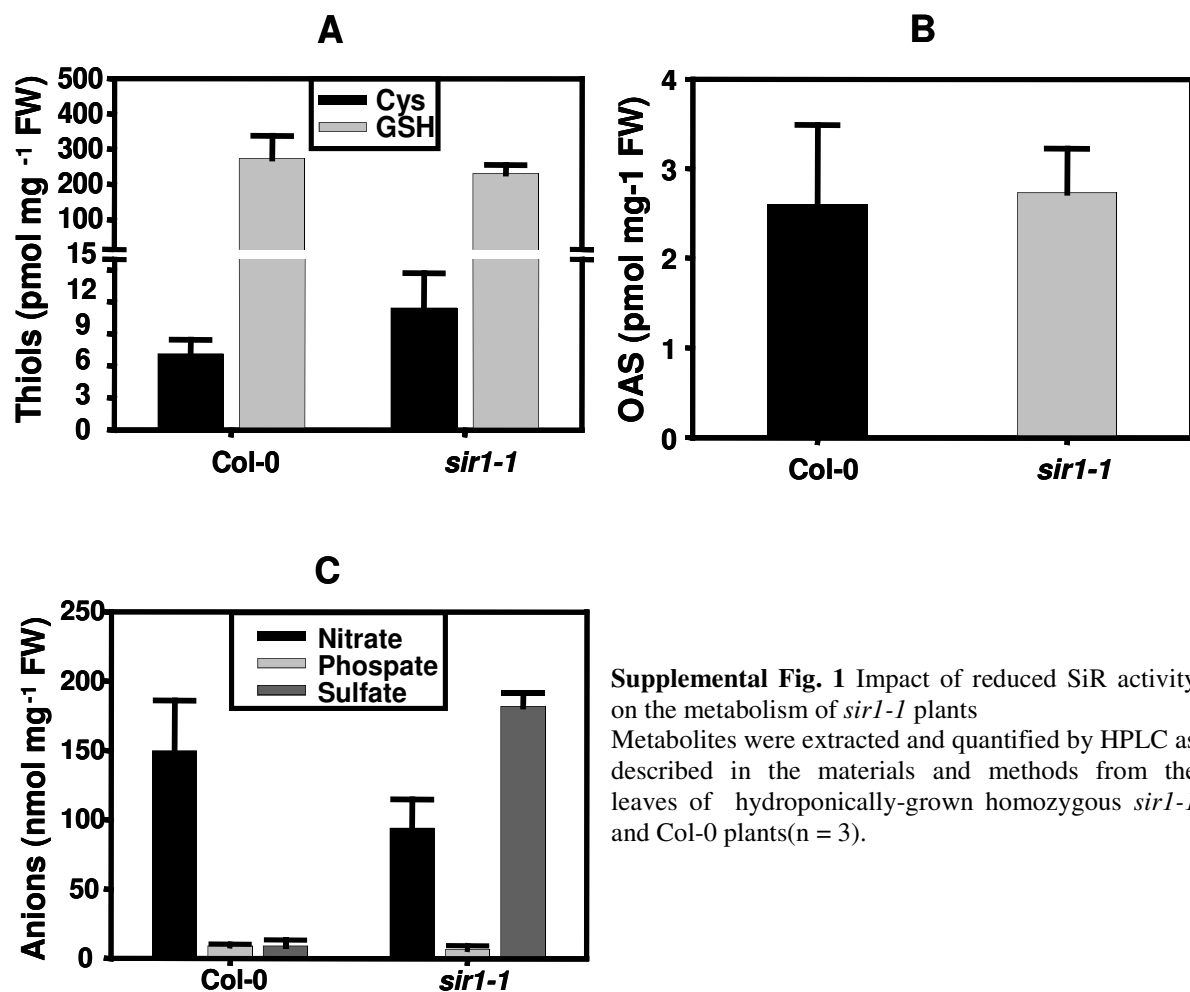
- Wu, L.** (2004). Review of 15 years of research on ecotoxicology and remediation of land contaminated by agricultural drainage sediment rich in selenium. *Ecotoxicol Environ Saft* **57**, 257-269.
- Xiang, C., Werner, B.L., Christensen, E.M., and Oliver, D.J.** (2001). The biological functions of glutathione revisited in *Arabidopsis* transgenic plants with altered glutathione levels. *Plant Physiol* **126**, 564-574.
- Yamaguchi, Y., Yamamoto, Y., Ikegawa, H., and Matsumoto, H.** (1999). Protective effect of glutathione on the cytotoxicity caused by a combination of aluminum and iron in suspension-cultured tobacco cells. *Physiol Plant* **105**, 417-422.
- Yonekura-Sakakibara, K., Onda, Y., Ashikari, T., Tanaka, Y., Kusumi, T., and Hase, T.** (2000). Analysis of reductant supply systems for ferredoxin-dependent sulfite reductase in photosynthetic and nonphotosynthetic organs of maize. *Plant Physiol* **122**, 887-894.
- Yoshimoto, N., Takahashi, H., Smith, F.W., Yamaya, T., and Saito, K.** (2002). Two distinct high-affinity sulfate transporters with different inducibilities mediate uptake of sulfate in *Arabidopsis* roots. *Plant J* **29**, 465-473.
- Yoshimoto, N., Inoue, E., Saito, K., Yamaya, T., and Takahashi, H.** (2003). Phloem-localizing sulfate transporter, Sultr1;3, mediates re-distribution of sulfur from source to sink organs in *Arabidopsis*. *Plant Physiol* **131**, 1511-1517.
- Yu, B., Xu, C., and Benning, C.** (2002). *Arabidopsis* disrupted in SQD2 encoding sulfolipid synthase is impaired in phosphate-limited growth. *Proc Natl Acad Sci USA* **99**, 5732-5737.
- Zhao, F., McGrath, S.P., Blake-Kalff, M.M.A., Link, A., and Tucker, M.** (2002). Crop responses to sulphur fertilisation in Europe. Proceedings No. 504. Int Fert Soc York.
- Zhao, F.-J., Tausz, M., and De Kok, L.** (2008). Role of sulfur for plant production in agricultural and natural ecosystems. In: *Sulfur metabolism in phototrophic organisms*, R. Hell, C. Dahl, and T. Leustek, eds (Dordrecht, The Netherlands: Springer), pp. 425-444.
- Zhu, Y.L., Pilon-Smits, E.A., Tarun, A.S., Weber, S.U., Jouanin, L., and Terry, N.** (1999). Cadmium tolerance and accumulation in Indian mustard is enhanced by overexpressing *γ-glutamylcysteine synthetase*. *Plant Physiol* **121**, 1169-1178.

Supplementary data

P2+P3 CCATCATA-CTCA--TT-GC--TGATCCATGTAGATTT**CGCGGAC-ATGAAGCCATTAACACACGCCCCCTTAT**
AtSR ACGTGATAGCGCACGTTAGCTTTGA-CCAT-TGCTTTTGTTCCTATTAGTTTTTTAAACACACGCCCCCTTAT

Supplemental data 1. Sequence alignment of the T-DNA and gene specific primer fragment of *sir1-1* with the genomic sequence of wild-type *SiR* gene.

The unmatched sequences (red) obtained from the the sequence analysis of gene specific and T-DNA specific primer combination (P2 + P3) represent the bases of the T-DNA, and hence the position of the T-DNA insertion towards the right border of *SiR* gene in *sir1-1*.



Supplemental Fig. 1 Impact of reduced SiR activity on the metabolism of *sir1-1* plants
 Metabolites were extracted and quantified by HPLC as described in the materials and methods from the leaves of hydroponically-grown homozygous *sir1-1* and Col-0 plants(n = 3).

Supplementary data

MIPs code	Identity, description	category	Change (% age)	P- value
At3g19710	branched-chain amino transferase	Glucosinolat-synthesis	1.72	0.004
At5g25980	myrosinase	Glucosinolat-synthesis	1.61	0.031
At5g26000	myrosinase	Glucosinolat-synthesis	1.59	0.004
At4g13770	cytochrom P450	Glucosinolat-synthesis	1.53	0.022
At1g16400	cytochrom P450, CYP79F2	Glucosinolat-synthesis	1.42	0.022
At4g03060	AOP2	Glucosinolat-synthesis	1.27	0.006
At1g24100	glucosyl transferase	Glucosinolat-synthesis	1.19	0.016
At1g54040	epithiospecifier protein,	Glucosinolat-synthesis	1.14	0.03
At2g22330	cytochrome P450 CYP79B3	Glucosinolat-synthesis	1.12	0.04
At3g56060	mandelonitrile lyase-like protein	Glucosinolat-synthesis	-1.3	0.034
AT5G63980	PAPS Phosphatase	Sulfur-metabolism	1.36	0.038
AT3G22740	AtHMT-3	Sulfur-metabolism	1.23	0.03
AT4G01850	SAM2	Sulfur-metabolism	1.22	0.033
At1g62180	APR2-RT	Sulfur-metabolism	-1.16	0.034
At5g65720	cysteine desulphydrilase	Sulfur-metabolism	-1.19	0.043
At5g44070	phytochelatin synthase	Sulfur-metabolism	-1.21	0.032
AT3G56300	CysteinyI-tRNA synthetase	Sulfur-metabolism	-1.24	0.048
At5g10180	Sultr2;1	Sulfur-metabolism	-1.37	0.018
AT1G13420	sulfotransferase family protein	Sulfur-metabolism	-1.43	0.03
At5g43780	ATP sulfurylase precursor	Sulfur-metabolism	-1.84	0.003
AT5G04590	sulfite reductase	Sulfur-metabolism	-3.22	0
AT2G25450	similar to ACC oxidase	Sulfur-induced	1.71	0.036
AT4G12470	lipid transfer protein family protein	Sulfur-induced	-1.24	0.014
ATCG01270	chloroplast encoded hypothetical protei	Sulfur-induced	-1.6	0.042
At5g24770	VEGETATIVE STORAGE PROTEIN 2	REDOX	11.37	0.001
At5g24780	VEGETATIVE STORAGE PROTEIN 1	REDOX	8.98	0.001
At2g47880	Glutaredoxin	REDOX	1.61	0.032
At2g03980	hydrolase family protein	REDOX	1.18	0.034
At2g32880	MATH domain-containing protein	REDOX	1.14	0.03
At4g23150	pad2 regulateded	REDOX	-1.1	0.047
At2g43570	chitinase	REDOX	-1.16	0.025
At1g03680	Thioredoxin	REDOX	-1.17	0.038
At3g54660	Glutathione Reductase I	REDOX	-1.17	0.039
At5g63030	Glutaredoxin	REDOX	-1.18	0.03
At2g05380	glycine-rich protein	REDOX	-1.23	0.012
At2g29580	zinc finger family protein	REDOX	-1.29	0.018
At4g31870	AtGpx7	REDOX	-1.32	0.017
At5g06290	2-Cys Prx B	REDOX	-1.37	0.004
AT2G41680	dihydrolipoyl dehydrogenase	REDOX	-1.43	0.03
At3g11630	2-Cys Prx A	REDOX	-1.44	0.027
At4g03520	Thioredoxin	REDOX	-1.48	0.022
AT3G25250	OXI1	REDOX	-1.6	0.022
At2g14610	PR1	REDOX	-1.6	0.022
At3g57260	PR2	REDOX	-1.73	0.004
At2g44290	Lipid transfer protein	REDOX	-1.78	0.004
At2g29450	ATGST U5	GSH-Transfer	1.53	0.035
At2g02930	putative glutathione S-transferase	GSH-Transfer	-1.29	0.024
At2g25080	putative glutathione peroxidase AtGpx1	GSH-Transfer	-1.55	0.021
At4g02520	ATGST F2	GSH-Transfer	-2.17	0.009
AT1G19670	CHLOROPHYLLASE	pathogens-related	2.17	0.002
At1g66100	THI1.1	pathogens-related	1.36	0.038
AT2G06050	OPR3	pathogens-related	1.22	0.011
At1g72260	THI2.1	pathogens-related	1.19	0.031
AT5G13160	AVRPPHB SUSCEPTIBLE 1	pathogens-related	-1.15	0.038
AT1G59870	ATP binding cassette transporter	pathogens-related	-1.4	0.024
AT3G20770	ETHYLENE-INSENSITIVE3	pathogens-related	-1.48	0.007
AT4G16860	RPP4	pathogens-related	-1.51	0.009
AT3G44480	RPP10	pathogens-related	-1.51	0.025
AT4G16950	RPP5	pathogens-related	-1.54	0.012
AT1G75040	PR5	pathogens-related	-1.59	0.006
At5g18170	glutamate dehydrogenase	amino acid synthesis	-1.19	0.022
At5g05730	ASA1	amino acid synthesis,	-1.22	0.033
At4g39540	shikimate kinase - like protein	amino acid synthesis	-1.26	0.033
AT3G44300	nitrilase	Auxin-Biosynthesis	1.5	0.006
AT5G15230	gibberellin-regulated (GASA4) mRNA	Hormon induced/related	1.36	0.01
AT3G44310	NIT1	Auxin-Biosynthesis	1.24	0.022
AT4G24620	hosphoglucose isomerase	Asc-biosynthesis	-1.26	0.022
AT4G14560	auxin induced gene (IAA1)	Hormon induced/related	-1.31	0.033

Supplemental data 2. The impact of reduced SiR activity on the expression of sulfur metabolism-related genes in the leaves

Total mRNA was extracted from the leaves of seven weeks old hydroponically-grown Col-0 and *sir1-1* plants. The mean \pm SD from three independent extractions of wild-type and *sir1-1* are shown. The genes in green background indicate significant down-regulation ($P < 0.05$), whereas, those in the white background represent significantly up-regulated genes ($P < 0.05$).

Supplementary data

MIPs code	Identity	Category	change (% ac	P-value
At5g23020	Mam2	Glucosinolat-Synthesise	3.10	0.000
At1g47600	myrosinase, TGG4	Glucosinolat-Synthesise	1.49	0.004
At3g09710	transcription factor	Glucosinolat-Synthesise	1.14	0.016
At4g03060	AOP2	Glucosinolat-Synthesise	0.81	0.001
At3g56060	mandelonitrile lyase-like protein	Glucosinolat-Synthesise	0.81	0.017
At2g31790	glucosyl transferase	Glucosinolat-Synthesise	0.75	0.004
At5g26000	myrosinase, TGG1	Glucosinolat-Synthesise	0.75	0.029
At5g07690	Myb29	Glucosinolat-Synthesise	0.57	0.012
At4g08620	Sultr1;1	Sulfur-metabolism	3.61	0.000
At1g78000	Sultr1;2	Sulfur-metabolism	2.10	0.001
At1g62180	APR2	Sulfur-metabolism	2.00	0.001
At2g17640	AtSAT2	Sulfur-metabolism	1.67	0.000
AT5G20980	plastidic methionine synthase	Sulfur-metabolism	1.60	0.000
At3g12520	Sultr4;2	Sulfur-metabolism	1.50	0.001
AT3G17390	S-adenosylmethionine synthetase	Sulfur-metabolism	1.47	0.002
AT1G13590	AtPSK1	Sulfur-metabolism	1.47	0.018
At4g04610	APR1	Sulfur-metabolism	1.46	0.011
At5g13550	Sultr4;1	Sulfur-metabolism	1.46	0.002
At5g17920	cobalamin-independent methionine synthase	Sulfur-metabolism	1.45	0.001
AT3G03780	cytosolic methionine synthase	Sulfur-metabolism	1.31	0.046
At4g21990	APR3	Sulfur-metabolism	1.30	0.009
AT4G01850	SAM2	Sulfur-metabolism	1.28	0.011
AT4G13940	S-adenosyl-L-homocysteinehydrolase	Sulfur-metabolism	1.27	0.001
AT3G25900	homocysteine S-methyltransferase	Sulfur-metabolism	1.26	0.014
AT3G23800	selenium binding protein	Sulfur-metabolism	1.20	0.026
AT3G45070	sulfotransferase family protein	Sulfur-metabolism	1.20	0.030
AT2G03750	sulfotransferase family protein	Sulfur-metabolism	1.20	0.034
AT1G28170	sulfotransferase family protein	Sulfur-metabolism	1.19	0.008
At2g43750	OAS-TL B	Sulfur-metabolism	1.14	0.006
At2g22250	putative cystein lyase	Sulfur-metabolism	1.14	0.048
At4g39940	APK 2	Sulfur-metabolism	0.88	0.039
AT1G02500	SAM	Sulfur-metabolism	0.85	0.032
At5g27380	glutathione synthetase, GSH2	Sulfur-metabolism	0.83	0.029
AT3G49780	Encodes a phytoalkyltransferase	Sulfur-metabolism	0.81	0.009
AT3G55400	methionyl t-RNA Synthetase (mito)	Sulfur-metabolism	0.79	0.001
At5g44070	phytochelatin synthase	Sulfur-metabolism	0.73	0.001
AT1G01010	putative selenocysteine lyase	Sulfur-metabolism	0.73	0.021
At3g22890	APS1	Sulfur-metabolism	0.65	0.004
At4g14680	APS2	Sulfur-metabolism	0.65	0.006
AT1G13420	sulfotransferase family protein	Sulfur-metabolism	0.57	0.000
AT5G04590	sulfite reductase	Sulfur-metabolism	0.44	0.001
At5g43780	ATP sulfurylase precursor	Sulfur-metabolism	0.38	0.000
AT5G67400	peroxidase 73	Sulfur-induced	3.55	0.000
AT5G48850	male sterility MS5 family protein	Sulfur-induced	3.16	0.000
AT4G04830	methionine sulfoxide reductase	Sulfur-induced	3.01	0.000
AT4G40090	arabinogalactan-protein (AGP3)	Sulfur-induced	2.85	0.004
At1g36370	glycine/serine hydroxymethyltransferase	Sulfur-induced	2.80	0.001
At4g25220	similar to glycerol-3-phosphate transporter	Sulfur-induced	2.14	0.001
At1g70880	Bet V allergen protein (SLIM 1 regulated)	Sulfur-induced	1.86	0.016
At4g31330	predicted protein	Sulfur-induced	1.44	0.004
AT3G49960	identical to peroxidase ATP21a	Sulfur-induced	1.41	0.003
AT5G57090	auxin transport protein (EIR1)	Sulfur-induced	1.37	0.002
AT2G44460	Putative thioglucosidase	Sulfur-induced	1.25	0.002
At2g34330	unknown protein	Sulfur-induced	1.24	0.008
At1g23730	Putative carbonic anhydrase	Sulfur-induced	1.16	0.006
At4g34730	putative ribosome binding factor A	Sulfur-induced	0.86	0.048
AT4G25990	chloroplast import apparatus CIA2-like	Sulfur-induced	0.84	0.024
AT5G17750	AAA-type ATPase family protein	Sulfur-induced	0.84	0.020
At4g34020	DJ-1 family protein	Sulfur-induced	0.79	0.011
At2g42550	putative protein kinase	Sulfur-induced	0.78	0.041
At2g03540	hypothetical protein	Sulfur-induced	0.74	0.002
At1g18870	isochorismate synthase	Sulfur-induced	0.73	0.035
ATCG01270	chloroplast encoded hypothetical protein	Sulfur-induced	0.72	0.005
AT1G75290	similar to an isoflavone reductase	Sulfur-induced	0.72	0.004
AT4G08870	arginas	Sulfur-induced	0.69	0.024
AT3G51600	nonspecific lipid transfer protein 5 (LTP5)	Sulfur-induced	0.67	0.020
AT1G64940	cytochrome P450	Sulfur-induced	0.64	0.005
AT3G45140	lipoxigenase (LOX2)	Sulfur-induced	0.64	0.026
At4g21830	methionine sulfoxide reductase domai	REDOX	2.73	0.000
AT1G30510	root-type ferredoxin	REDOX	1.63	0.020
AT5G22140	dihydrolipoyl dehydrogenase	REDOX	1.23	0.003
AT3G44190	dihydrolipoyl dehydrogenase	REDOX	1.22	0.006
At5g03870	putative GRX	REDOX	1.14	0.015
At3g52960	type II Prx E	REDOX	1.04	0.014
At2g48110	expressed protein	REDOX	0.86	0.003
At2g47870	CC	REDOX	0.85	0.015
At1g33960	AtIG1	REDOX	0.84	0.029
At3g52070	GDSL-motif lipase	REDOX	0.81	0.016
AT5G08410	ferredoxin-thioredoxin reductase,	REDOX	0.80	0.025
AT5G08740	dihydrolipoyl dehydrogenase	REDOX	0.78	0.008

Continue on next page

At3g62960	CC	REDOX	0.77	0.011
At2g24850	Encodes a tyrosine aminotransferase	REDOX	0.77	0.011
At3g02730	Thioredoxin	REDOX	0.77	0.010
At3g54660	Glutathione Reductase I	REDOX	0.74	0.000
At1g31170	Sulfiredoxin Srx	REDOX	0.73	0.006
At1g64500	putative GRX	REDOX	0.73	0.001
At2g32680	Putative R-gene	REDOX	0.73	0.000
At1G10960	ferredoxin, chloroplast, putative	REDOX	0.72	0.041
At3g63080	glutathione peroxidase -like protein	REDOX	0.72	0.011
At2G04700	ferredoxin thioredoxin reductase catalytic beta	REDOX	0.72	0.006
At3g54900	CGFS	REDOX	0.70	0.011
At3G27820	peroxisomal membrane	REDOX	0.70	0.002
At2g44290	Lipid transfer protein	REDOX	0.68	0.006
At2g38270	CGFS	REDOX	0.68	0.006
At5g63030	CPYC	REDOX	0.67	0.003
At4g03520	Thioredoxin	REDOX	0.66	0.004
At3G16250	ferredoxin-related	REDOX	0.62	0.004
At3g15360	Thioredoxin	REDOX	0.59	0.001
At3g06050	type II Prx F	REDOX	0.58	0.033
At5G01600	Encodes a ferretin protein	REDOX	0.58	0.001
At2g47880	CC	REDOX	0.58	0.004
At2g05380	glycine-rich protein (GRP3S)	REDOX	0.58	0.005
At2G41680	dihydropyridyl dehydrogenase	REDOX	0.57	0.000
At2g46680	encodes a putative transcription factor	REDOX	0.54	0.009
At4g31870	AtGpx7	REDOX	0.48	0.000
At3g26060	2-Cys Prx Q	REDOX	0.48	0.004
At5G21105	L-ascorbate oxidase	GSH-Asc-cycle	1.28	0.031
At1g7190	putative glutathione transferase	GSH-Transfer	1.25	0.020
At5g41210	ATGST T1	GSH-Transfer	0.85	0.034
At5g27380	glutathione synthetase GSH2	GSH-Transfer	0.83	0.029
At2g02390	ATGST Z1	GSH-Transfer	0.80	0.047
At4G32320	L-ascorbate peroxidase	GSH-Asc-cycle	0.77	0.040
At2g29450	ATGST U5	GSH-Transfer	0.75	0.024
At2g25080	putative glutathione peroxidase AtGpx 1	GSH-Transfer	0.73	0.010
At1g78380	similar to glutathione S-transferase	GSH-Transfer	0.70	0.003
At5G21100	L-ascorbate oxidase	GSH-Asc-cycle	0.64	0.014
At1G77490	L-ascorbate peroxidase	GSH-Asc-cycle	0.58	0.000
At2g02930	putative glutathione S-transferase	GSH-Transfer	0.54	0.000
At4g02520	ATGST F2	GSH-Transfer	0.39	0.002
At1G43160	ERF-Familienmitglied	pathogens-related	1.75	0.029
At5G05170	CELLULOSE SYNTHASE 3	pathogens-related	1.32	0.009
At4G23550	Encodes WRKY DNA-binding protein 29	pathogens-related	1.16	0.048
At5G06950	TGA2	pathogens-related	0.91	0.029
At1g19610	DEF1.4 Defensin	pathogens-related	0.89	0.018
At2G39940	CORONATINE INSENSITIVE 1	pathogens-related	0.88	0.045
At5G13160	A VRRPB SUSCEPTIBLE 1	pathogens-related	0.86	0.032
At1G08720	ENHANCED DISEASE RESISTANCE 1	pathogens-related	0.84	0.006
At3g52430	PAD4, PHYTOALEXIN DEFICIENT 4	pathogens-related	0.82	0.039
At4G20380	LESION SIMULATING DISEASE	pathogens-related	0.79	0.004
At5G45250	RESISTANT TO P. SYRINGAE 4	pathogens-related	0.78	0.003
At3G48090	ENHANCED DISEASE SUSCEPTIBILITY 1	pathogens-related	0.77	0.003
At1G19670	ATGLH1, COR1, CHLOROPHYLLASE	pathogens-related	0.75	0.031
At4G11260	RFR1	pathogens-related	0.73	0.003
At1G74710	SID2, SALICYLIC ACID INDUCTION DEFICIENT 2	pathogens-related	0.72	0.037
At3G20770	ETHYLENE INSENSITIVE3	pathogens-related	0.69	0.003
At1g05010	EFE, ethylene forming enzyme	pathogens-related	0.68	0.008
At5g14930	leaf senescence-associated protein	pathogens-related	0.67	0.000
At3G44480	RFP1	pathogens-related	0.64	0.000
At5G44420	LOW-MOLECULAR-WEIGHT CYSTEINE-RICH transcription factor	pathogens-related	0.62	0.002
At3G54000	transcription factor	pathogens-related	0.62	0.002
At1G75040	FR5	pathogens-related	0.61	0.025
At1G59870	ATP binding cassette transporter	pathogens-related	0.58	0.000
At4G16950	RFP5	pathogens-related	0.46	0.001
At4G16860	RFP4	pathogens-related	0.43	0.002
At3g19450	cinnamyl alcohol dehydrogenase	amino acid synthesis	1.47	0.001
At2G41220	Glutamate synthetase	amino acid synthesis	1.42	0.014
At4G34200	mitochondrion, amino acid binding	amino acid synthesis	1.41	0.003
At4G31990	aspartate aminotransferase	amino acid synthesis	1.27	0.026
At1G17745	phosphoglycerate dehydrogenase activity	amino acid synthesis	1.27	0.029
At3G48450	nitrate-responsive NOL protein, putative	amino acid synthesis	1.12	0.032
At4g39330	cinnamyl alcohol dehydrogenase CAD1	amino acid synthesis	0.87	0.031
At3G58750	Encodes a peroxisomal citrate synthase	amino acid synthesis	0.86	0.045
At5G53460	NADH-dependent glutamate synthase	amino acid synthesis	0.80	0.008
At3g48560	acetolactate synthase	amino acid synthesis	0.79	0.026
At3G19480	oxidoreductase activity	amino acid synthesis	0.79	0.039
At4g39540	shikimate kinase - like protein	amino acid synthesis	0.79	0.012
At5g37600	glutamate-ammonia ligase	amino acid synthesis	0.78	0.003
At5g05730	encodes the alpha subunit of anthranilate synthase	amino acid synthesis	0.73	0.029
At2g35370	glycine decarboxylase complex H-protein	amino acid synthesis	0.66	0.041
At1g09240	putative nicotianamine synthase	amino acid synthesis	0.63	0.008
At3g30775	proline oxidase, mitochondrial precursor	amino acid synthesis	0.59	0.017
At1G75750	gibberellin-regulated protein 1 (GASA1)	Hormon induced/related	2.00	0.000
At1g77330	Acc-Oxidase	Ethylenebiosynthesis	1.93	0.003
At5g20960	INDOLE-3-ACETALDEHYDE-OXIDASE	Hormon induced/related	1.66	0.008
At5G15230	gibberellin-regulated (GASA4) mRNA	Hormon induced/related	1.32	0.011
At4g08950	putative phi-1-like phosphate-induced protein	Hormon induced/related	1.32	0.032
At3g47290	phosphoinositide-specific phospholipase C family protein	Hormon induced/related	1.27	0.004
At2G45790	phosphomannomutase	Asc-biosynthesis	1.24	0.011
At2g22250	putative cystein lyase	bolism, Cystein degradation	1.14	0.048
At3G24220	9-cis-epoxycarotenoid dioxygenase	ABA-Synthesis	0.87	0.049
At3G53360	3-oxo-5-alpha-steroid 4-dehydrogenase	Brassinosteroid-Synthesis	0.64	0.028
At3G44310	NIT1	Auxin-Biosynthesis	0.61	0.011
At3G16770	AtEBP, ethylene-inducible	Hormon induced/related	0.55	0.002
At3G14588	Auxin (indole-3-acetic acid) induced gene (IAA1)	Hormon induced/related	0.54	0.001
At3g49700	ACC-Synthase	Ethylenebiosynthesis	1.24	0.004
At2g19590	ACC-Synthase	Ethylenebiosynthesis	1.11	0.028

Supplemental data 3. The impact of reduced SiR activity on the expression of sulfur metabolism-related

genes in the roots

Total mRNA was extracted from the roots of seven weeks old hydroponically-grown Col-0 and *sir1-1* plants. The genes in green background indicate significant down-regulation ($P < 0.05$), whereas, those in the white background represent significantly up-regulated genes ($P < 0.05$).

A

P1+P4 TTTGACCATTGTCTTTTGTCTCTATTAGTTTTTAAACACACGCCCCCTTATGATGACATCGCTTCAGGATATATTCAATT(

ALSIR TTTGACCATTGTCTTTTGTCTCTATTAGTTTTTAAACACACGCCCCCTTATTC - GATTTT - CT - CACCC - ACC - - CAAA - (

B

P2+P7 AGAGTGAGTGGCTTTGGGTGGGTGAG - AANTCTCNTNGGGGNCNNGTGTAAATGGCTTCNTGTCCGNGAAATCTACA - TG

ALSIR AGAGTGAGTGGCTTTGGGTGGGTGAGAAAAATCGAATAAGGGGGCGTGTGTTAA - -AAAAC - TAATAGAG - AA - CAAAAGAC

Supplemental data 4. Sequence alignment of the T-DNA and gene specific primer fragments of *sir1-2* with the genomic sequence of wild-type *SiR* gene.

(A) The unmatched sequences (red) obtained from the the sequence analysis of gene specific and T-DNA specific primer combinations (P1 + P4) represent the position of the T-DNA insertion towards the left border *SiR* gene in *sir1-2*. (B) The unmatched sequences (red) obtained from the the sequence analysis of gene specific and T-DNA specific primer combinations (P2 + P7) represent the position of the T-DNA insertion towards the right border *SiR* gene in *sir1-2*.

List of abbreviations

APS	ammonium persulfate
Ac-COA	acetyl-coenzymeA
AP	alkaline phosphatase
APR	Adenosine-5'-phosphosulfate reductase
BCIP	5-bromo-4-chloro-3-indolyl phosphate toluidin salt
BSA	bovine serum albumin
Col-0	<i>Arabidopsis thaliana</i> wild-type Columbia-0
cpm	counts per minute
dpm	disintegration per minute
DTT	1,4-dithiothreitol
EDTA	ethylenediamine tetraacetic acid
HBED	N, N'-bis(2-hydroxybenzyl)ethylenediamine-N, N'-diacetic acid
HEPES	4-(2-hydroxyethyl)-1-piperazineethanesulfonic acid
HPLC	high performance liquid chromatography
ICP	Inductively Coupled Plasma Emission Spectroscopy
IMAC	immobilized metal affinity chromatography
HR	hypersensitive response
IPTG	isopropyl- β -D-thiogalactopyranoside
K_m	Michaelis constant
KDa	Kilo Dalton
MBB	monobromobimane
NBT	nitro-blue tetrazolium
PAGE	polyacrylamide gel electrophoresis
PMSF	phenylmethylsulphonylfluoride
rpm	rounds per minute
SDS	Sodium dodecylsulfate
SULTR	Sulfate transporters
T-DNA	Transferred DNA used for insertional mutagenesis
TEMED	N,N,N',N'-Tetramethylethylenediamine
Tris	2-Amino-2-(hydroxymethyl)propane-1,3-diol

Acknowledgments

First and foremost, I lay down my grateful estrangement before Allah Almighty let me with encouragement to take this job to its end, and the respect for his last Prophet Muhammad (peace be upon him) for enlightening and guiding the mankind to the true path of life.

From the core of my heart, deepest sense of gratitude is forwarded to my supervisor professor Rüdiger Hell, whose dynamic supervision, lasting mood of keen interest and constructive criticism brought the material exposed in this thesis to its final shape. Even in his countless engagements he was present all the time to help me.

Thanks are extended to professor Thomas Rausch for his valuable suggestions and helpful discussions, particularly in selenium fertilization experiments.

Special thanks are extended to Dr. Markus Wirtz for useful ideas and genuine help in conducting the research. His critical suggestions and consistent advice throughout the entire PhD project helped me a lot in my proceedings.

I am thankful to Dr. Andreas Meyer for his suggestions and advice from time to time. Special thanks are due to Sarah Hassel for technical assistance and Corinna Heeg for her best wishes and help on numerous occasions. I feel my vocabulary limited in finding words for thanking to all my former and current lab members, who always gave me hands in difficult times and maintained an excellent atmosphere in the lab. I would like to thank M. Reichelt and J. Gershenzon, MPI Jena, for determination of glucosinolates, and R. Hänsch and R. Mendel, Univ. Braunschweig, Germany, for sulfite oxidase assays.

I am greatly thankful to Higher Education Commission of Pakistan (HEC) and Deutscher Akademischer Austausch Dienst (DAAD) for providing financial support for the project. I would like to acknowledge all the colleagues of my department in NWFP Agricultural University, Peshawar, Pakistan for taking the teaching load during my absence.

At the end, I express my deepest feelings of gratitude to my kind and respectable parents whose care, support and valuable advice remained everlasting assets throughout my career. I am inspired to acknowledge my amazing family members, available all the time to uphold me. Final thanks to Saima and Sher Azam Khan for everything.